NUREG/CR-1340
SSS-R-80-4217
R6, RA

State-of-the-Art Study Concerning Near-Field Earthquake Ground Motion

Annual Report
September 1978 - September 1979

Manuscript Completed: January 1980
Date Published: August 1980

Prepared by
H. J. Swanger, J. R. Murphy, T. J. Bennett and R. Guzman

Systems, Science and Software
P. O. Box 1620
La Jolla, CA 92038

Prepared for
Division of Reactor Safety Research
Office of Nuclear Regulatory Research
U.S. Nuclear Regulatory Commission
Washington, D.C. 20555
NRC FIN No. B6491

ABSTRACT

This report presents a status summary of a continuing investigation into the applicability of theoretical earthquake source modeling to the definition of design ground motion environments for nuclear power plants located in the near-field of potentially active faults. A wide variety of proposed near-field ground motion prediction procedures are described and evaluated. It is concluded that existing empirical procedures for predicting near-field ground motion characteristics are not adequately constrained by the available strong motion data, leading to order of magnitude uncertainty in the prediction of some parameters. On the other hand, the review of the proposed theoretical source descriptions has identified a number of model parameters and assumptions which are also not well constrained either by data or theory and which may affect the near-field ground motion estimates predicted by these models. Preliminary parametric study results are presented, for example, which demonstrate that different, commonly employed assumptions concerning the initiation and stopping of earthquake faulting can have a significant effect on the computed near-field ground motion characteristics.

TABLE OF CONTENTS

TABLE OF CONTENTS (Continued)

TABLE OF CONTENTS (Continued)

LIST OF ILLUSTRATIONS

LIST OF ILLUSTRATIONS (continued)

LIST OF ILLUSTRATIONS (continued)

I. INTRODUCTION

1.1 BACKGROUND

In September, 1978, Systems, Science and Software (S^3), under contract to the Nuclear Regulatory Commission, began work on a two-year research program which focuses on a state-of-the-art evaluation of near-field earthquake source modeling. The primary objective of this study is to provide a critical evaluation of the various earthquake source models which have been proposed, both in terms of the soundness of the physical concepts involved and their ability to describe the observed trends in the measured data. In order to achieve this objective, a research program consisting of a number of related tasks has been formulated. The first task consists of a systematic literature search in which various empirical and theoretical models which have been proposed for use in estimating near-field earthquake ground motion parameters are reviewed, compared and evaluated. The second task focuses on an investigation of the scaling relations associated with the various theoretical models. The dependence of the seismic source function on variables such as magnitude/moment and the dynamic parameters of faulting are systematically investigated for each model of interest. Where necessary, calculations are performed so that scaling laws can be deduced over the same range in variables for each model. At this point the models can be quantitatively compared and evaluated with regard to the consistency and plausibility of their predictions. Under the third task, the applicability of various promising models are critically assessed through comparisons of model predictions with observed strong motion data. In order to accomplish these comparisons, selected source models are employed in conjunction with highly simplified models of the propagation path to make predictions corresponding to a number of near-field ground motion observations. Those models which are

found to be consistent with the observed peak amplitudes, spectra and time histories are then identified and their relative strengths and weaknesses are analyzed and documented. Once this program has been completed, the applicability of existing theoretical earthquake source models to the specification of design ground motion parameters for nuclear power plants located in the near-field of active tectonic features will be critically assessed and documented. This report provides a summary of the research conducted in support of these objectives during the first year of this contract.

1.2 CHARACTERISTICS OF STRONG EARTHQUAKE SHAKING IMPORTANT TO THE DESIGN OF SAFETY RELATED ITEMS IN NUCLEAR POWER PLANTS

Before proceeding to a detailed consideration of the ground motion issues, it is appropriate to establish the framework within which this investigation is being carried out. This is necessary because while a complete description of the seismic source function for earthquakes would encompass the consideration of a very wide frequency band extending from DC to perhaps several hundred Hertz, the objective of this study is not to analyze the source for its own sake but rather to assess the capability of available source models with regard to the definition of those characteristics of the near-field ground motion which are important in the design of nuclear power plants. The purpose of this section, therefore, is to provide a brief overview of the seismic response characteristics of nuclear power plants with emphasis on defining the characteristic frequencies associated with safety related items.

A definition of the structures, systems, and components important to safety during earthquakes is provided in U. S. NRC Regulatory Guide 1.29 titled, "Seismic Design Classification". These structures, systems, and components (including

their foundations and supports) should be designed to withstand, without loss of function, the effects of the safe shutdown earthquake (SSE). The plant features thus designed, designated Seismic Category I, are those necessary to ensure:

1. The integrity of the reactor coolant pressure boundary,

2. The capability to shut down the reactor and maintain it in a safe shut down condition, or

3. The capability to prevent or mitigate the consequences of accidents that could result in potential off-site exposures.

The following types of items can be identified as safety related (Seismic Cateogory I) in nuclear power plants:

- Stability of subsurface materials and foundations (bearing capacity and liquefaction).
- Stability of slopes (soil slopes and rock slopes).
- Buildings (containment building, auxiliary building, fuel handling building, control building).
- Piping and supports.
- Long buried structures (electrical duct banks, tunnels, and well casings).
- Equipment (pressure vessels, heat exchangers, pumps, air handling equipment, water chillers, control panels, cable trays, HV&AC ducts, electric switch gear, supports and other types of equipment).
- Cooling towers.
- Embankments and earth and rock-fill dams.
- Fuel handling equipment (cranes, upenders, spent fuel storage racks).

Traditionally, the frequency range considered to be of importance for the earthquake resistant analysis and design of nuclear power plants has been 0.5 to 33.0 Hz. This is the frequency range within which the design spectra of many

nuclear power plants have been defined. The primary basis for specifying this frequency range is that the significant natural frequencies of most Seismic Category I items fall well within it. Exceptions to this are a few Category I items whose natural frequencies are in the 0.25 to 0.5 Hz range. Examples of these are in the sloshing modes of water reservoirs and the spent fuel pool, hanging cable trays, and the low frequency pendulum vibrations of loads suspended by Category I cranes. However, because a major portion of the Seismic Category I items are housed within Category I buildings, the significant natural frequencies of the buildings have the largest effect on the seismic design of nuclear power plants. The significant natural frequencies of the buildings determine both their own seismic response and the amplitude of the in-structure design response spectra (in-structure design response spectra determine the seismic design of most Category I equipment). The fundamental frequencies of Category I buildings (containment building, auxiliary building, fuel handling building, and others), which are very massive and stiff, vary between approximately 2 Hz for buildings on relatively soft soils to approximately 12 Hz for buildings on sound bedrock.

It appears that the highest frequencies of significant interest should be between 15 Hz and 20 Hz. This is because the fundamental frequencies of portions of Category I buildings, such as deep beams vibrating vertically or of very stiff equipment, rarely, if ever, exceed the 15 to 20 Hz range.

Within the above defined frequency band, the structural response, of course, depends on the details of the ground motion time history; especially amplitude level and duration. These two parameters together define the excitation amplitude at the characteristic frequencies of the structures of interest. The duration of strong shaking is particularly important for purposes of assessing nonlinear response effects

such as those associated with liquefaction and fatigue (i.e., deterioration or failure due to cyclic loading).

In view of the above discussion, it is appropriate to consider the role of peak ground acceleration in defining the design ground motion for nuclear power plants. After the 1971 San Fernando earthquake, the earthquake engineering and seismological community became acutely aware of the potential for experiencing peaks of high acceleration (i.e., 1 g or more) in the near-field of earthquakes. In fact, since 1971 there have been isolated observations of large peak accelerations from a number of earthquakes of modest size (i.e., $M < 6$). However, it is important to note that many of these have been isolated, high frequency peaks which are not necessarily representative of the general level of the ground motion experienced at the site. For example, Page, et al. (1972) lowpass filtered the S16E component of the 1971 San Fernando earthquake accelerogram recorded at Pacoima Dam and found that in the frequency band below about 9 Hz, the original 1.22 g peak acceleration was reduced to 0.93 g. Moreover, it can be shown that the standard Regulatory Guide 1.60 response spectra, normalized to a peak acceleration of 0.75 g, bounds most of the response spectra of the 1971 Pacoima Dam recordings. The reason for this is that, for the low-damped response spectra used in the design of nuclear power plants, the linear response in a given frequency band is relatively insensitive to components of the forcing function lying outside the band. For example, consider the amplitude of the five percent damped response spectrum at 10 Hz due to sinusoidal forcing functions with frequencies of 20 Hz and 10 Hz. It can be shown that the response at 10 Hz due to one cycle of a 20 Hz sine wave is an order of magnitude smaller than that due to two cycles of a 10 Hz sine wave of the same amplitude. Thus, the possibility of isolated, high frequency acceleration peaks does not, of itself, necessarily have any implications with respect to the

design response spectral amplitudes in the frequency range of interest. In fact, for structures which have some ductility, the duration of a particular level of shaking may be the most important factor in defining the response characteristics. Thus, for example, Husid (1967) in his analysis of the response of a single-degree-of-freedom elasto-plastic structure, showed that the amplitude of shaking at Parkfield in 1966 would have had to be five times as great as that in El Centro in 1940 to produce the same effects because of its much shorter duration.

In summary, safety related items in nuclear power plants respond primarily to components of the ground motion which lie in a restricted frequency band. Moreover, the amplitude of the response spectrum over the frequency range of interest may not be closely related to the peak acceleration level, particularly for sites in the near-field of the earthquake source. Therefore, in the present study, the effort is not focused on the analysis of peak ground motion parameters alone, but rather on the physics of the faulting process which control the characteristics of the motion which define the response over the frequency range of importance in the design of nuclear power plants.

1.3 FOREWORD

The following sections present a summary of the current status of our investigation of near-field earthquake ground motion. In Section II, a critical review of the various proposed empirical procedures for predicting near-field ground motion parameters (i.e., peak motion, spectra and time histories) is presented, together with descriptions of some selected applications of these procedures. A state-of-the-art review of theoretical source modeling is presented in Section III where the various proposed theoretical models are classified and compared. Section IV presents the results of some preliminary parametric studies which have been conducted using a particular theoretical model and provides some additional

insight into the question of how various assumptions about the nature of the source affect the computed near-field ground motion. This is followed in Section V by a summary, together with a statement of conclusions and a discussion of future plans for the research effort.

II. REVIEW OF PROPOSED EMPIRICAL PROCEDURES FOR PREDICTING NEAR-FIELD EARTHQUAKE GROUND MOTIONS

2.1 BACKGROUND

Before proceeding with more detailed considerations, some background discussion is appropriate. Descriptions of ground motion for use in engineering design typically involve identification of earthquake sources and assessment of the size (magnitude or epicentral intensity) of potential earthquakes from these sources. In addition, to account for incompleteness in our understanding of earthquake causes and possible sources, it may be desirable to design certain structures to some level of earthquake which is viewed as the background level for some large region -- i.e., the largest earthquake which could reasonably be expected to occur at a location whose geologic and seismic characteristics are indistinct from those generally existing throughout the region. Thus, the Nuclear Regulatory Commission's Seismic and Geologic Siting Criteria, Appendix A to 10 CFR Part 100, require identification of the earthquake potential determined to be the background level for the region (tectonic province), which is taken to be the largest historical earthquake not associated with some known geologic structure. In the latter case, the maximum intensity of the historical earthquake is assumed to occur at the site and peak acceleration values determined from empirical relationships (e.g., Trifunac and Brady, 1975; Murphy and O'Brien, 1977) are normally used to scale a set of empirically derived standard response spectra (e.g., Newmark, Blume and Kapur, 1973) for use in design. In the former case, which is more closely tied to the present problem, the earthquake epicenter is assumed to occur on the structure with which it is associated at its nearest approach to the site. Ground motions in this case too are frequently derived from empirical relationships (e.g., Schnabel and Seed, 1973) between

magnitude, distance, and acceleration level; and the resulting acceleration is again normally used to scale the standard response spectra. However, the reliability or level of conservatism in this procedure becomes difficult to define when determinations are required outside the range of data which were used in developing the empirical relationships. Of particular interest in the present study is the relevance of these empirical procedures to describe ground motion for use in engineering design of structures in the near-field* of potential earthquakes.

The state of the art for predicting earthquake ground motion on the basis of analyses of empirical data has been summarized in two recent papers: one by Bernreuter (1977) and the second by Boore, et al. (1978). The existing techniques can be viewed from several perspectives; for this report we have broken them down into three categories: (1) techniques resulting in specification of a single parameter, such as peak acceleration level; (2) techniques resulting in specification of frequency content of the ground motion, such as Fourier or response spectra; and (3) techniques resulting in specification of time histories of the ground motion.

2.2 PEAK MOTION RELATIONS

The majority of the methods relying on empirical data have related the earthquake magnitude and distance to a single ground motion parameter, and primarily to peak acceleration. Some of these studies have limited their consideration to the region beyond the near-field, where data are more plentiful,

---

*For the purpose of the discussion in this section, the term "near-field" refers to the area surrounding the source within a distance approximately equal to the dimensions of the fault rupture (i.e., the geometrical near-field).

or have considered data in the near- and far-field separately; but others have not drawn such distinctions. The strong motion data base is generally recognized to be incomplete in the near-field for earthquakes of all sizes, but particularly for large earthquakes. However, the empirical data have been extrapolated to describe the ground motion for such cases. When this has been done, the computations were found to be highly sensitive to the behavior of the attenuation function and to the dependence of acceleration level on magnitude. Because of this sensitivity, some investigators have sought to establish additional constraints on the problem by considering limitations arising from seismic wave transmission and earthquake source theory. In the following sections, the most widely used methods are discussed with focus on their application in the near-field.

Page, et al. (1972) developed methods for describing near-field ground motion for use in the design of the trans-Alaska oil pipeline. For earthquakes in the magnitude range 5.5 to 8.5, the report describes the expected behavior of peak horizontal ground accelerations, velocities and displacements and also the duration of strong motion for sites 3 to 5 km from the causative fault. The earthquakes used as the data base for the study were in the magnitude range from 5.3 to 7.7; however, the data above magnitude 7.0 are all at distances greater than about 45 km from the faults. The study did not consider the effects of site conditions.

To derive the near-field ground motion, data recorded at a distance of 5 km from the fault in the 1966 Parkfield earthquake were used to represent the ground motion for magnitude 5.5, and the Pacoima Dam record (filtered to remove frequencies above 8 Hz) obtained at a hypocentral distance of 3 km from the 1971 San Fernando earthquake was used to represent magnitude 6.5. The ground motions shown in the report

for magnitudes greater than 6.5 were obtained by extrapolation. It is noted that the extrapolation was guided by consideration of the fact that peak accelerations increase with magnitude at all distances and that Brune's source theory suggests proportionality between peak acceleration and effective stress; however, the details of these considerations are unclear. In the end, Page, et al. adopt a peak acceleration of 1.25 g for magnitude 8.5; then, for magnitudes between 6.5 and 8.5, the acceleration values are interpolated. However, the interpolation is not linear, and again no details are given. Similar procedures are followed for estimating the ground velocities and displacements.

Weaknesses in the approach of Page, et al. appear to be their reliance on one or two records which are taken to be representative of a given magnitude earthquake and the lack of a satisfactory basis to support the extrapolation. However, it should be noted that Page, et al. recognized these weaknesses in their methodology; and the report includes numerous caveats regarding applicability of their conclusions.

Schnabel and Seed (1973) developed a different approach for deriving earthquake ground motion. Their report presents predicted maximum accelerations for rock sites at distances between one and 100 miles from the fault rupture and for magnitudes from 5.2 to 8.5. The data used in their study included earthquakes in the magnitude range from 5.0 to 7.7* and records in the distance range from about one to 100 miles; for earthquakes above magnitude six no data within a distance of six miles from the fault were used.

---

*Schnabel and Seed rate the 1952 Kern County earthquake as magnitude 7.6 while the USGS rating is 7.7.

To derive acceleration levels within and beyond the range of the data, Schnabel and Seed considered a theoretical model to represent the propagation of seismic waves outward from an extended source. They represented the attenuation as the product of (1) a term representing geometrical spreading from an areal source having lateral and vertical extent, and (2) a term representing frequency dependent damping. For reasonable assumptions on the damping factor, they found the geometrical spreading term to be dominant for the sizes of earthquakes under consideration and distances within 50 miles of the causative fault. While the behavior of the attenuation function with distances was treated in detail, Schnabel and Seed did not provide a complete description of how the absolute levels of the attenuation curves were fixed for particular magnitudes. However, it appears that they were developed by constraining the theoretical attenuation curves for specific earthquakes to pass through individual data points. For a given magnitude interval the results were then averaged and enveloped to obtain the curves presented in the report. There is no obvious explanation of how they determined the curve for magnitude 8.5 or the probable upper bound curve shown in the report. An additional finding of interest in the present study is that the approach is relatively insensitive to several parameters describing source and transmission characteristics: the vertical extent of faulting, the upper limit of faulting, shear velocity in the surrounding medium, and damping factor.

The small number of strong motion records used for each magnitude interval is considered to be a weakness of this study because it both places in question the reliability of the mean curves and results in underestimates of the scatter of the data. This has become apparent with the acquisition in recent years of additional strong motion records at close distances from small earthquakes having peak accelerations

above those predicted by the curves. Boore, et al. (1978) also note that the theoretical curves for geometrical spreading developed by Schnabel and Seed are based on assumptions which strictly apply to total radiated energy; their application to peak acceleration values is questionable. Finally, the use of acceleration measurements at fairly large distances (50 to 100 miles) to constrain the theoretical attenuation curves and thereby predict strong ground motion near the source places high reliance on the accuracy of an attenuation model which, at best, can provide only a very crude approximation to the distance decay rate of time domain peak motion parameters.

Donovan (1973) adopted an approach used by Esteva and Rosenblueth (1963) and Esteva (1970) to analyze a data base consisting of 678 acceleration observations obtained worldwide and including the 1971 San Fernando earthquake data. Magnitudes of earthquakes in the data sample range from less than five to more than eight and hypocentral distances are between about three and 450 km, with the majority of data at small distances being for small earthquakes. Attenuation relations of the form:

$$a = a_0 e^{AM} R^{-B} \quad \text{and} \quad a = a_0 e^{AM} (R + 25)^{-B}$$

where M is magnitude, R is hypocentral distance, and a_0, A and B are constants, were fit to the data and certain subsets of the data using least squares techniques. Donovan notes that, although both equations result in similar attenuation values except at small distances, the fit to the data using the latter equations is somewhat better. The latter relationship also avoids the problem of extreme accelerations as R approaches 0, which was the original intent of Esteva (1970) in proposing this representation. However, it also should be noted that the assumption of the constant 25 in the denominator

is completely arbitrary and strongly controls predictions of acceleration levels at distances near the source. This is probably the greatest weakness of the approach since it diminishes its usefulness for predicting ground motion near the source.

Orphal and Lahoud (1974) also performed statistical analyses using the same form of the attenuation relationship as that used by Donovan without the constant in the distance term. A regression analysis was first performed on data from the 1971 San Fernando earthquake to determine distance dependence. They take the focal depth as 14 km so that the data cover a hypocentral distance range from 15 to 350 km for the magnitude 6.4 event. They next performed a second regression analysis on data from a set of earthquakes in the magnitude range from 4.1 to 7.0 to determine the dependence on magnitude. The peak accelerations from these earthquakes were first normalized by multiplying by the previously derived distance attenuation factor $R^{1.39}$, and the regression was then performed on the normalized values. By analogy to the distance dependence of peak ground motion values observed for underground nuclear tests, Orphal and Lahoud developed similar prediction equations for peak velocities and displacements.

The distance dependence in the relationship developed by Orphal and Lahoud is completely controlled by a single event, the 1971 San Fernando earthquake. While this tends to place in question its general reliability, the relationship does accurately predict peak accelerations in a worldwide data base reported by Ambraseys (1969) for earthquakes in the magnitude range 3.9 to 7.7. With regard to ground motion near faults, the relationship accurately predicts near fault motions observed in the 1966 Parkfield earthquake. However, as with the other statistical relations, the near-field motion level predicted by this model is controlled by the attenuation relation which was derived from primarily far-field data.

Trifunac (1976a) proposed a more complex form for relating peak ground motion parameters to earthquake magnitude and distance:

$$\log_{10} X = M + \log_{10} A_0(R) - \log_{10} X_0(M)$$

where X is taken to be peak acceleration, peak velocity, or peak displacement, the attenuation with distance described by $A_0(R)$ is assumed to be the same for each of the ground motion parameters and X_0 is a magnitude-dependent scaling parameter derived empirically. The magnitude-dependent scaling factor was assumed to have the form:

$$\log_{10} X_0 = Ap + BM + C + Ds + Ev + FM^2$$

where p is a confidence level associated with the estimate, s represents site conditions (rock or soil), and v represents the component of motion (horizontal or vertical). A regression analysis was performed on the peaks of acceleration, velocity and displacement using data from the Caltech strong motion data sample. Earthquake magnitudes in the sample are between 3.8* and 7.7 and the epicentral distance range is from about 5 to 400 km. Trifunac assumed that the distance dependence $A_0(R)$ was the same as that described by Richter (1958) as used in developing the magnitude scale.

The prediction equations which result from the regression analysis are shown to flatten out at distances below about 10 to 20 km. However, Richter lacked data in this range to support the adopted distance dependence; and, as noted

*The lower limit of the magnitude range was cited as 3.0 by Trifunac but this appears to have been an error corrected in subsequent papers.

elsewhere, strong motion data do not exist to confirm or deny such behavior. More fundamentally, the Richter attenuation relationship, $A_0(R)$, was derived from measurements made on Wood-Anderson seismographs. Although this instrument had somewhat better response at high frequencies than the typical observatory seismograph of today, its sensitivity does not compare with the modern broad-band strong motion instruments which recorded the preponderance of the peak motion data reported by Trifunac. Therefore, it is unclear that the Richter attenuation relationship should have any relevance to the attenuation of recorded peak acceleration values. Furthermore, the use of the same attenuation function to represent the distance decay of acceleration, velocity and displacement peaks is difficult to justify on physical grounds and is contrary to the findings of other investigators (e.g., Orphal and Lahoud, 1974; McGuire, 1978a) who have determined significantly different attenuation relationships from statistical analyses of the individual peak motion parameters. Another factor is that Schnabel and Seed (1973) found the influence of source dimensionality on the attenuation relation to be very important, particularly in proximity to the fault; however, Trifunac considered this to be beyond the scope of his report. This coupled with the lack of confirmatory strong motion data near the source were considered to be the greatest weaknesses in the proposed approach. Trifunac's analysis also does not take into account frequency-dependent attenuation due to damping; however, as pointed out by Schnabel and Seed (1973), this deficiency may not be too serious when considering only the peaks of the motions. In addition, the data sample used by Trifunac has been criticized because more than half the records are from the 1971 San Fernando earthquake which could be a source of potential bias.

In a more recent study, McGuire (1978a) performed a regression analysis on the horizontal components of the strong

ground motion data from 140 records from the Caltech data sample. The data used were for earthquakes in the magnitude range from 4.5 to 7.7 and for hypocentral distances from about 10 km to just over 200 km. In his regression analysis, McGuire used a relationship of the form:

$$\ln X = A + BM + C\ln R + DY_s$$

where X was taken as peak acceleration, peak velocity, peak displacement, or PSRV spectral level at 1 Hz for two percent damping, A, B, C and D were constant coefficients which may be different for different ground motion descriptors, M was magnitude, R was hypocentral distance, and Y_s was one or zero for soil or rock sites, respectively. The form of the relationship neglecting the site term is equivalent to that suggested by Esteva and Rosenblueth (1963) and subsequently used by others as described above. Because it does not include an additive constant in the hypocentral distance term, values predicted by McGuire's relationship do not tend to flatten out at small distances. However, it should be noted that McGuire deliberately excluded observations at nearer distances from his data base and does not consider the relationships to be appropriate for predicting ground motion at locations in the near-field. McGuire's report advocates the use of judgement and physical arguments for considering the near-field problem and offers additional caveats about extrapolating the data to higher magnitude levels.

Figure 1 shows comparisons of the near-field acceleration levels predicted by the relations described above at epicentral distances of five and 30 km (assuming zero focal depth). All of the relations shown are for hardrock sites except for those of Orphal and Lahoud and Donovan which are based on samples composed of both hardrock and alluvium data.

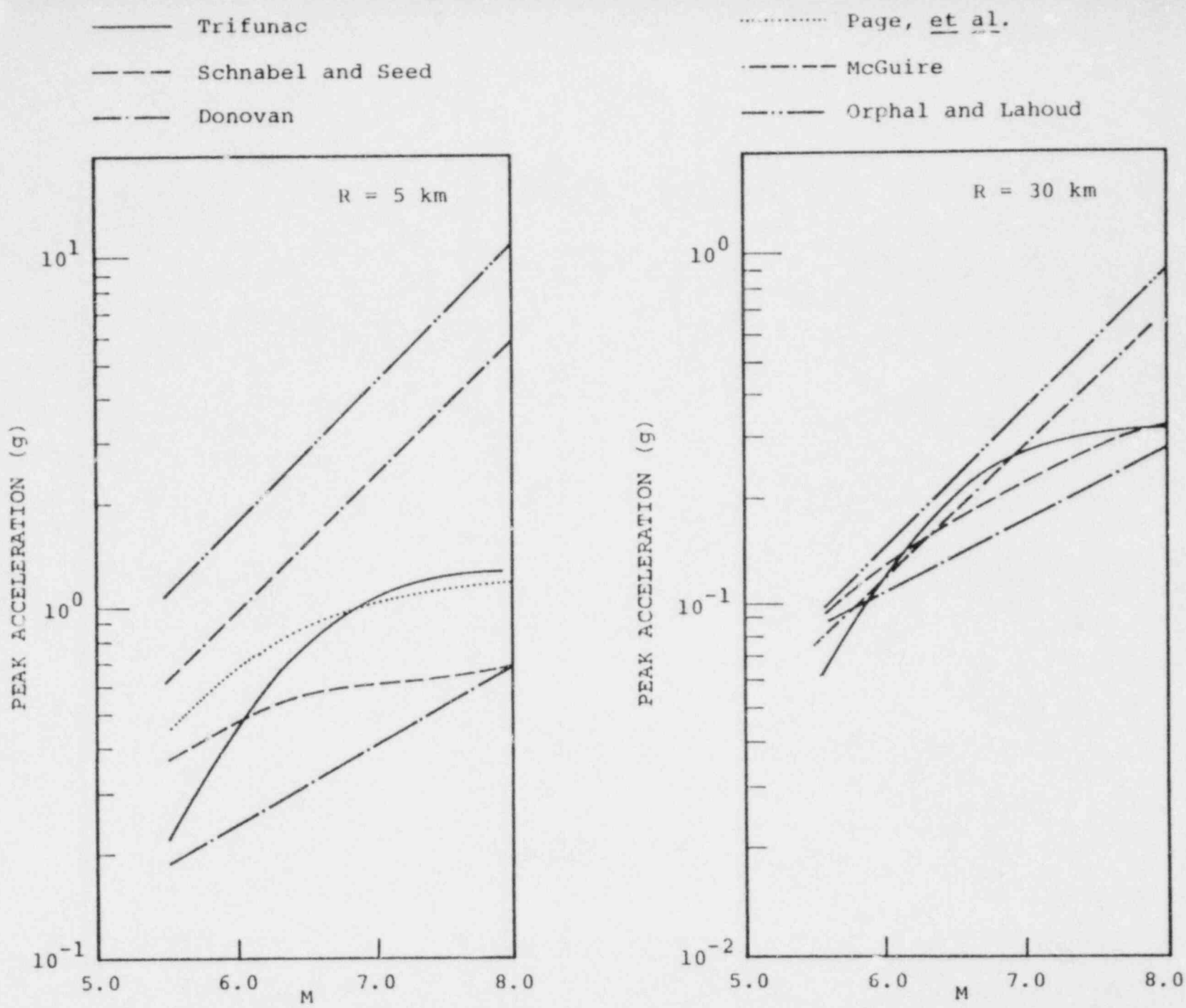

Figure 1. Peak accelerations as a function of magnitude at distances of 5 and 30 km estimated from empirical relationships.

This figure graphically illustrates the nature of the present problem. That is, at an epicentral distance of 30 km, over the magnitude range from 5.5 to 7.0 where the prediction equations are well constrained by the available empirical data, the range of the peak acceleration values obtained from all the proposed scaling laws described above is less than a factor of two. However, at the near-field range of 5 km which is of primary interest in this investigation, the variability exceeds an order of magnitude. This illustrates the sensitivity of the near-field predictions to the various assumptions concerning the dependence on magnitude and distance, particularly at large magnitudes and short epicentral distances. Thus, since adequate data are not available to reconcile these discrepancies, near-field estimates of strong ground motion parameters will have to be constrained by insights gained from theoretical source modeling.

2.3 GROUND MOTION SPECTRA PREDICTIONS

For the most part, the above discussions have treated descriptions of earthquake motion in terms of single ground motion parameters (acceleration, velocity or displacement) with no particular regard for the frequency content or time dependence of the motion. Such representations of the ground motion are clearly incomplete. While single ground motion parameters may provide descriptions adequate for engineering, certain simple classes of structures and over limited frequency ranges, more complex structures and systems with a broad range of critical frequencies require more refined engineering analysis methods and more complete descriptions of the earthquake ground motion. The spectral representation of ground motion in terms of Fourier or response spectra has been studied by several individuals.

Newmark, Blume and Kapur (1973) developed a set of normalized response spectra commonly used for design of nuclear power plants. Newmark and his associates conducted a study independent from that of Blume and his associates, and the results were meshed in the report cited above. Newmark, et al. studied 28 horizontal components of strong motion and 14 vertical components for earthquakes in the magnitude range from 5.3 to 7.7 and epicentral distances in the range from near zero to 120 km. Blume, et al. studied a somewhat different sample of 33 horizontal components of strong motion for earthquakes in the magnitude range from 5.[illegible] to 7.8 and epicentral distances from near zero to 80 km. In both cases the time histories were normalized before computing response spectra; the normalization performed by Newmark, et al. was more refined than that of Blume, et al. as time histories were normalized to different levels to evaluate the effects on spectral shape of maximum values of ground acceleration, ground velocity, and ground displacement. Response spectra corresponding to these normalized time histories were computed and analyzed statistically to obtain estimates of the spectral shapes having a 50 percent and 84.1 percent probability of exceedance. The results, reported as amplification factors, were smoothed to a somewhat simpler form which was recommended for use in engineering design. The actual implementation of these spectral shapes for use in design is achieved by scaling the spectra to acceleration values derived from empirical relationships between acceleration and information on the size and distance of potential earthquakes, as noted above.

Criticism of the study has focused on the broadband shape of the spectra which is not thought to be representative for expected earthquakes. The sources of this problem are in the data base, which contains earthquakes covering a fairly wide range of magnitude, epicentral distance, and soil conditions, and in the consequent analysis of the data which fails

to discriminate the effects of these factors on the spectral shape. In addition, no particular consideration in the analysis was given to representing ground motion in the near-field, which would limit the usefulness of this procedure in such applications. In fact, the spectral shape is assumed to be independent of distance, contrary to the findings of most other investigators.

Trifunac (1976b) performed a regression analysis on the Fourier amplitude spectra computed for the Caltech data sample, as described above. The earthquakes were again in the magnitude range from 3.8 to 7.7 and in the epicentral distance range from 5 to 400 km. The numerical model used by Trifunac was analogous to that which he used in the single parameter representation discussed above except all coefficients in the scaling function were made functions of frequency (or period) and anelastic attenuation was included. Trifunac again takes the distance-dependent term $\log_{10} A_0(R)$ to be the empirical relation derived by Richter (1958) in defining the magnitude scale for Southern California. The data were broken down into sets corresponding to magnitude groups 3.0 to 3.9, 4.0 to 4.9, 5.0 to 5.9, 6.0 to 6.9 and 7.0 to 7.9, and predictions of the Fourier amplitudes with some specified confidence level are provided for magnitudes of 4.5, 5.5, 6.5 and 7.5. The Fourier spectra for other magnitudes are obtained by interpolation and extrapolation.

An interesting observation which Trifunac notes rather tentatively is that the Fourier spectral amplitudes cease to increase linearly with magnitude in the range between about M = 4.0 and 5.5 and may reach a maximum in the range from M = 7.5 to 8.5. However, this observation apparently arises from the quadratic dependence on M which Trifunac assumes for the scaling function. McGuire (1978b) notes that this behavior is completely dependent on the 1952 Kern County

earthquake (M = 7.7) records and considers the statistical significance of this observation to be misleading because of potential biases from source, travel path and site effects.

While the report specifically shows estimates of the Fourier amplitude spectra at epicentral distances of zero km, Trifunac notes that the estimates are purely extrapolations of the spectra derived for larger distances and cannot be tested. However, the consequences of this extrapolation are important for the near-field problem and should be noted. Trifunac finds that the shape of the Fourier spectra remains relatively the same over the distance range from 20 to 200 km. McGuire (1978b) points out that this lack of change in frequency content with distance does not appear realistic and is possibly due to biases in the data base caused by small earthquake accelerograms being available only for close distances while at large distances only large earthquake accelerograms [illegible]ilable. As a result, for large earthquakes at small d[illegible]ances, Trifunac's model would tend to underestimate the high frequencies and overestimate low frequencies. Again, as was noted in conjunction with the peak amplitude review presented in Section 2.1 above, one of the primary objections to Trifunac's selected analysis procedure relates to his unverified assumption that Richter's attenuation relationship, which is based on data recorded through the bandwidth-limited Wood-Anderson seismometer, is applicable in the analysis of broadband strong motion data.

McGuire (1978b) performed a regression analysis very similar to that of Trifunac (1976), discussed above, but using a simpler statistical model and a different sample of strong motion data. The mathematical model used by McGuire was of the form:

$$\ln FS(T) = b_1 + b_2 M + b_3 \ln R + b_4 Y_s$$

where M is magnitude, R is epicentral distance, Y_s is a 0 or 1 indicating rock or soil, respectively, and the b's are coefficients dependent on the period T and determined by the regression analysis. McGuire deliberately limited the data sample by restricting the number of records from any one earthquake or any single site; he found this reduced possible biases in estimating the variance of the data. The resulting data sample contained earthquakes in the magnitude range from 4.5 to 7.7 and epicentral distances from about 5 to 220 km. McGuire further restricted his consideration to the horizontal components of motion.

McGuire studied in some detail the question of whether a statistical model with linear dependence on magnitude or one with quadratic dependence (as proposed by Trifunac) better represented the data. He found the simpler, linear model provides as good a fit to the Fourier spectral amplitudes as the quadratic model. McGuire further compared his proposed model with that of Trifunac for two events recorded near the source; the 1971 San Fernando earthquake recorded at Pacoima Dam and the 1940 El Centro earthquake record. The models were found to be nearly equivalent in their predictive capability for the two events; both predict somewhat lower than observed spectra at frequencies above about 10 Hz. Based on this, McGuire concluded that his model is adequate to estimate the Fourier spectral amplitude of acceleration recorded close to the rupture surface for intermediate-sized earthquakes (i.e., magnitude 6.5). As noted above, McGuire's model also appears to provide a more realistic presentation of the shift from higher to lower frequencies at greater distances. McGuire concludes that extrapolation beyond the data base to larger magnitudes and closer distances using his model is more reliable than extrapolation using the Trifunac model.

The most obvious criticism of the McGuire study would appear to be the limitations of the data sample and, as a consequence, the reliability of resulting estimates. McGuire has further limited a sample which is by its very nature limited. While he provided a reasonable justification for his selected approach, the consequences tend toward increased estimates of the data variance and a reduction of confidence in any single estimate based on the data.

Figures 2 and 3 show sample comparisons of the velocity spectra predicted by the Newmark, et al., Trifunac and McGuire models at epicentral distances of 5 and 30 km (again assuming zero focal depth) for sites on alluvium. It should be noted that while the Trifunac and McGuire predictions are for Fourier spectra of velocity, the Newmark, et al. predictions are for 0.5 percent response spectra with amplitude level arbitrarily normalized to the mean of the other two at a period of 1.0 second. However, it is well known that the undamped response spectrum is an upper bound to the Fourier spectrum and, moreover, numerous studies have shown that low damped (e.g., 0.5 percent) response spectra have the same average shape as the corresponding Fourier spectra over the period range in which there is significant energy in the seismic signal (i.e., probably for periods greater than about 0.2 seconds in this application). Therefore, it is reasonable to compare the shapes of the various spectral predictions shown in Figures 2 and 3. It can be seen from these figures that the Trifunac and McGuire estimates are remarkably consistent at these distances over the magnitude range from six to eight. However, the Newmark, et al. spectral estimates are in poor agreement with the other two. In particular, as has been noted by previous investigators, the Newmark, et al. spectra are significantly broader than the others. Moreover, the shape of the Newmark, et al. spectra is independent of magnitude and distance in disagreement with the findings of both Trifunac

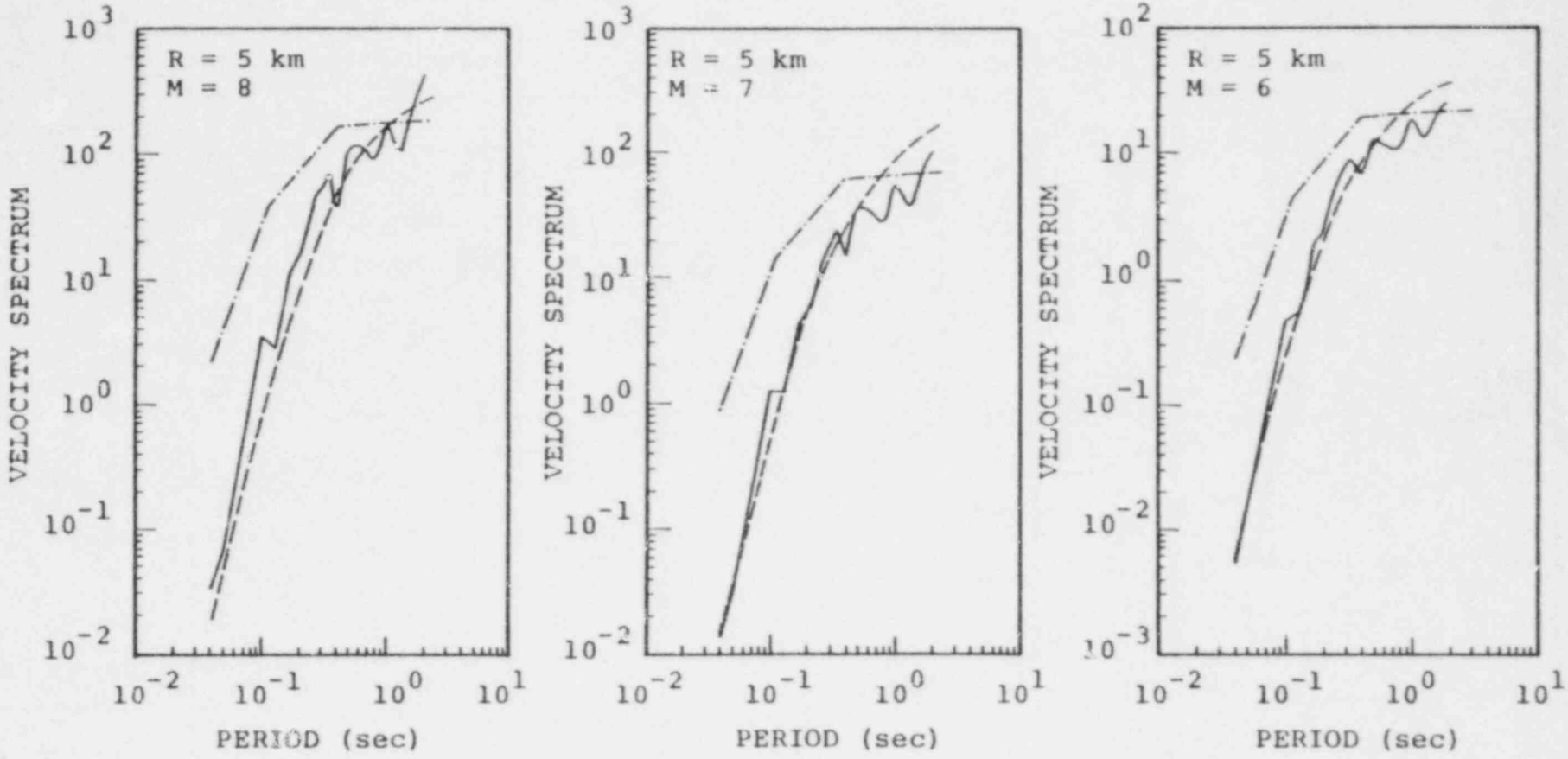

Figure 2. Estimates of spectra at an epicentral distance of k km for magnitudes 6, 7 and 8 from empirical relationships.

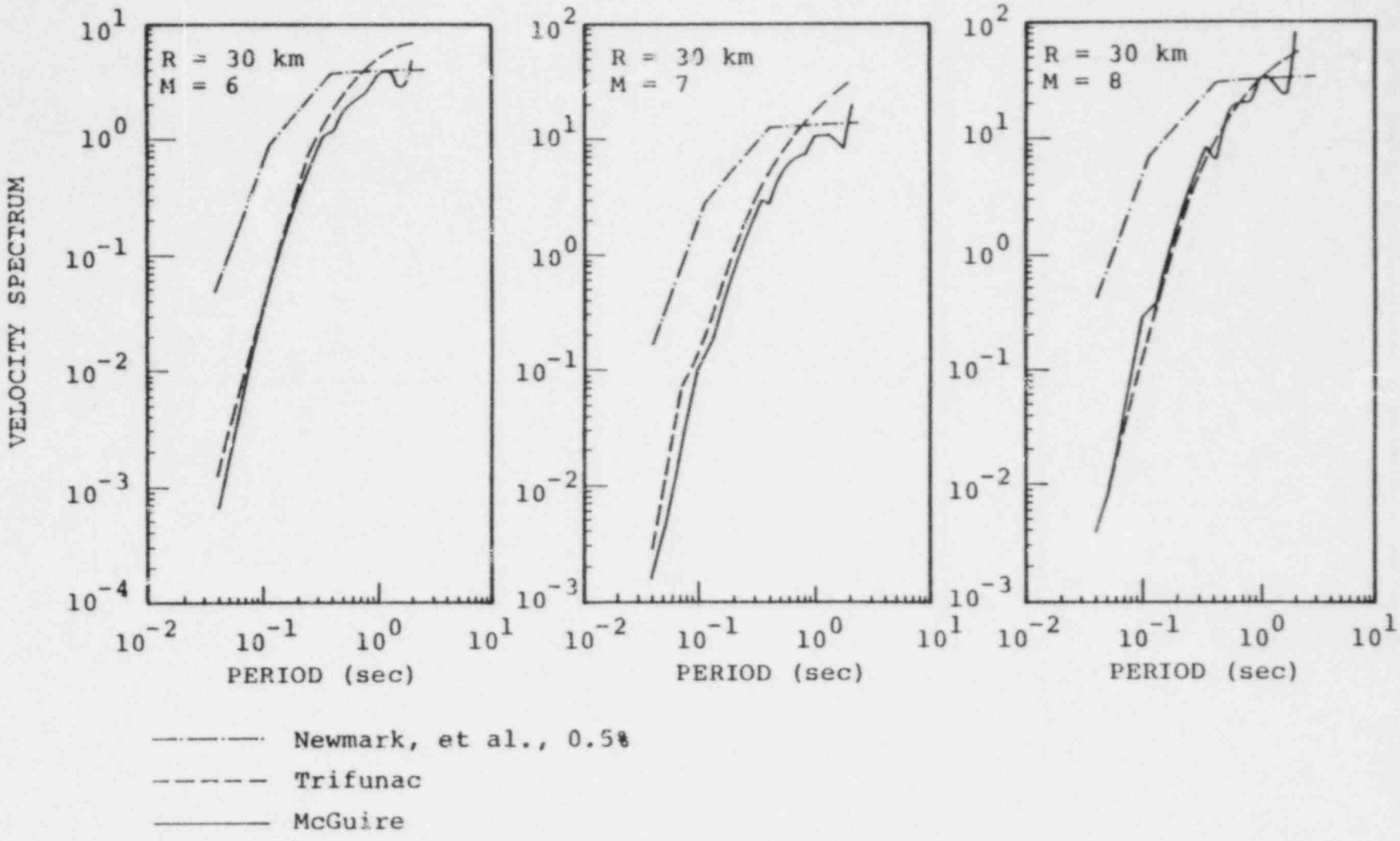

Figure 3. Estimates of spectra at an epicentral distance of 30 km for magnitudes 6, 7 and 8 from empirical relationships.

and McGuire. As with the peak motion estimates, there are not sufficient data available to quantitatively test any of these predictions at close epicentral distances. Therefore, it will be necessary to test the reasonableness of the various prediction schemes against simulations performed using theoretical models of the earthquake source.

2.4 TIME HISTORY PREDICTIONS

Attempts have also been made to develop empirically based procedures for predicting earthquake ground motion time histories. The different approaches which have typically been adopted in these investigations can be subdivided into two classes. In the first, no attempt is made to characterize the source or propagation path, but rather the objective is to generate ground motion time histories which satisfy some specific constraints. Thus, for example, much research has been directed toward defining functions of time which have response spectra that provide least upper bounds to the design response spectra established for particular sites. This approach was apparently first proposed by Housner (1947, 1955) who concluded that the extreme irregularity of recorded ground acceleration could be explained by large numbers of waves arriving at times determined by factors other than observed source and propagation properties. He proceeded to represent the ground motion as a series of sinusoidal acceleration wavelets occurring randomly in time. The amplitudes and periods of the wavelets were taken to be variable parameters which could be adjusted until the corresponding response spectrum matched a prespecified design response spectrum. More recently, more elaborate statistical models have been developed which employ white noise or filtered white noise in place of Housner's sinusoidal wavelets. For example, Bycroft (1960), Rosenblueth and Bustamente (1962), Crandall, et al. (1966), Brady (1966) and Brady and Husid (1966) have used white noise

to represent strong motion and used the results in studies of structural response. Housner and Jennings (1964) and other workers in this area have further refined the input by filtering the white noise and using that in their analyses of structural response to earthquake ground motion.

The most serious limitations of such models relate to the fact that there exists a multitude of time histories with grossly different characteristics which can satisfy such requirements. For example, Trifunac (1971) pointed out that the 1966 Parkfield earthquake was a relatively short duration, small magnitude event producing little damage, but it had comparable spectral amplitudes to the 1940 El Centro earthquake which had a longer duration, higher magnitude, and produced much damage. Moreover, they all rest on the assumption that an accurate design response spectrum can be specified for the site of interest and, as was noted above, it is not at all clear that such a capability exists for the near-field locations of interest in the present investigation.

The second class of empirical approaches for estimating ground motion time histories encompasses techniques which more truly represent predictions in that the source and propagation path are explicitly considered. This approach is typified by the work of Rascon and Cornell (1968) who modeled the earthquake as a series of elemental sources extended along a fault and computed the ground motion as a superposition of waves arriving from the individual sources according to a derived probability distribution which is dependent on the wave type and other empirical source and transmission properties. In testing their model they compared simulated ground motion time histories with actual strong motion records for the 1934 (M = 6.5, R = 64 km) and 1940 (M = 7.1, R = 11 km) El Centro earthquake records and the 1952 (M = 7.7, R = 43 km) Taft

record.* The response spectra computed for the simulated motions were found to be comparable to those for th real records. The chief weakness in the model was viewe to be that it only considered direct body waves. In addition, the model was again tested on only a very limited data sample. Finally, the model relies on empirically derived relationships such as those described in earlier sections of this report and their applicability to the prediction of near-field ground motion parameters has yet to be verified.

In summary, existing empirical procedures for predicting earthquake ground motion time histories rely heavily on empirical definitions of the peak amplitude and spectral characteristics of the expected motion. Thus, the applicability of such procedures to near-field sites is subject to all of the uncertainties associated with the specification of these other ground motion parameters.

2.5 EXAMPLES OF EMPIRICAL GROUND MOTION ESTIMATES IN THE NEAR-FIELD OF EARTHQUAKES FROM NUCLEAR POWER PLANT LICENSING EXPERIENCE

A number of nuclear power plant license applications have been considered for sites in the near-field of potential earthquake sources. In some of these, site-specific procedures have been employed which incorporate modifications and extensions of the general empirical procedures discussed above. In this section, some examples are presented with a brief synopsis of considerations which went into describing ground motion for these cases. The following examples are considered: San Onofre Nuclear Generating Station Units 2 and 3, San Joaquin Nuclear Project, and Humboldt Bay Power Plant Unit 3. Detailed descriptions of the procedures employed in these cases can be

*Magnitudes and distances here are those identified by the U. S. Geological Survey; Rascon and Cornell used somewhat different estimates of the distance for the two El Centro events.

found in the Preliminary Safety Analysis Reports, Final Safety Analysis Reports and Safety Evaluation Reports prepared for the individual sites. The following sections will highlight selected portions of these investigations which illustrate some different approaches to specifying near-field ground motion parameters.

2.5.1 San Onofre Nuclear Generating Station Units 2 and 3

One of the problems addressed in conjunction with this site study concerned the estimation of the ground motion characteristics to be expected due to the possible re-occurrence of a major earthquake on the Newport-Inglewood fault which was the source area for the magnitude 6.3 Long Beach earthquake of 1933. This involved estimating the response that San Onofre would have exhibited during the 1933 earthquake as well as for larger earthquakes that might occur on the same fault system. These estimates were obtained using a semi-analytical method which attempted to compensate for the frequency dependent attenuation with distance as well as local response differences between the San Onofre site and the locations at which the 1933 earthquake was actually recorded. In this approach, the ground motion spectrum, R, was represented functionally by the expression:

$$R = C\ Gs^{-1}\ f(M)\ \exp\left(\frac{-s\omega}{2Q\beta}\right)$$

where C = constant; G = site factor; f(M) = function of magnitude; s = distance; ω = frequency; Q = specific attenuation (assumed = 250); β = shear wave velocity (assumed = 3.2 km/sec).

The characteristics of the site response at San Onofre relative to sites which recorded the 1933 earthquake were determined by using the records obtained at San Onofre, Vernon, Long Beach and Subway Terminal during the 1968 Borrego Mountain earthquake. The ratios of site response for this earthquake at

San Onofre to that at other stations were computed from the spectra of the two records. Then using the above equation the response at San Onofre to the 1933 earthquake was estimated by adjusting spectra observed at Vernon, Long Beach and Subway Terminal during the 1933 event for the differences in site effects and frequency-dependent attenuation. For earthquakes larger than that of 1933, the spectra were considered to be directly proportional to rupture length based on the results of Aki (1967). Thus, for earthquakes with rupture length larger than the 30 km rupture length estimated for the 1933 earthquake, the spectra were assumed to increase by a factor equal to the ratio of the two rupture lengths.

2.5.2 San Joaquin Nuclear Project

In Amendment 2 of the Early Site Review Report, a near-field earthquake of magnitude 7 at a hypocentral distance from the site of 16.5 miles on the Pond-Poso Creek fault was postulated. To determine the design level of shaking associated with this event, the existing four records which were considered to best represent the overall characteristics of the design earthquakes were used. They were the 1940 El Centro record, the 1971 Holiday Inn record, the 1933 Vernon record and the 1952 Taft record. For the first three records the magnitude and source-site distances were very similar to those of the design event. Also, the travel path between the source and the station included a deep sedimentary valley and the local geologic conditions were comparable. The 1952 Taft record was selected because it was recorded in the general vicinity of the site.

A linear scaling was performed to adjust the representative records to the level of shaking of the design event. To do this, scaling factors were calculated using the attenuation relationships of acceleration as a function of magnitude and distance reported by Housner (1965), Schnabel and Seed (1973)

and Donovan (1973). The scaling factors were obtained by dividing the acceleration that corresponds to the magnitude and distance of the design event by the acceleration that corresponds to the magnitude and distance of the representative records. This procedure depends only on the shape and relative position of the attenuation curves and not their absolute levels. The representative records (two horizontal accelerogram components) were linearly scaled by the most conservative of the calculated scaling factors and their response spectra were computed. Regulatory Guide 1.60 design spectra were compared to the computed spectra and visually fitted to clearly envelope more than 84 percent of the data points in computed spectra. This procedure (Guzman and Jennings, 1976) led to Regulatory Guide spectra normalized to 0.35 g.

2.5.3 Humboldt Bay Power Plant Unit 3

As a result of the June 7, 1975 earthquake in the vicinity of the plant, the seismic ground motion was re-evaluated in the report titled "Ground Motion Analysis for the Humboldt Bay Nuclear Power Plant" by Tera Corp. (12/24/75). In this report, deeply buried faults under the site were postulated to be capable of producing a 6.1 magnitude event at a depth of 25 km. Based on scaling of the records obtained at the site on June 7, 1975, the characteristics of the postulated maximum earthquake were determined. In this case, the scaling was based on the assumptions that the amplitude of the motion attenuates as 1/r with distance and scales as $e^{0.8M}$ with magnitude. Therefore, scaling the 6/7/75 records (which are said to have recorded an average maximum acceleration of 0.18 g) from magnitude 5.5 to 6.1 and from 32 km to 25 km yielded an average maximum acceleration of 0.37 g for the design event. The estimated duration of shaking was 6 seconds.

2.6 CONCLUDING REMARKS

In the above discussion an attempt has been made to summarize and illustrate the various empirical prediction procedures which have been proposed for predicting the strong ground motion characteristics of earthquakes. It has been demonstrated that the applicability of these procedures to the near-field regime, which is of primary interest in the present investigation, is questionable. The principal reason for this uncertainty is that the existing near-field data base is not complete enough to adequately constrain the empirical scaling laws. Thus, empirical prediction procedures which are applicable outside the near-field regime, have been extrapolated into the near-field using either statistical or simplified physical arguments. Neither of these alternatives has proved to be completely satisfactory. Thus, as was illustrated in Figure 1, statistical extrapolations into the near-field are critically dependent on the assumed functional forms of the scaling laws and different, reasonable assumptions can lead to near-field ground motion estimates which vary by more than an order of magnitude. Moreover, attempts to base the extrapolation into the near-field on simple physical arguments concerning the nature of the source and propagation path frequently lack credibility, either because the justification is ambiguous or even, in some cases, at variance with the predictions of some detailed deterministic models of the earthquake source and propagation paths of interest. Thus, additional theoretical insight is required to provide a better understanding of how to perform this extrapolation in a quantitatively accurate fashion.

III. A REVIEW OF THE CHARACTERISTICS OF THEORETICAL EARTHQUAKE MODELS AND THEIR UTILITY FOR PREDICTING STRONG GROUND MOTION

3.1 INTRODUCTION

There is much interest in applying techniques for computing synthetic seismograms to supplement the use of empirical data for specification of design motion near earthquakes. Information obtained from such computations may be useful in cases where empirical results are of questionable value because of lack of data. Such cases include: (1) motion at close distances from an event (within 10 km), (2) motion near rather large events ($M_s > 7.5$), (3) cases where two- or three-dimensional propagation effects may be of importance. In the first two cases our strong motion data is rather sparse. In practice, intuitive input has been necessary to extrapolate data from other circumstances. In the third case, empirical studies have not been useful in quantifying such effects.

The purpose of this chapter is to review the various theoretical models of the earthquake source which might be used to synthesize near-field strong ground motion. Only recently have deterministic calculations of ground motion characteristics been considered as a means for establishing design criteria for engineering structures. Synthetic seismogram computations are widely used in seismology, but have been applied to compute high frequency (5 to 20 Hz) near-field (within 20 km of the source) ground motion on only a few occasions. Most applications involve analysis of recordings at frequencies much lower than are normally of interest for engineering applications. For example, synthetic seismograms are often used to study teleseismic (range greater than 1000 km) ground motion (frequencies of order 0.05 Hz). The objective of such studies is to infer moments and fault dimensions of events. Recently, techniques have been developed for analysis of short period teleseismic recordings (Somerville, et al.,

1976; Bache and Barker, 1978). These recordings offer information in part of the frequency range of engineering interest (about one hertz) and may be used to supplement information obtained from strong motion recordings.

Numerous authors have computed strong ground displacements for comparison to doubly integrated processed accelerograms. Synthetic ground velocities (Boore and Stierman, 1976) and accelerations (Kawasaki, 1975; Bouchon and Aki, 1977) are relatively sparse in current literature. Emphasis on modeling of strong ground displacements rather than velocities or accelerations has come about largely because of a lack of efficient computational tools needed for high frequency computations. Recent advances in this area have now made high frequency calculations more practical.

There are a few studies in which computations have been made to supplement or extend the empirical data base (Swanger and Boore, 1978b; Herrmann and Nuttli, 1975). These applications have been limited to special interest problems and the methods em· oyed are not sufficiently general to be used for constructing design motion for a wide frequency band, range of epicentral distances, or source sizes. Recently, algorithms have been proposed for a deterministic synthesis of design motion which may be applicable to a wide variety of problems of engineering interest (Wiggins, et al., 1978; Archuleta, et al., 1978). These methods require rather sophisticated computational techniques to adequately represent the physical processes of seismic sources and radiation of seismic energy through the earth. Both of these processes are quite complicated and not thoroughly understood. Computer simulation of such processes requires numerous assumptions to be made. Many of these assumptions are made on strictly intuitive grounds and have yet to be properly evaluated quantitatively.

Because of the large number of uncertainities in deterministically simulating the production and propagation of

seismic energy, the number of possible techniques which may be used for such a purpose is enormous. These techniques may vary in the degree of sophistication by which they represent the earthquake process or they may vary because they represent quite different assumptions about the physics.

In the following sections the various types of theoretical models of the earthquake source which could be used for deterministic simulation will be discussed in detail. Emphasis will be placed on the physical properties of the models and the properties of high frequency radiation produced by these models. The first section will be a brief summary of the physical processes generally thought to be important in the earthquake process. Next will be a brief summary of the general types of theoretical models used to approximate these physical processes. This will be followed by a detailed description of specific models which are separated into three general classes. These are:

1. analytical models which are constructed by specifying a displacement field on the fault (kinematic models),

2. analytical models which are based on an approximation of the consequences of some prescribed stress condition on the fault, or

3. numerical dynamic models which are formulated by specifying the initial conditions of the physical system and solving for the displacement field compatible with the physical equations governing the response of the medium.

3.2 THE PHYSICS OF EARTHQUAKES

Before discussing the various models of the earthquake source, it is useful to summarize the physical mechanisms which appear to be important in the process. It was first hypothesized early in this century (Reid, 1911) that the slip occurring during

an earthquake is due to the release of concentrations of tectonic stresses, and it is this assumption that motivates nearly all dynamical earthquake studies. It is assumed that the stresses are built up until a critical stress is reached. This critical stress is related to the strength of the materials or the cohesive stresses on a preexisted fracture zone (fault). Upon reaching this stress level, stress is released and shear fracture, which is usually assumed to be brittle, occurs. As the stress level is dropped at one place it is increased at nearby points, causing the fracture to propagate.

When fracture occurs, slip results. The stress level to which the initial stress drops is determined by the frictional stresses which oppose this slip. Often used to represent this process is a Coulomb friction model which has a static and a dynamic friction level. The critical stress of fracture is then the static frictional stress and the stress drop is the difference between the static and dynamic frictional stresses. One consequence of this model is that slip reversals will not occur except under extreme circumstances. In some cases one might envision slip to be frictionless, such as when heat generated by the initial sliding causes melting on the fracture surface (Richards, 1976). In recent years, more complicated models of the cohesive forces opposing slip have been developed. These models generally involve complicated coupling of the slip or slip velocity, frictional stress, and rupture velocity, and these relationships are generally known as fracture or rupture criteria.

The rate at which the edge of the fracture propagates cannot exceed the velocities of elastic wave propagation. It is sometimes assumed that the rupture velocity tends to be bounded by the seismic shear velocity, but most friction models indicate rupture velocity can approach the compressional velocity (Burridge, 1973). In general, one can expect the rupture velocity in the direction of the prestress to be

different from that perpendicular to the prestress. Of great concern in present research are the mechanisms which cause rupture to stop.

Of importance for high frequency radiation from earthquake is the possibility of spatial variations in prestress and material strengths. The presence of stress concentrations or local barriers to sliding may cause strong radiation of high frequency energy (Das and Aki, 1977), and it has been suggested that such effects may dominate in near fault accelerations.

The purpose of dynamic earthquake studies is to examine the physical consequences of the above processes and determine what slip histories and seismic radiation are compatible with these processes.

3.3 CLASSIFICATION OF THEORETICAL MODELS

Theoretical models can be conveniently separated into a few distinct classes. These classifications are motivated by what initial conditions of the earthquake source are assumed to be known and what procedures are used to obtain the quantities necessary to compute the seismic radiation. The major classes of models are:

1. Kinematic Models - These models assume that the entire slip and rupture history on the fault is known. The slip history on the fault is all that is required to compute the seismic radiation. The details of the slip history, which is important to the high frequency radiation, are sometimes included to satisfy some dynamic rupture constraint. Usually the details are motivated by a desire for mathematical simplicity.

2. Simple Dynamic Models - These models are analytic approximations describing some aspects of the stress release process. These models are normally used for interpretation of earthquake source parameters and for providing constraints on the characteristics of kinematic models.

3. Numerical Dynamic Models - These models assume that the initial stress conditions are known. The dynamic rupture process is then modeled to obtain a slip history which can be used to compute the resulting ground motion. These models, even in the simplest cases, require extensive computations.

Economic constraints suggest that a routine model for simulating near-field ground motions will probably be kinematic. Simple dynamic models are generally not detailed enough to be used and numerical models are probably too expensive to apply routinely. These solutions for the rupture process are very important for determining what kinds of specifications of slip and rupture histories are truly valid physically.

3.4 KINEMATIC SOURCE MODELS

3.4.1 Introduction

Most models of the earthquake source employed in the computation of synthetic seismograms are based on analytical approximations of the earthquake displacement field. Very few models actually claim to be a detailed representation of the earthquake process. Instead, analytical models are usually constructed to allow for generation of a radiation field which is intended to be comparable to certain features of the radiation field of earthquakes. Since we are interested in the

radiated energy as an end product, analytical models of earthquakes can be quite useful for synthetic seismogram computations, even if the models poorly describe physical processes on the fault surface. It would be better to have a model which can describe the actual dynamic nature of the earthquake source so we could be certain that the resulting motion due to such a model would be realistic. Unfortunately, we do not know what an earthquake is like in detail. Most of our information about the earthquake process comes from our observations of the seismic waves radiated from earthquakes. In some cases theory or controlled experiments (Archuleta and Brune, 1975) are of some help in constraining models, but, in general, models must be evaluated in terms of the properties of their radiated energy and via comparisons to observations.

Even though some knowledge of the gross mechanical properties of earthquakes existed as early as Reid (1911), mathematical descriptions of the earthquake source and its radiation of seismic energy did not appear until almost fifty years later. Theoretical difficulties in relating the conditions governing slip on the fault to the radiation of energy caused much of the delay. The work of de Hoop (1958), Maruyama (1963), and Burridge and Knopoff (1964) provided the necessary background in a usable form.

3.4.2 Haskell Model

One of the earliest and most widely used mathematical descriptions of an earthquake source is that due to Haskell (1964). Haskell applied his model to improve our understanding of the seismic spectrum and later (Haskell, 1969) to the generation of strong motion time histories. The original model has been widely used as a tool for interpreting strong ground

displacements and many of the more recent kinematic models differ only in subtle details.

The principle physical elements of the Haskell model are as follows:

1. Rectangular fault surface.

2. One-dimensional rupture propagation at a constant velocity across one of the primary fault dimensions.

3. Slip history after arrival of the rupture identical everywhere on the fault surface.

4. Slip history generally used is a ramp of constant duration everywhere on the fault.

Other kinematic models generally relax or alter these basic assumptions. A consequence of this simple description is that relatively few free parameters need be specified. Besides orientation parameters, those needed to describe the source are the two fault dimensions, direction of rupture propagation (usually chosen to be in the long dimension), rupture velocity, slip velocity, and slip duration (rise time). Other useful parameters which result from the necessary ones are fault slip (product of slip velocity and rise time) and seismic moment (product of fault slip, fault area, and the rigidity of the elastic medium).

The simple structure of this model allows for useful interpretations of the far-field* seismic spectrum and relatively easy computation of near-field motions in simple types of elastic media. Much of our understanding of the seismic spectrum has come from geometrical far-field studies of the consequences of this model (Haskell, 1964 and 1966; Aki, 1967). Most computations of synthetic strong ground motion have employed the original model or ones with slight deviations. In an elastic wholespace, calculation of the ground motion requires a double integration over the fault dimensions. Haskell (1964) first performed this integration numerically to produce displacement, velocity and acceleration time histories, though the last was beset with numerical instabilities. Wholespace calculations were made more efficient by the work of Boatwright and Boore (1975) and Sato (1975), who demonstrated that the integration in the direction of rupture can be performed analytically. Recently, the complete analytical solution has been obtained by Madariaga (1978) using the Cagniard-de Hoop method.

---

*The terms "far-field" and "near-field" are often used in different contexts for describing certain varieties of wave propagation phenomena. In order to clarify ambiguities which may arise in discussions to follow, the terms will be defined here. There are two types of simplifications in the characteristics of observed radiation which occur when the observer is far from the source. By "far-field" we mean that the distance from source to receiver is many times longer than the wavelengths of observed motion. This has nothing to do with source dimensions. By "near-field" we mean distances within a few wavelengths of the source. Mathematical descriptions of the radiated energy are considerably simpler in the far-field than in the near-field, even for point sources. Descriptions of the properties of motion observed from extended sources are simplified when the observer distance is large compared to the dimensions of the source. We will call this situation the "geometrical far-field." For example, when examining the characteristics of the accelerations recorded at Pacoima Dam from the San Fernando earthquake, we are considering far-field motion in the geometrical near-field.

Computations in more realistic earth structures are few. Anderson (1976) applied the model to computing synthetic displacements in an elastic halfspace by a two-dimensional integration of the halfspace Green's functions (point source responses). In the special case of a vertical fault, Israel and Vered (1977) showed that one spatial integration can be computed analytically within the framework of Cagniard's method for computing motion a halfspace. Similar simplifications can be applied to particular cases involving layered media calculations. In general, the simple form of the Haskell model allows for many computational simplifications in computing synthetic seismograms which are not available for more complex kinematic earthquake models.

The characteristics of the seismic radiation produced by a Haskell fault model are best illustrated by the analytical solution obtained by Madariaga (1978). Madariaga pointed out two distinct types of radiation fields produced. One consists of spherical waves that appear to be radiated from the four corners of the fault. These are due to the stopping and starting of the rupture. The high frequency character of the seismic ground motions is controlled by the character of the wave at its onset (first motion). Except between the planes $y = 0$ and $y = H$ (Figure 4), the first motion for a step displacement on the fault is a step in ground velocity. This implies that for the standard ramp displacement on the fault, the first motion acceleration will be a step with amplitude proportional to the slip velocity on the fault (Figure 5). This type of radiation is observed everywhere in the medium and is the only radiation seen for $y < 0$ and $y > H$.

In the region $0 \leq y \leq h$ (forming a cylinder of infinite radius) another type of radiation is present. These are cylindrically propagating waves associated with the one-dimensional nature of the rupture. Madariaga points out that this type of radiation is similar in nature to that generated by a propagating line dislocation (Boore and Zoback, 1974). This radiation

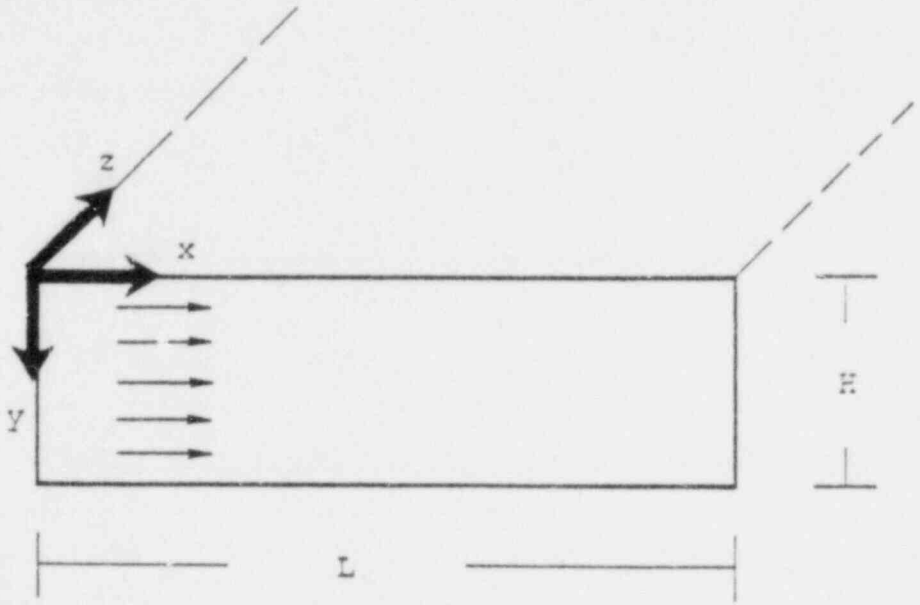

Figure 4. Geometry of a Haskell rectangular fault model. Propagation of slip is one-dimensional in the x-direction.

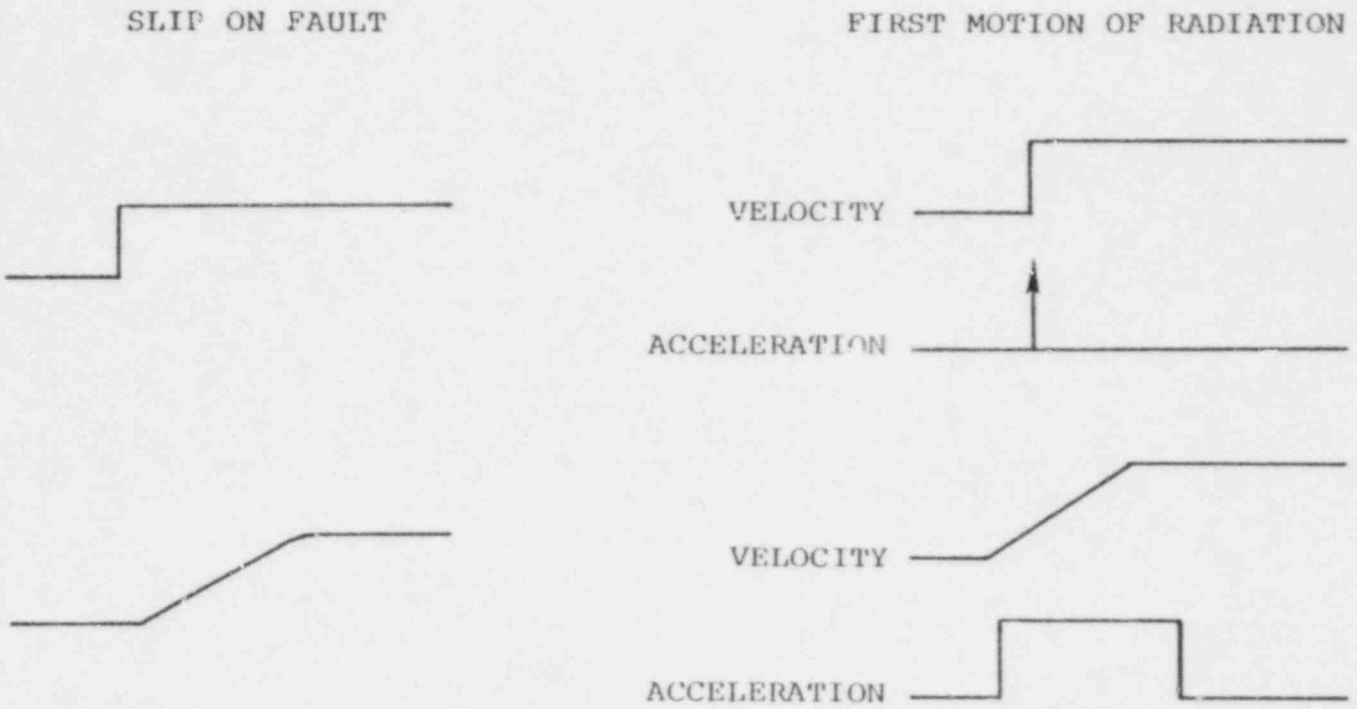

Figure 5. First motions of the spherical waves generated by a Haskell model for step and ramp slip histories.

has the characteristic that the first motion in velocity due to a step slip history contains a square root singularity. As a consequence, in the region $0 \leq y \leq H$ accelerations produced by even a ramp slip history will be infinite (Figure 6). Because of the singular nature of the radiation in this region, the high frequency character of the ground motion will be controlled by these waves, rather than by the spherical waves which are also present in this region.

The singular accelerations radiated from a Haskell fault model in certain geometries suggests that computations of accelerograms might produce numerical problems. Computations involving long, thin vertical faults (long dimension horizontal) may not present difficulties since likely observer positions will be outside the cylindrical region where accelerations are infinite. Calculations like those of Boore and Joyner (1978) may not be affected. Computations for obliquely dipping faults (like the 1971 San Fernando, California earthquake) may have inherent instabilities associated with time domain calculations. Such may be the cause of apparent instabilities in the calculations of Niazy (1975). Frequency band limited calculations, limited due to discretization or intrinsic attenuation in the medium, will, of course, produce finite accelerations. The time domain peak amplitudes are, however, bound to be artifacts of the computational method or attenuation of the medium rather than being due to some physical parameter associated with the rupture process. This particular characteristic of the model may make it undesirable for deterministic modeling of high frequency strong ground motion, even though it may be useful for wavelengths much larger than a fault width.

A difficulty commonly identified with the Haskell model is the possibility of strong focusing of energy due to the one-dimensional nature of the rupture. It is often hypothesized that a long fault with a rupture velocity very near the shear

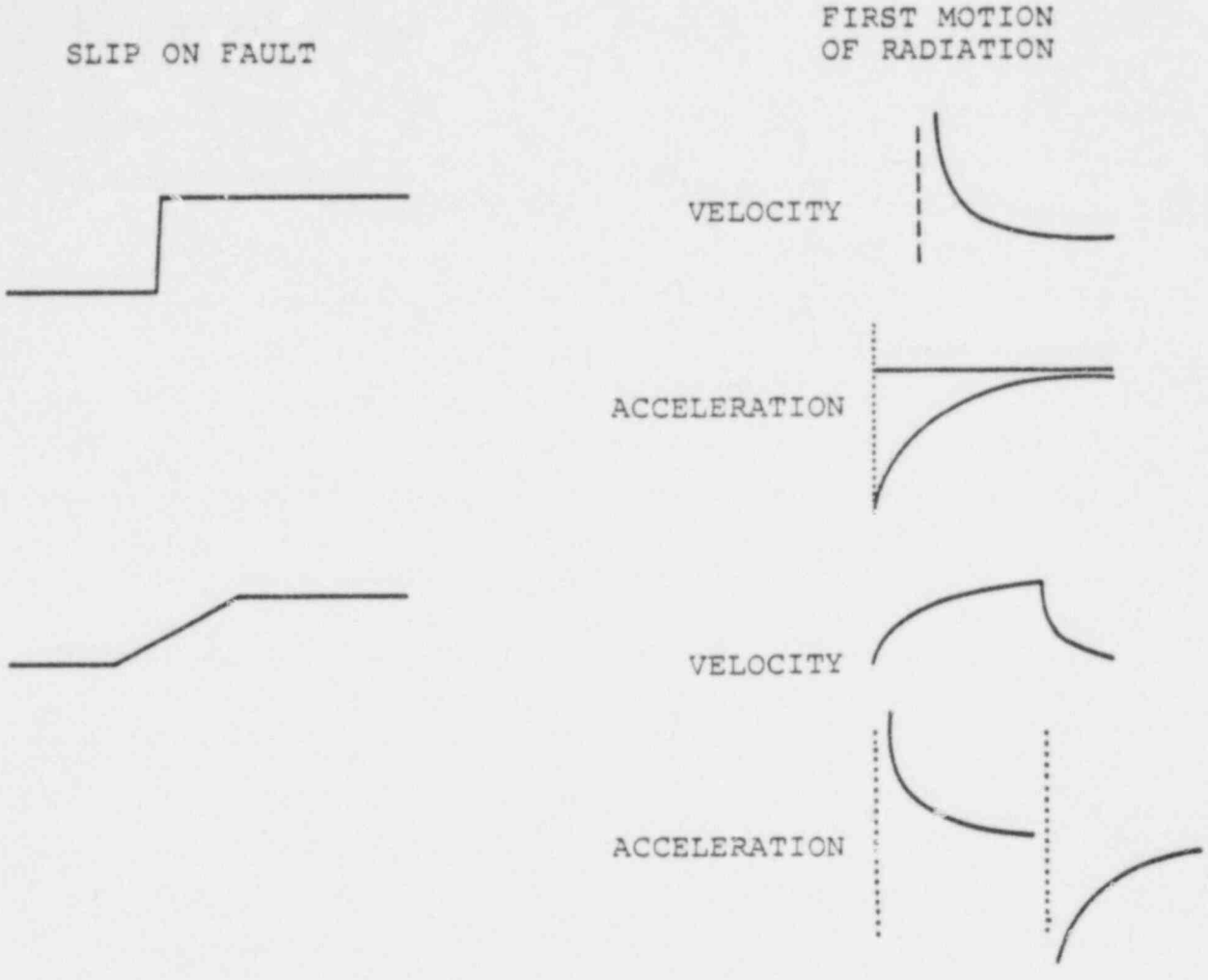

Figure 6. First motions of the cylindrical wave generated by a Haskell model in the region $0 \leq y \leq H$ for step and ramp slip histories.

wave velocity will "focus" high frequency energy toward an observer close to the fault surface. This may be a misleading concept. All of the singularities in the motion computed by Madariaga correspond to P or S wave arrivals from the starting and stopping of the rupture. This suggests that the source of high frequency motion is not due to the coherent part of the rupture, but rather to the sudden starting or stopping of coherent rupture. This supports the observation of Boore (1977) suggesting that the high frequency motion for a long, narrow Haskell fault is insensitive to the length, and that of Boore and Joyner (1976) that coherency in rupture should be viewed as a destructive interfering effect on the high frequencies rather than a focusing effect. The high frequencies are generated most efficiently by a sudden change in rupture state, i.e., stopping and starting.

Certain modifications to the original Haskell model can be made which may remove the potential for infinite accelerations. One possibility is employment of a source slip function with continuous first and second time derivations, such as that used by Israel and Kovach (1977). Such a solution provides the desired result, but does not find support in the physics of faulting. A more common approach is to have rupture propagate in two-dimensions rather than one. Such a procedure has been used by Heaton and Helmberger (1977) and Hartzell, et al., (1978). Madariaga (1978) suggests employing nonuniform slip on the fault, tending to zero at the lateral edges. Such changes are compatible with the physics of the problem. The consequences of such modifications of the high frequency characteristics of the radiated motion have not been fully explored.

3.4.3 Savage Model

Savage (1966) proposed a kinematic model of an earthquake which contains some desirable features not found in the

original Haskell model. This model consists of an elliptical fault surface on which rupture is assumed to initiate from one focus of the ellipse and spread radially outward until the edge is reached. Final slip on the fault may be a constant or may vary spatially, as does the static displacement field for constant stress drop on the fault surface. The source time history is generally considered to be constant, like the ramp function commonly used in Haskell models. Like the Haskell model, the Savage model possesses rather simple representations of the displacement field produced in the geometrical far field. For constant slip on the fault, the geometrical far-field displacement has an analytical form. One numerical integration is required for spatially varying slip.

The differences between the Savage model and the Haskell model (Table 1) include features that make the former more desirable for high-frequency, near-field computations. Initiation of rupture from a point and/or variation of slip over the fault surface probably keep near-field accelerations finite. No published computations of accelerations in the geometrical near field exist to date for this model, so consequences of the model in such cases are unclear at this time. Boore and Stierman (1974) have employed the model to compute strong ground velocities.

3.4.4 Variations on Savage and Haskell Models

Most kinematic models used in computations to date tend to differ from the original Haskell and Savage models by only a detail or two. Rather than summarizing each individual model separately, we will discuss these models according to their differences from the Haskell and Savage models. Exceptions are those models which are analytical approximations to some dynamical result which will be discussed later.

TABLE 1

COMPARISON OF HASKELL AND SAVAGE CHARACTERISTICS

	Haskell	Savage
Fault Surface	Rectangle	Ellipse
Rupture	One-Dimensional	Two-Dimensional
Fault Slip	Constant	Constant or varying at the static field for constant stress drop
Slip History	Constant Form	Constant Form
Free Parameters	Length	Semi-Major Axis
	Width	Semi-Minor Axis
	Rupture Velocity	Rupture Velocity
	Final Slip	Final Slip
	Rise Time	Rise Time
	Rupture Direction	Focus of Rupture Initiation
	Orientation Parameters	Orientation Parameters

A feature common to most recent kinematic descriptions is the initiation of rupture from a point within the rupture surface. This feature has been employed by Heaton and Helmberger (1977), Hartzell, et al. (1978), and Del Mar Technical Associates (DELTA) (1978) within the framework of a rectangular fault with constant slip. The possible consequences of this modification have been discussed above.

The form of the slip time history is the subject of numerous recent discussions. Within the framework of any model with a constant slip history on the fault, the frequency content of the radiation can be easily manipulated by varying the nature of the slip history. For such models the spectrum of the radiation is simply proportional to the spectrum of the slip history at a point on the fault. The ramp type slip function employed by Haskell (1969) was recognized as a low frequency approximation even though Brune (1970) showed that this form has some dynamical significance in the rupture process.

Ohnaka (1973) proposed a general form for the slip history based on physical arguments developed from an elastic rebound description (Reid, 1911) of a earthquake. This time history has the form of a ramp which smoothly approaches the final slip by an exponential damping of slip velocity.

A number of kinematic models proposed recently are motivated by the work of Kostrov (1964) and numerical results from dynamic earthquake simulations (Madariaga, 1976) which will be discussed in detail later. Kostrov showed the slip of a uniformly expanding circular shear crack under constant effective stress takes the form

$$D(r,t) = \dot{D}_0 \sqrt{t^2 - r^2/v^2} \text{ for } t > r/v \quad ,$$

where $\dot{D}_0$ is the slip velocity at the center of the crack (proportional to stress drop), r is the distance from the center, and v is the rupture velocity. At the center of the

crack the slip history is a ramp, but elsewhere the high frequencies are enhanced by a square-root singularity in velocity. Even though the slip function suggested by this physical model varies spatially on the fault, some features of the dynamic slip function have been employed in constant slip models.

Hartzell, et al. (1978) used the form

$$D(t) = D_0 \sqrt{1 - \left(\frac{(t-\tau_R)}{T} - 1\right)^2} \quad , \quad 0 \leq t - \tau_R < T \quad ,$$

$$= D_0 \quad , \qquad\qquad t - \tau_R > T \quad ,$$

where D_0 is the final slip, τ_R is the arrival time of the rupture front and T is a "rise time." This type of slip history has the same square-root singularity in velocity and high frequency asymptotic behavior as the dynamic solutions, but does not contain the spatial dependence of the slip suggested by the dynamics.

DELTA (1978) employed a slip history which includes the characteristic of dynamic solutions that the high frequencies are enhanced at the initiation of slip. It is argued that in an actual rupture process the stress must be bounded everywhere and this will cause initial slip velocity to be bounded. The value of the initial slip velocity will be related to the maximum shear stress the material can withstand. This maximum shear stress, which DELTA calls the "dynamic stress," is related to the initial slip velocity by an analytical formula obtained from studies of rupture dynamics. This initial velocity is applied over an arbitrarily short time span. The remainder of the slip is a ramp of smaller velocity chosen to obtain the desired final slip.

In all of the slip functions above (Figure 7), the high frequency content is controlled not only by the value of slip

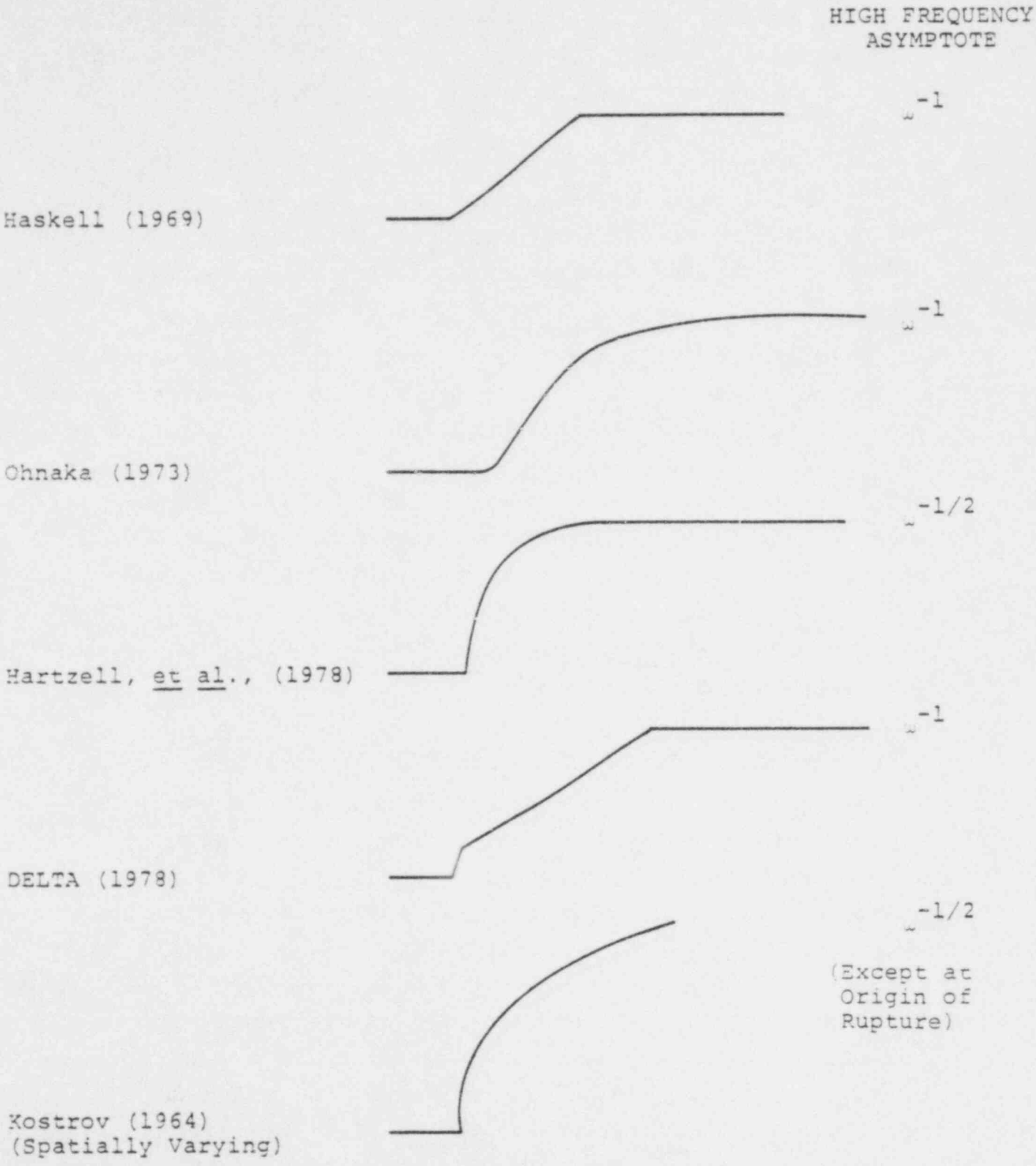

Figure 7. Proposed slip functions.

velocity chosen, but also by the characteristic times (rise times) chosen. This is particularly true with DELTA's model which contains two characteristic times. In practice, DELTA chose the initial rise time to be shorter than any of the periods of interest. This can cause the high frequency asymptote over the range of frequencies of interest to be flat. The double ramp time history allows more flexibility than most others, but it also requires specification of more free parameters.

Most kinematic models used to date have slip constant on the entire fault or constant over each of a small number of discrete fault segments (Trifunac and Udwadia, 1974; Boore, 1977). An exception mentioned earlier is the Savage model which has been used by Boore and Stierman (1974). Aki (1968) used the static displacement over the fault width in modeling strong ground displacements at Parkfield, California. The majority of the employments of nonconstant slip distributions are associated with analytic approximations to dynamic solutions for propagating shear cracks.

3.4.5 Analytic Approximations to Dynamic Solutions

Several kinematic models have been used recently which employ certain features of dynamic solutions for propagating shear cracks. One of the earliest models of this type is that of Brune (1970). Brune showed that for instantaneous rupture over a circular fault, the slip begins as a ramp with velocity proportional to effective stress. Using exponential damping to arrest the slip, Brune formulated simple descriptions of the far-field displacement time histories and spectra in terms of the fault dimension and stress drop. The model has been used extensively for interpretation of far-field characteristics of ground motion (Thatcher and Hanks, 1973, for example) but is generally not used for seismogram synthesis, largely due to the instantaneous rupture assumption.

Sato and Hirasawa (1973) used the Kostrov (1964) dynamic solution to approximate the far-field displacement field due to a circular crack. The analytical solution is used until the rupture reaches a prescribed radius. Slip was terminated simultaneously everywhere on the fault. The numerical results of Madariaga (1976) suggest that slip termination for a circular crack will be controlled by the inward propagation of shear and compressional waves from the fault boundary. Bouchon (1978) used the Kostrov analytic solution to prescribe slip until the arrival of the compressional waves radiated from the stopping of the rupture. Such effects are inferred from numerical studies. Such numerical results will later be discussed more thoroughly.

3.4.6 Specification of Free Parameters

Most kinematic models have similar free parameters which must be chosen in order to deterministically synthesize near field ground motion. Free parameters associated with nearly all models are the final slip, fault dimensions, rupture velocity and "rise time." Appropriate values for these parameters must be chosen by considering either comparable observations of such parameters or considerations of relevant rupture physics.

Generally, the size of a potential earthquake event of engineering interest is given in terms of a magnitude measure. Magnitude is normally defined as the logarithm of the amplitude measured on a particular instrument and is normalized to a particular distance. For the purposes of deterministic modeling of ground motion, one must relate the prescribed design magnitude to fault model parameters, such as fault dimensions and slip. Often, design magnitude is actually obtained from an estimate of potential fault dimensions. In such cases a compatible slip must be obtained. Past measurements of gross fault parameters and their relationship to magnitude can be used. Attempts to construct empirical scaling relationships have been

made (Aki, 1966; Kanamori and Anderson, 1975; Geller, 1976). Given present data, the uncertainties in such empirical formulas are quite large. Uncertainties in the measured quantities used are also rather large. At best, empirical results can provide bounds for specification of such parameters.

Given the fault dimensions, another approach is to choose a slip which is compatible with some prescribed static stress drop. The expressions of Keilis-Borok (1959) are often used. Kinematic models with constant slip on the fault actually have infinite average stress drop (Madariaga, 1978). The value of slip which is obtained from stress drop formulas is the average slip on a fault in static equilibrium for a given static stress drop. Choice of an appropriate static stress drop is also plagued by order of magnitude scatter in observed values. This can be crucial in computing motions since, for most models, computed motions will be proportional to the stress drop chosen when other parameters are chosen independently.

Values chosen for rupture velocity can have a strong influence on computed ground motion (Boore, 1977). Theoretical studies of expanding shear cracks suggest rupture velocities may exceed the seismic shear velocity for frictional sliding with cohesion (Burridge, 1973). Without cohesion, values may be as large as the compressional velocity (Burridge and Levy, 1974). Measured rupture velocities (as summarized in Geller, 1976) show a wide range of values. Closer examination of these measurements suggest that in most cases the values are poorly resolved. Even for the most widely studied individual events, contradictions in measured values exist. For the 1966 Parkfield, California event "measured" values are 2.2 to 2.3 km/sec (Eaton, 1967; Filson and McEvilly, 1967; Aki, 1968), 2.4 to 2.5 km/sec (Trifunac and Udwadia, 1974), 1974), and 2.8 to 3.0 km/sec (Anderson, 1974). Recent work

by Archuleta and Day (1979) presents satisfactory fits to near-field displacements assuming a rupture velocity of 3.1 km/sec.

The characteristic time of slip of the fault must also be chosen for synthesis. Generally, physical arguments relating arrest of slip to rupture propagation and fault dimensions are used to determine appropriate rise times. It is usually assumed that the narrow fault dimension will control the time of slip. The discussion of Savage (1972) is particularly useful for this choice. Choice of rise time can also strongly influence computed motion. For ramp type slip histories and a prescribed final slip, far-field motions can increase significantly as rise time is shortened, particularly for periods comparable or shorter than the rise time.

Often the effects of chosen source parameters on computed ground motion are rather complicated. This is particularly the case for variations in rupture velocity when the radiation is propagated through layered earth models (Boore, 1977; Swanger and Boore, 1978a). A variation in a particular parameter can cause different effects within the framework of a different kinematic model. In the geometrical far-field the tradeoffs can usually be resolved, but in strong motion studies many remain unresolved. Sensitivities to such parameters must be examined on a case by case basis.

3.4.7 Kinematic Models and High Frequency Observations

The large majority of applications of kinematic source models to synthetic seismogram computations for comparison to strong ground observations have involved displacements rather than accelerations. Such comparisons tell very little about the performance of these models at frequencies higher than one hertz. At displacement frequencies very little information is available which can be used to differentiate one model from

another. Anderson and Richards (1975) compared the displacement motion characteristics in the near field from a number of kinematic source models including a Haskell model, Savage model and a simple crack approximation. They concluded that the differences in the models reflected by near-field displacements are so subtle that they could not be resolved from comparisons to observations.

Boore and Stierman (1976) used a Savage model with variable slip to compute ground velocity for comparisons to recorded motion from the Point Mugu, California, earthquake. Their calculations included a geometrical far-field approximation. Good fits to the data were obtained, yet a few of the source parameters could not be resolved given the limited observations available for that event. Since the comparisons could not resolve gross fault parameters, they can not justifiably be used as support for the model.

Kawasaki (1975) used a Haskell type model to compute accelerations for comparison to the largest motions at Parkfield, Station No. 2. The fault model parameters used were not chosen to model the entire rupture surface, but only a small section in the vicinity of the observer.

The most extensive computations of high frequency motion employing a kinematic source model is that of DELTA (1978). Their model consisted of a rectangular fault surface with rupture initiating from a corner of the fault and extending in two-dimensions. The slip time histories are assumed to be constant on the fault and had the double ramped form described earlier. Computations of synthetics were made for comparison to the observed motion near three California earthquakes. Comparisons of smoothed response spectra were made instead of a time domain waveform comparison.

There are a few details in DELTA's model which make it difficult to evaluate in the context of other kinematic models. Integration over the fault surface was performed using a rather

coarse grid spacing (1 by 1-3 km) making the rupture slightly incoherent for the range of frequencies of interest employing the methods used by DELTA. Additional incoherence in rupture was added artificially by randomly altering the times of rupture arrival at the grid corners. The effect of such incoherence on high frequency motion can be severe (Boore and Joyner, 1978). Concerning high frequency radiation, it might be more appropriate to view DELTA's model as stochastic rather than deterministic. Sensitivities to the probabilistic parameters involved in this case are unknown.

3.4.8 Summary

Kinematic models of the earthquake source are those which prescribe the entire slip and rupture history. Studies employing such models for synthesis of high frequency motions which can support a preference for a particular kinematic model are nonexistence. Since many of the models employed to date were not constructed for such purposes, this is not surprising. More realistic high frequency radiation may be obtained from kinematic models by introducing refinements suggested by dynamic model calculations (discussed in the next section). This can only be evaluated by future computations which clarify the characteristics of high frequency radiation for such source models and by careful consideration of the relevance of the dynamic approximations. Further work is also necessary to constrain the values of free parameters used in applications of kinematic models.

3.5 SIMPLE DYNAMIC SOURCE MODELS

3.5.1 Introduction

The problem of interest in this study is the computation of high-frequency (1-20 Hz) characteristics of ground motion near an earthquake. At these frequencies there is little evidence suggesting that simple kinematic models like those described in the previous section are adequate for predicting ground motion in a deterministic manner. The details of the particular earthquake model used can influence the characteristics of the motion produced to the extent that the uncertainties involved may be larger than those that can be tolerated in design applications.

A major difficulty in choosing an appropriate model is that our data set of recordings near earthquakes is much too sparse for determining the slip history present on a fault. Far-field data are much more plentiful, but it can be shown (Kostrov, 1968) that the slip history cannot be uniquely determined from far-field observations alone. Far-field data can be used to find the best representation of an earthquake source within the framework of a pre-chosen model, but there is no guarantee that such a model is appropriate for near-field studies.

Observations alone appear to be insufficient for determining an appropriate earthquake model for near-field studies, but some constraints may be found by careful consideration of the physics of the earthquake source. Viewing the earthquake as a dynamic process driven by changes in the local stress field can lead to conclusions about how many of the free parameters needed to describe the earthquake slip history can be constrained on physical grounds. Our knowledge of earthquake dynamics is still rather primitive, but studies to date do provide some useful information about the nature of slip on the fault under realistic conditions.

In this section we will summarize some of the findings of analytical studies of the earthquake rupture process and mechanisms of stress release and crack propagation in an elastic medium. We shall examine the results of relatively simple problems performed which have given insight into the nature of dynamic earthquake processes. Some of these results have been incorporated in kinematic models of earthquakes and were mentioned briefly in the previous section. Here we will examine these findings in terms of their relevance for simulating high-frequency strong ground motion.

3.5.2 Self-Similar Solutions for Crack Problems

One of the more important problems in earthquake dynamics was first solved by Kostrov (1964). He examined the motion of a uniformly expanding circular shear crack in an infinite homogeneous medium under constant stress drop. This solution is very important to the understanding of the characteristics of the slip on an earthquake fault during and just after initiation of the rupture. The characteristics of this solution have been used to specify the form of the slip function for kinematic models as was described in Section 3.4.4.

Suppose we have a uniformly expanding planar circular shear crack in an infinite homogeneous medium whose edge is moving outward from the center at a velocity v. Everywhere on the crack the shear stress is forced to be constant at a level σ_o below the initial stress level. Kostrov solved for the distribution of slip with time on the crack surface. The solution takes the form

$$u(x,t) = A\sigma_o \sqrt{v^2t^2 - x^2}, \qquad x < vt,$$

$$0, \qquad x > vt,$$

where u is the slip in the direction of the tractions associated with the initial shear stress and A is a constant dependent on the material elastic constants and rupture velocity v (Dahlen, 1974). There are a number of important features to this solution:

1. The solution is "self-similar." At any given instant of time, the basic shape of the spatial slip distribution is the same (Figure 8). In this particular case the slip distribution is identical to the static slip distribution except for a scaling constant.

2. The slip function at the center of the crack is a simple ramp. Away from the center of the crack, slip velocity becomes singular as the rupture front passes through. In general, the high frequency content of the slip function increases as one moves away from the center of the crack.

3. Stress is singular just ahead of the crack edge.

Kostrov noted that the initial assumption that the crack should expand circularly is actually a restrictive one. In general, it was shown that if the energy needed to advance the crack tip is the same everywhere on the edge of the crack, then rupture velocity is likely to vary with azimuth relative to the direction of the initial prestress.

Kostrov's results were extended by Burridge and Wills (1969) to an expanding elliptical fault surface on which the rupture velocity in the direction of the prestress and that in the perpendicular direction are different. Their solution contains essentially the same features as the circular crack problem. In this case, the slip of the fault surface takes the form

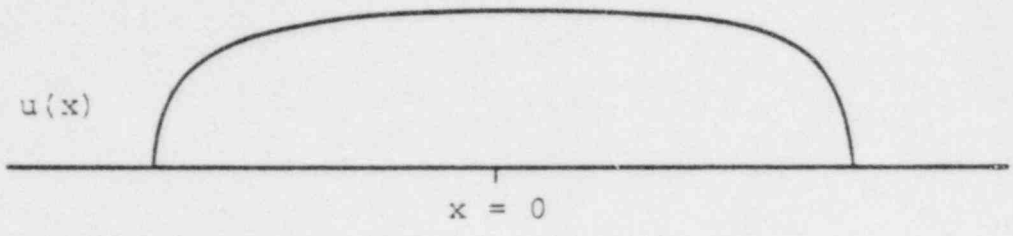

(a)

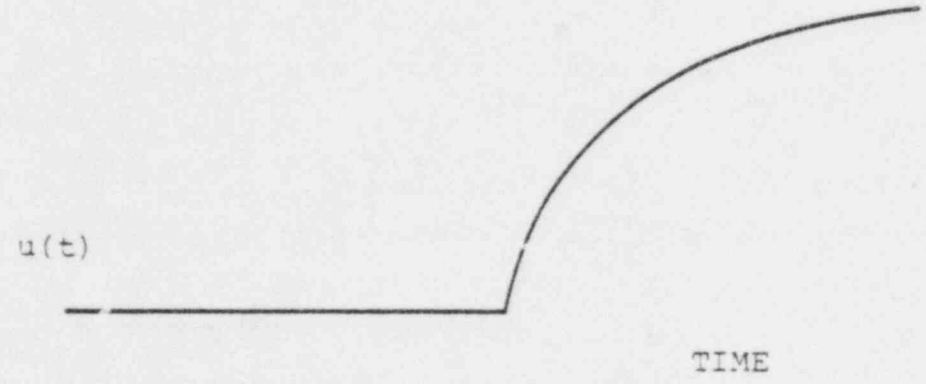

(b)

Figure 8. (a) Self-similar displacement of fault.
(b) Kostrov slip function.

$$u(x,y,t) = A \sqrt{t^2 - \frac{x^2}{v_x^2} - \frac{y^2}{v_y^2}} \quad ,$$

$$t > \sqrt{\frac{x^2}{v_x^2} + \frac{y^2}{v_y^2}} \quad ,$$

where v_x, v_y are the rupture velocities in the x and y direction. This solution also has the self-similarity properties of the circular case. The slip of the crack at any instant of time resembles the static displacement field on an elliptical crack with constant applied stress. It should be emphasized that the self-similar features of Kostrov's and Burridge and Willis's solutions will apply only for uniformly expanding cracks. In cases where the prestress varies spatially or the rupture velocity changes, self-similarity will be destroyed.

Richards (1973, 1976) examined the properties of the uniformly expanding elliptical crack in detail. It is shown that in order to keep the tractions finite in front of the rupture front in the direction of the prestress, the rupture velocity in that direction must be equal to the Rayleigh velocity of the medium. For the direction perpendicular to the prestress, the rupture velocity should approach the shear velocity. This choice of rupture velocities causes the stress ahead of the crack to be finite in those two directions, but still causes singular values at intermediate angles. There is no choice of the two rupture velocities which will cause stress to be bounded everywhere on the crack edge.

The self-similar solutions for the slip on the fault have been applied to the computation of earthquake ground

motion. Richards (1976) used the Kostrov solution directly and computed particle accelerations and stresses at the surface of an infinitely expanding crack. Others have chosen to make some assumption about the stopping of the rupture. Sato and Hirasawa (1973) and Bouchon (1978) assumed the rupture front stops abruptly and slip everywhere on the fault arrests at the same time. One consequence of this assumption is that most of the high frequency radiation results from the stopping process.

Even though Kostrov's solution and its extensions have been very important additions to our understanding of crack propagation, it has yet to be shown just how relevant they are when applied to earthquake ground motion problems. One problem is that the solutions imply singular stresses and particle velocities at the edge of the expanding rupture surface while we know that stresses are bounded by the strength of earth materials. This may not be too serious since solutions with mathematical singularities are often useful for physical problems in which only a finite frequency range is of interest. Rupture propagation is not a process where we would expect materials to exhibit linearly elastic behavior and it is still not clear how these results will change in the frequency range of interest when physical bounds are included in the problem.

Another difficulty with these solutions is the assumption of uniformly expanding rupture. We know that earthquake ruptures must stop. What we do not know is how they stop. This is very important when one considers the high frequency radiation from such sources. The results of Sato and Hirasawa (1973) suggest that the stopping of circular cracks can control the high frequency motions if the rupture is stopped instantaneously across the fault. The nature of high frequency radiation would probably be much different if rupture is allowed to decelerate slowly.

3.5.3 The Brune Model

The model of Brune (1970) is not a rigorous solution to a dynamic faulting problem as the above mentioned models, but is worth discussion since the majority of the measurements of stress drop on faults, which drives the dynamic processes, have been made under the assumption of the Brune model. His solution gives an approximation to the radiation field of an instantaneously forming circular crack having constant applied stress.

Brune recognized by use of physical arguments that the slip of a fault where a shear stress is applied instantaneously everywhere must initiate in the form of a ramp with particle velocity proportional to the applied stress, sometimes called effective stress. As in the propagating crack problems, effective stress can be viewed as the difference between the prestress and the frictional stress on the fault surface. To include fault finiteness, Brune assumed the particle velocity at the center of the fault should decrease and approach zero on a time scale comparable to the travel time of shear waves across the fault surface. He chose a exponential damper for velocity with e-fold decrease occurring after this characteristic time. For this simple model one can obtain effective stress from quantities usually measured from seismic radiation, namely seismic moment and corner frequencies.

Since the majority of our measurements of stress drop have come from the Brune model, it is important to understand how these values are related to the effective stress associated with other models. The most important quantity to be examined is the corner frequency associated with the seismic radiation. The corner frequency is the frequency of transition of the seismic displacement spectrum from the flat shape at low frequencies to the asymptotic decay at high frequencies. The location of the corner frequency is a function of some characteristic dimension in the source. This relationship is

crucial in stress drop estimation since for a given seismic moment, the inferred stress drop is inversely proportional to the third power of the characteristic dimension. In other words, a factor of two error in characteristic dimension causes a factor of eight difference in inferred effective stress. There has been great debate within the seismological community over what observed corner frequencies are and how they are related to the characteristic dimensions of the source (Molnar, et al., 1973; Savage, 1974; Dahlen, 1974; Madariaga, 1976).

Madariaga (1976) compared the corner frequencies assumed by Brune with those produced by propagating circular shear cracks. Brune assumed an azimuth independent relationship between corner frequency and fault radius. Madariaga showed that this average value may be in error at certain angles off the fault plane by 50 percent for the instantaneous forming shear crack and, possibly, by as much as 100 percent for subsonic ruptures (Figure 9). This implies that effective stress inferred by the Brune model may differ from that inferred from suddenly stopping circular crack models by as much as a factor of eight. Brune, et al. (1979) suggest that the differences in corner frequencies noted by Madariaga may only be due to differences in the way corner frequencies are determined from spectral data. In any case, the numerous discussions of what the corner frequency characteristics of earthquakes are and what they mean in terms of earthquake parameters are still rather confusing. Since most of our measurements of effective stress come from corner frequency measurements, there is still much uncertainty as to what values of effective stress are appropriate for earthquakes.

3.5.4 Volumetric Stress Relaxation Models

Most models of the dynamic earthquake process have assumed a mode of stress release on a planar fault boundary.

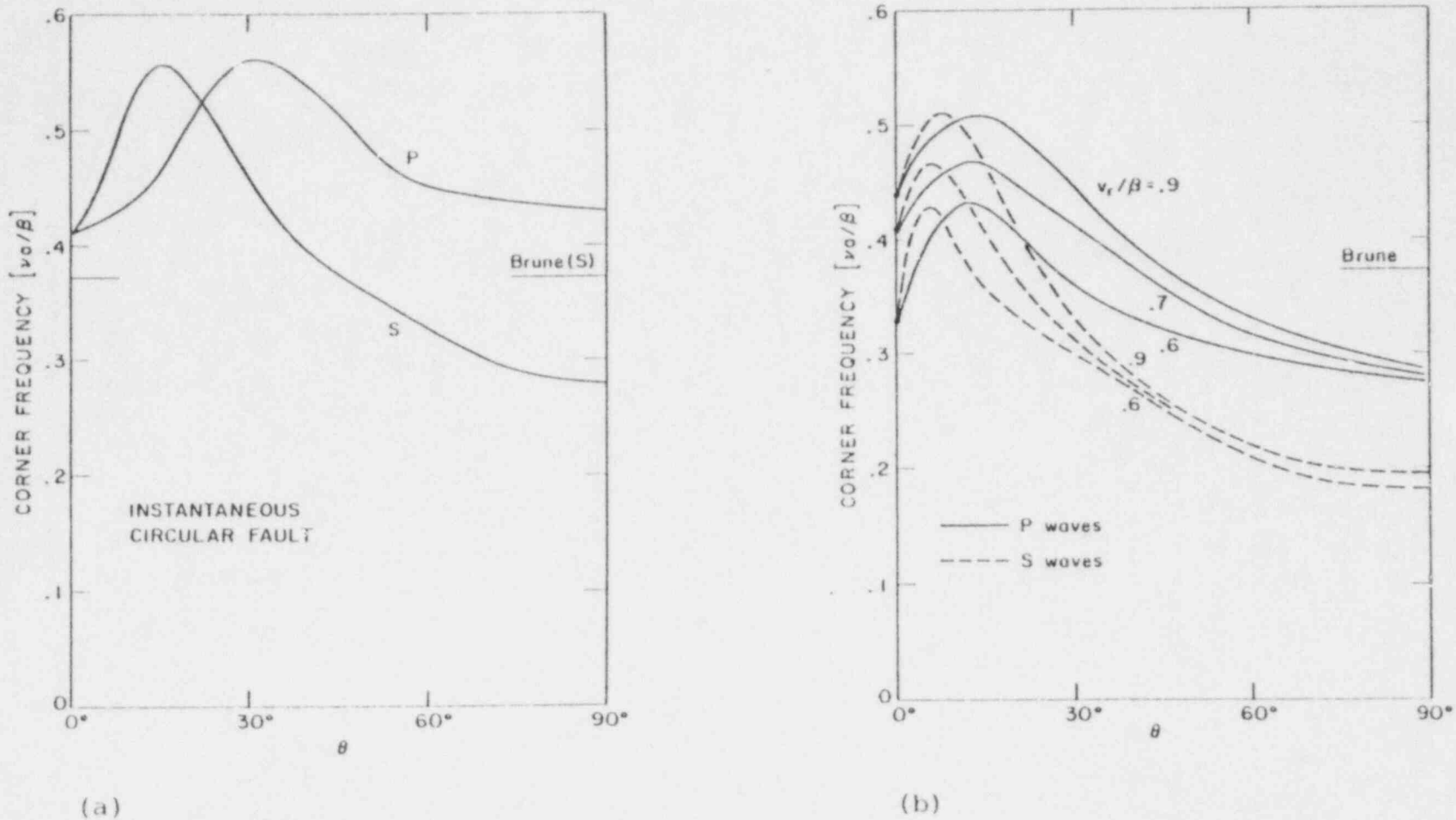

Figure 9. (a) Variation of corner frequencies as a function of azimuth for the instantaneous circular fault. Brune's approximation is included for comparison. (b) Variation of P and S corner frequencies as a function of azimuth for three values of the rupture velocity. (From Madariaga, 1976).

Archambeau (1968) and Minster (1973) have examined the consequences of stress relaxation in volumetric failure region. This view of the process might be useful if material failure in addition to shear fracture (e.g., melting) occurs in the source region.

In order to compute with the Archambeau/Minster model, several approximations are made. The only geometry for which the solution has been obtained is for stress release due to creation of a spherical value of weakened material. The spherical source region may expand or translate (Figure 10), but the zone of instantaneous stress relaxation remains spherical. The spherical nature of the source allows for many mathematical simplicities and may be useful for consideration of ground motion in the geometrical far-field, but it is not desirable for near-field studies.

Another important approximation employed in applications of the model is the transparency approximation. The stress changes in the earthquake process are caused by material failure which alters the elastic continuum. The transparency approximation models the stress release by applying fictitious body forces necessary to give a desired stress state at prescribed locations and times without altering the continuum. This ignores the possibility of the stress release at one part of the source influencing the stresses of another. It is not clear to what extent this approximation affects the seismic radiation, but it has been shown to give reasonable results in far-field and geometrical far-field studies (Bache and Barker, 1978; Bache, et al., 1979). Since the approximation ignores the buildup of stress concentrations associated with rupture, it probably is not useful in studies of high frequency ground motion where such details may be important.

Volumetric models have proven quite useful in the interpretation of seismic recordings in the geometrical

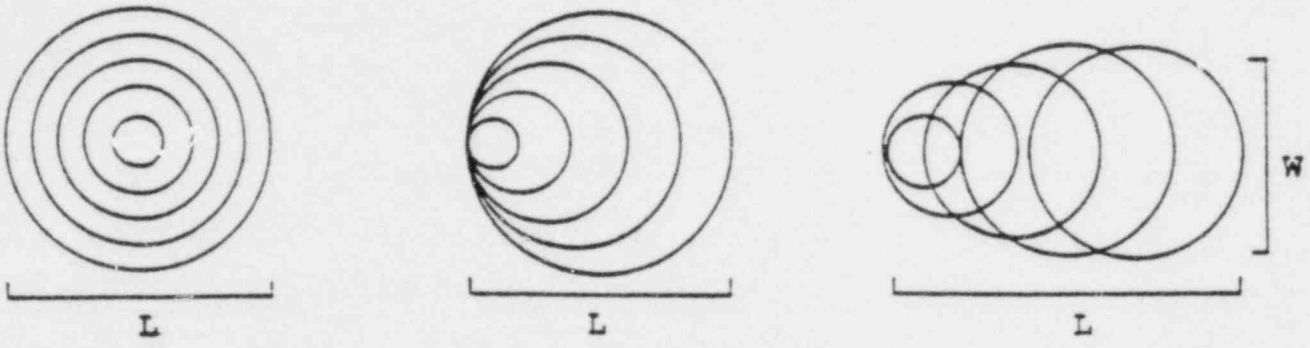

Figure 10. Three geometries for the Archambeau/Minster source model.

far-field (Bache and Barker, 1978), but these models as applied thus far do not appear to be very useful for near-field studies of high frequency motion. Both the unrealistic geometry and the transparency approximation are probably inappropriate for studies in the geometrical near-field.

3.5.5 Summary

In the previous section, we discussed the characteristics and limitations of kinematic models of the earthquake source. These models have been used extensively in interpretation of seismic signals, but there is little evidence that kinematic models in their present form are adequate at describing the high frequency radiation from seismic sources. In order to gain understanding as to how these models may be lacking in realistic earthquake features, it is important to examine the mechanical processes which cause the earthquake to occur.

Here we have reviewed some simple models of the dynamic rupture process and mode of stress relaxation which may be appropriate to the earthquake source. These models have been used extensively for interpretation of earthquake mechanism and features of these models have been added to kinematic models.

Kostrov's solution for the slip on a uniformly expanding crack under constant stress drop may be a very good approximation for the earthquake process at the initiation of rupture. This solution indicates that the slip time history should vary on the fault and in a manner such that the high frequencies are enhanced as rupture propagates outward from the initiation point. Except at the center of the fault; slip velocity is singular as the rupture front passes through. The solution generally has singular stresses at the rupture edge. This is certainly unphysical but may be a reasonable approximation for the seismic frequencies of interest here. The most

serious limitation in such crack propagation models is the stopping of the rupture. It has been shown that the bulk of the radiated high frequency energy comes from the stopping of the rupture if the rupture is terminated abruptly. It may well be that the nature of the high frequency radiation may be controlled by the manner by which earthquake ruptures stop, and these simple dynamic models tell us nothing about this process.

The Brune model has not been used for seismic synthesis, but has been important in the measurement of stress drop on faults. The level of effective stress in earthquakes is important to deterministic modeling since the level of high frequency motion will scale with this parameter. Most estimates of stress drops associated with the rupture process have come from a Brune model interpretation. Comparison of the Brune estimates of stress and those of other dynamic interpretations suggests that there may be large uncertainties as to what effective stresses are associated with the earthquake rupture process.

The contributions of fault dynamics to models of earthquakes used for seismic synthesis has to date been limited to considerations discussed here. Current research of the dynamic rupture process is involved with examining some of the uncertainties in these simple dynamic models.

3.6 NUMERICAL MODELS OF THE EARTHQUAKE SOURCE

3.6.1 Introduction

Earthquake source studies of the present decade have concentrated on understanding the mechanical processes of stress relaxation on earthquake faults and the consequences of such processes on the slip history on the fault. Relatively simple analytical models of stress relaxation, such as the Kostrov (1964) solution and the Brune (1970) model have been used extensively in earthquake source interpretation, but these models contain features which are unrealistic as elements of earthquake faulting processes. More sophisticated models of stress relaxation have to date defied analytical solution and most require extensive computations to implement.

Numerical models of stress release employing finite difference or finite element techniques are currently under study. Here we will review the results of this area of earthquake source studies. The present state of this research effort is at a point where we have a fair idea of the consequences of many types of initial conditions in prestress and material properties. What we do not know at this time is which of these conditions are most likely to be associated with real earthquake processes.

3.6.2 Constant Stress Release in Linear Elastic Materials with Prescribed Rupture Conditions

The most common numerical model of the earthquake process assumes the release of constant effective stress on a prescribed rupture surface with constant rupture velocity. In a simple geometry this problem was solved analytically by Kostrov (1964), except that Kostrov's solution does not include any stopping of the rupture, which appears to be important in the radiation of seismic energy. The analytic solutions indicate that models with constant effective stress and

constant rupture velocity are unphysical because of infinite stresses which form at the propagating crack tip. However, characteristics of the radiated energy produced by such models may be acceptable in the frequency range of engineering and seismological interest. The numerical solutions to this problem do not contain infinite stresses as part of the solution because the calculated stress is smoothed by the discrete grid approximation to the continuum. These solutions can thus be considered to be low-pass filtered solutions to the initial problem.

One of the earliest calculations of this type is that of Madariaga (1976). He examined the sudden stopping of the rupture on a circular boundary. This solution is identical to that of Kostrov (1964) until the time the rupture front reaches the boundary (Figure 11). When the rupture is terminated, waves radiate inward which slows the internal slippage. In nearly all frictional sliding models, the slip is not permitted to reverse, and slip is terminated when the slip velocity tries to change sign. In the circular case, this appears to occur with the arrival of shear waves radiated by the stopping of the rupture.

In the Kostrov solution, the slip distribution on the fault surface is at any time the slip distribution for a static stress drop equal to the difference between the prestress and the frictional stress. This difference is usually referred to as the effective stress. In the circular crack which stops, slip continues to occur near the center of the crack even after the rupture propagation has terminated. Since information in an elastic medium cannot propagate faster than the compressional velocity of the medium, the center of the crack does not "know" rupture has terminated until some time after the fact. Since slip continues without an increase in fault area, the final slip is somewhat larger than the static slip expected for the given initial effective stress.

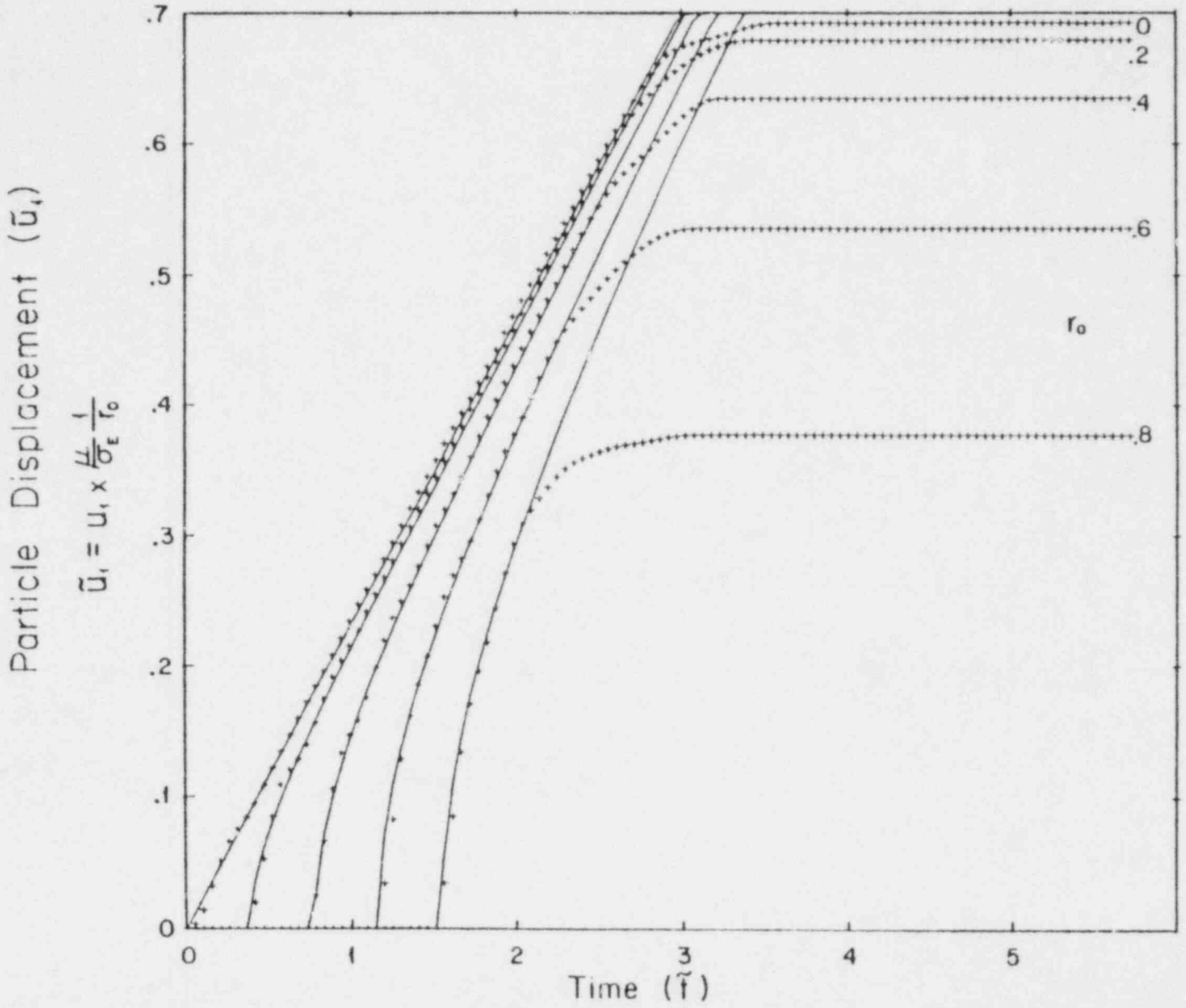

Figure 11. Comparison of particle displacements from Kostrov's self-similar rupture, $v = 0.9\beta$, with finite element solution (crosses) for a circular fault, radius r_o for five positions (from Archuleta, 1976).

This phenomena is often referred to as "overshoot", and is a common feature in most dynamic crack solutions which include the effects of rupture stoppage.

The termination of rupture has significant effects on the radiation of high frequency energy. Richards (1976) demonstrated that the Kostrov solution radiates seismic energy with a far-field displacement spectrum proportional to f^{-3} at high frequencies (f is frequency). When the rupture is abruptly terminated, Madariaga observed a high frequency asymptote of f^{-2} (Figure 12). This strongly suggests that the stopping of the rupture will control the high frequency behavior of radiated energy for the case of a circular fault. The simultaneous stopping on the circular boundary causes a great deal of constructive interference in the radiated energy.

3.6.3 Constant Effective Stress Faulting on Square Faults

Day, et al. (1978) considered stress relaxation on a square fault with rupture initiating at the center (Figure 13 and Table 2). Like the circular fault problem, the solution should be the Kostrov solution until the rupture reaches the closest edge (Figure 14). For the square fault, the healing phase from the rupture edge is not as coherent as that for a circular fault, but it is still very prominent. This can be observed very clearly in the stress history very near the fault as shown in Figure 15. Off the edge of the fault, there is a strong stopping pulse and one can see this phase propagating inward. The static stress value is reached soon after this phase arrival.

Day, et al. (1978) computed the radiated far-field displacement spectra and time histories at various positions off the fault, as shown in Figures 16 and 17. The spectral characteristics are quite similar to that found for the circular faulting of Madariaga (1976). At all the locations shown,

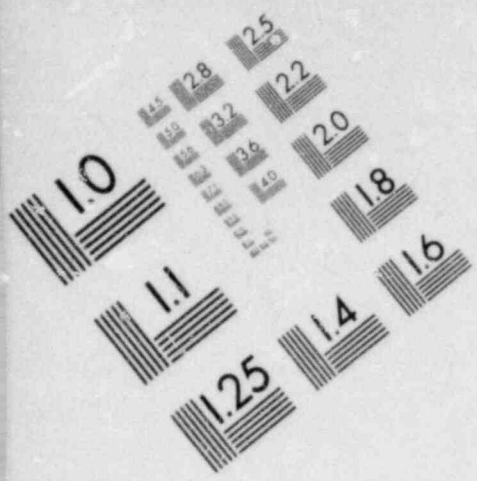

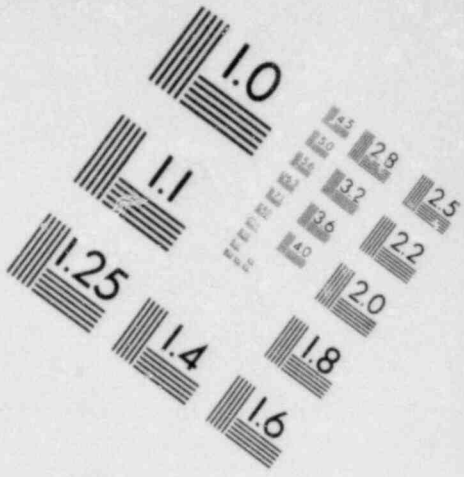

IMAGE EVALUATION
TEST TARGET (MT-3)

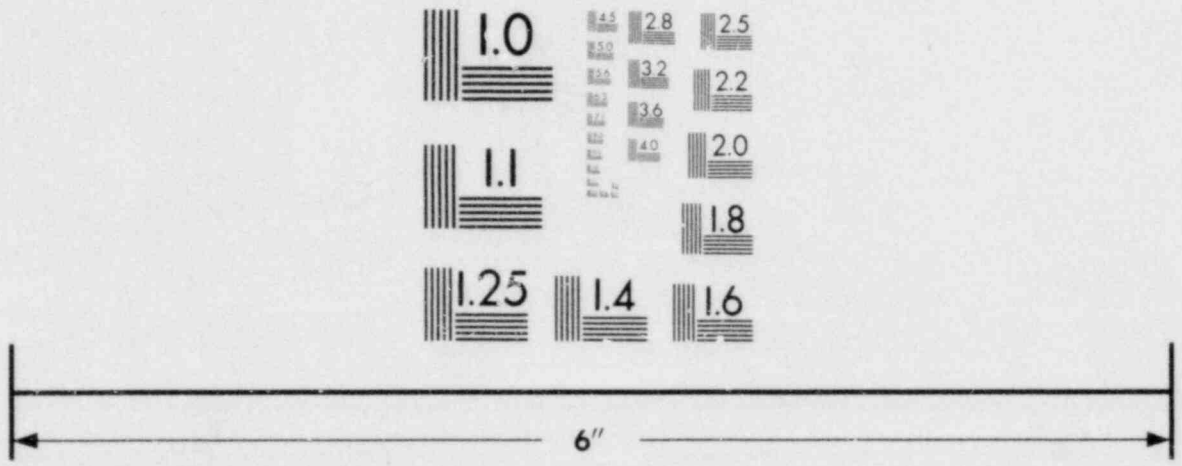

MICROCOPY RESOLUTION TEST CHART

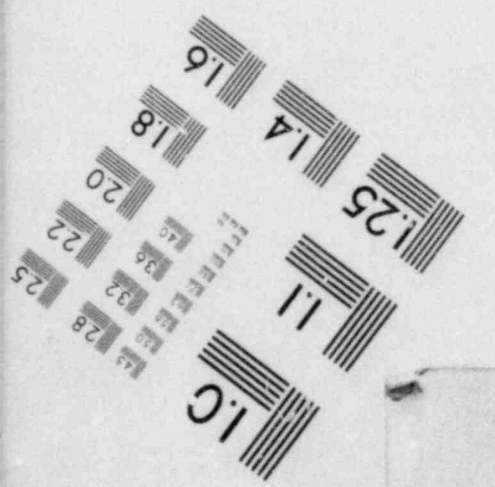

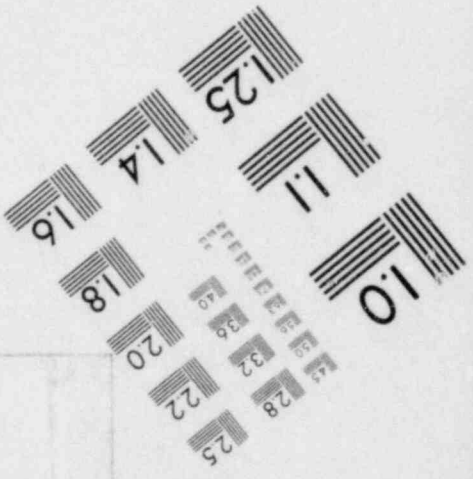

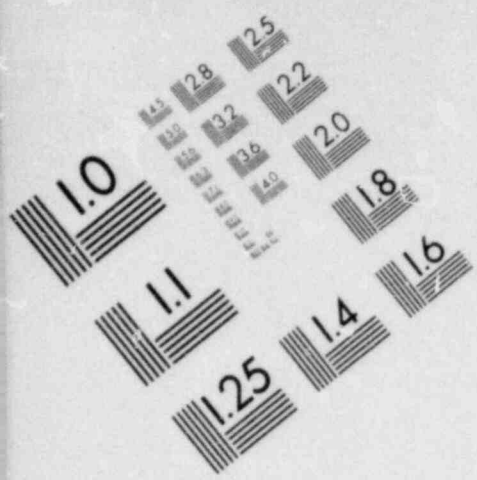

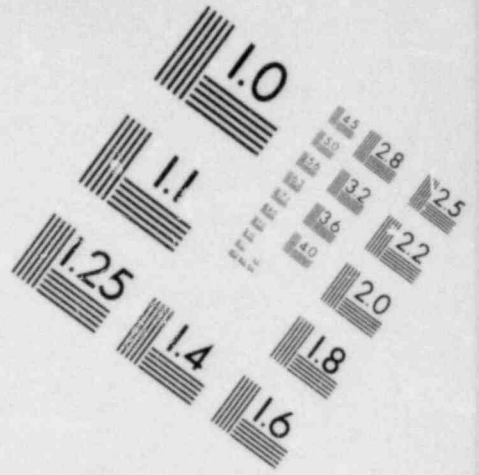

IMAGE EVALUATION
TEST TARGET (MT-3)

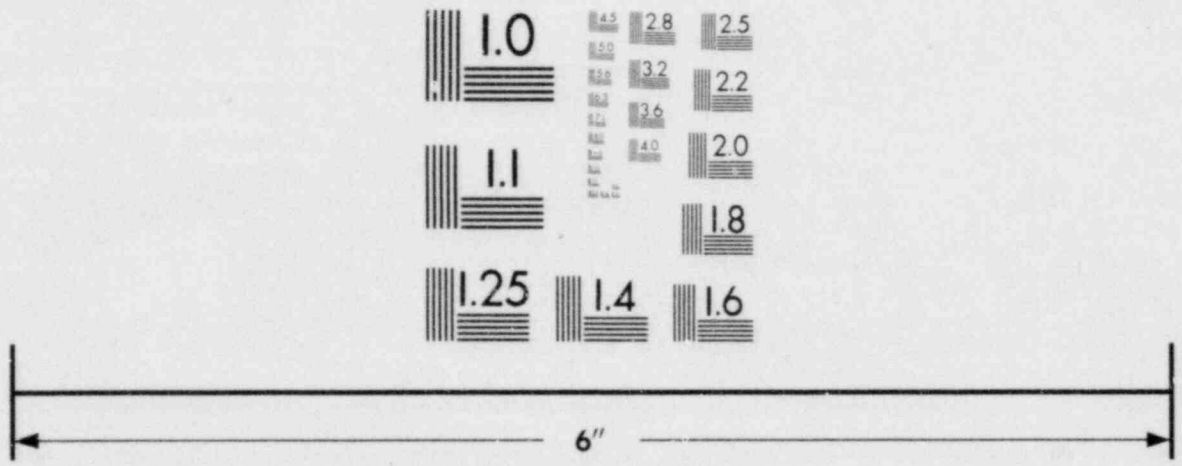

MICROCOPY RESOLUTION TEST CHART

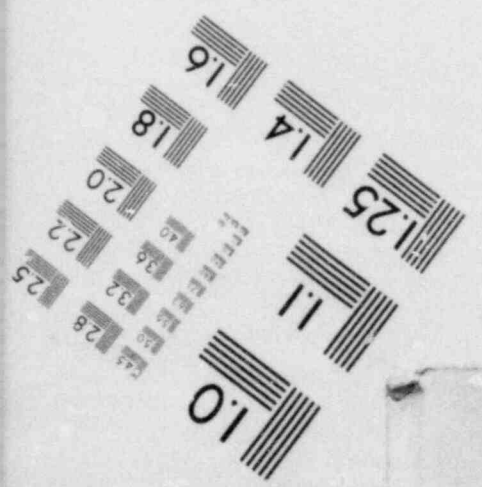

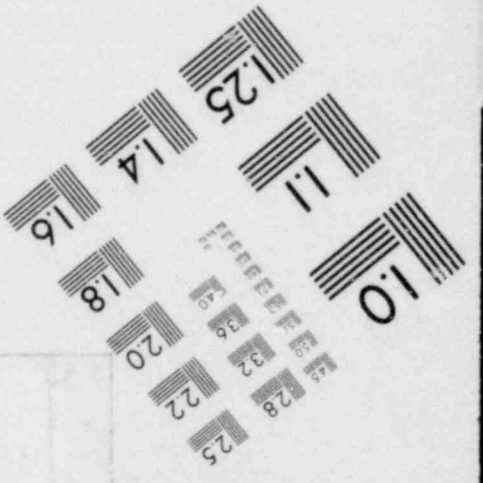

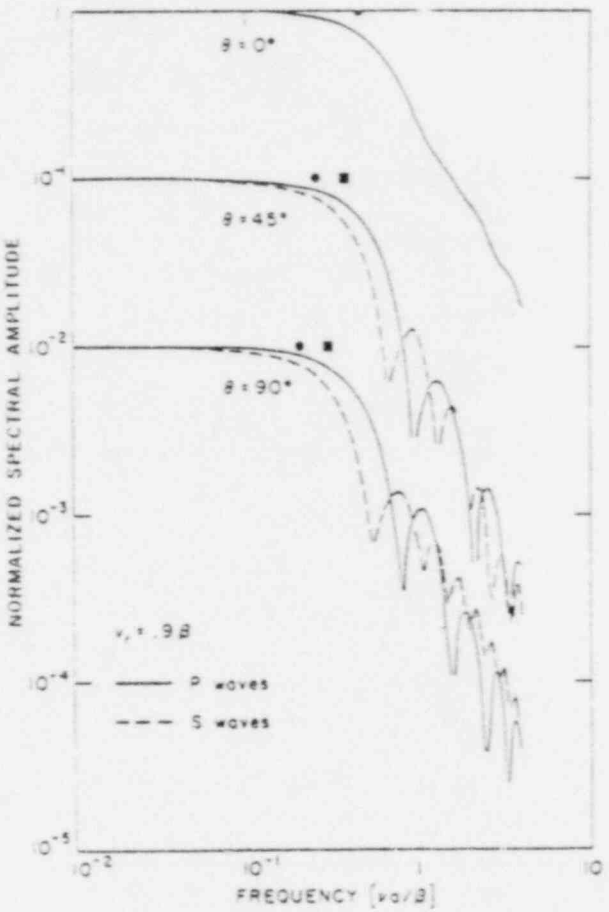

Figure 12. Far field spectrum of P and S waves radiated by a subsonic circular fault with v_r = 0.9β. The spectra of different θ are shifted by one decade in amplitude. The squares indicate the P corner frequencies while the circles indicate the S corner frequencies (from Madariaga, 1976).

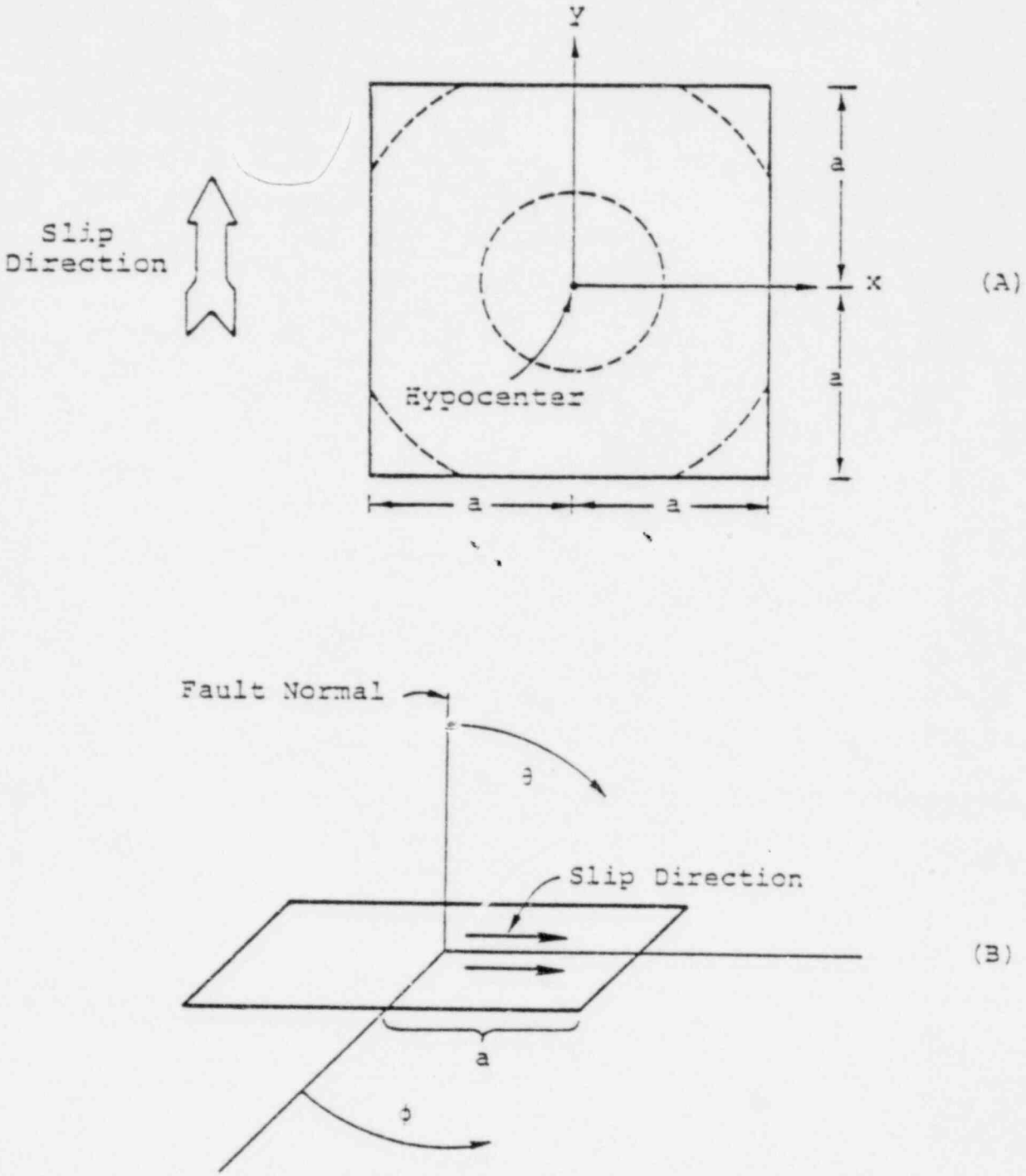

Figure 13. (A) The fault configuration for the finite difference simulation, and (B) the coordinate system for describing the radiated field.

TABLE 2

PARAMETERS EMPLOYED BY DAY, ET AL., 1978

P Wave Velocity	α = 5.93 km/sec
S Wave Velocity	β = 3.42 km/sec
Density	ρ = 2.74 gm/cm
Rupture Velocity	V_R = 3.08 km/sec
Tectonic Shear Stress	σ_T = 1 kbar
Frictional Stress	σ_f = 0.82 kbars
Fault Dimensions	2ax2a = 3 km x 3 km

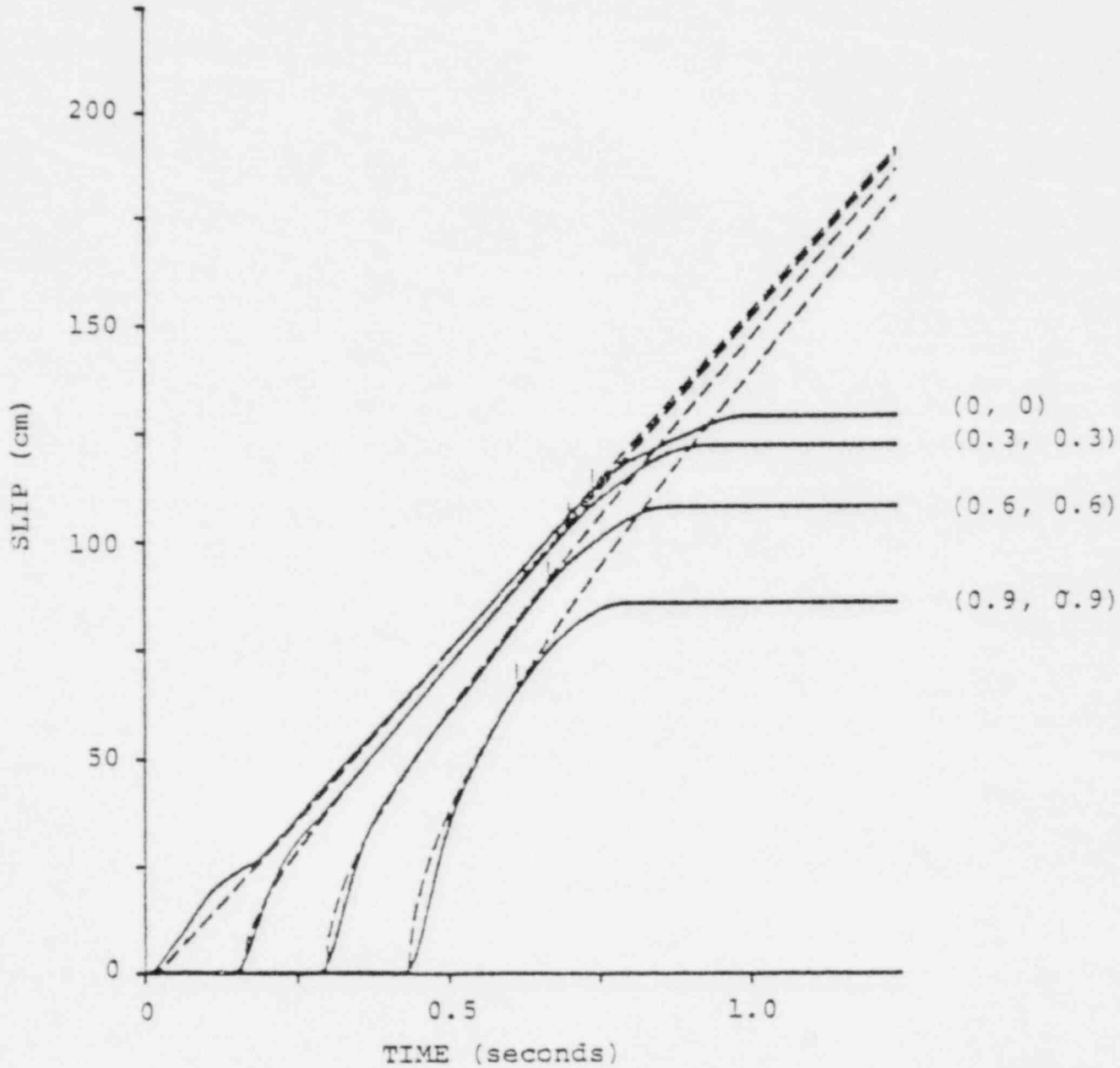

Figure 14. Relative displacement on the fault for the elastic case. The dashed curves are Kostrov's analytic solution; the solid curves are the finite difference results. x,y coordinates in kilometers are given in parenthesis. Vertical lines indicate the arrival times of edge effects due to fault finiteness.

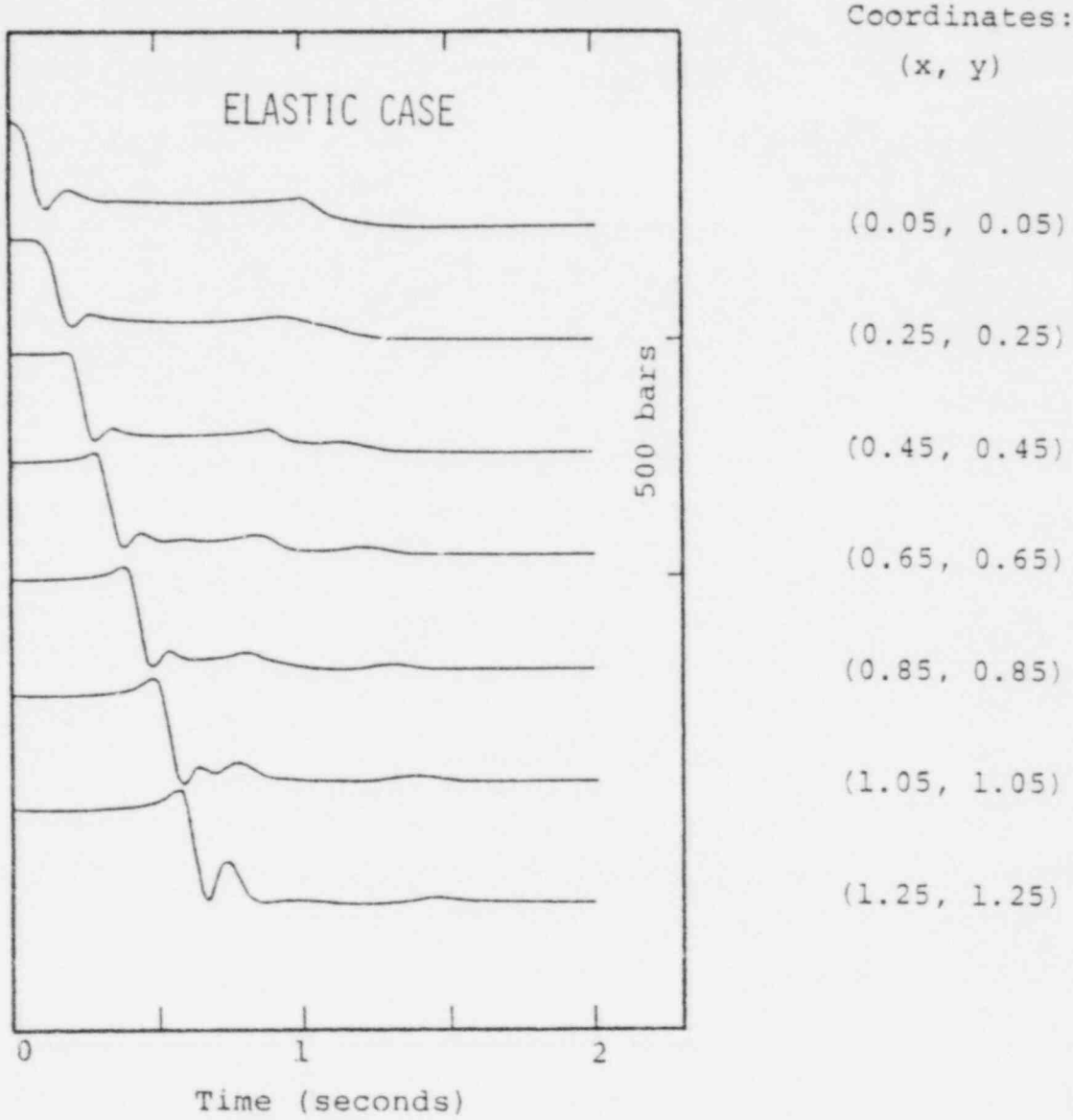

Figure 15. Time histories for the stress component σ_{yz} adjacent to the fault plane, for several hypocentral distances. Observation points are at a distance of 0.05 km from the fault plane; x and y coordinates are shown in parentheses. The stress scale for each time history is shown at the right.

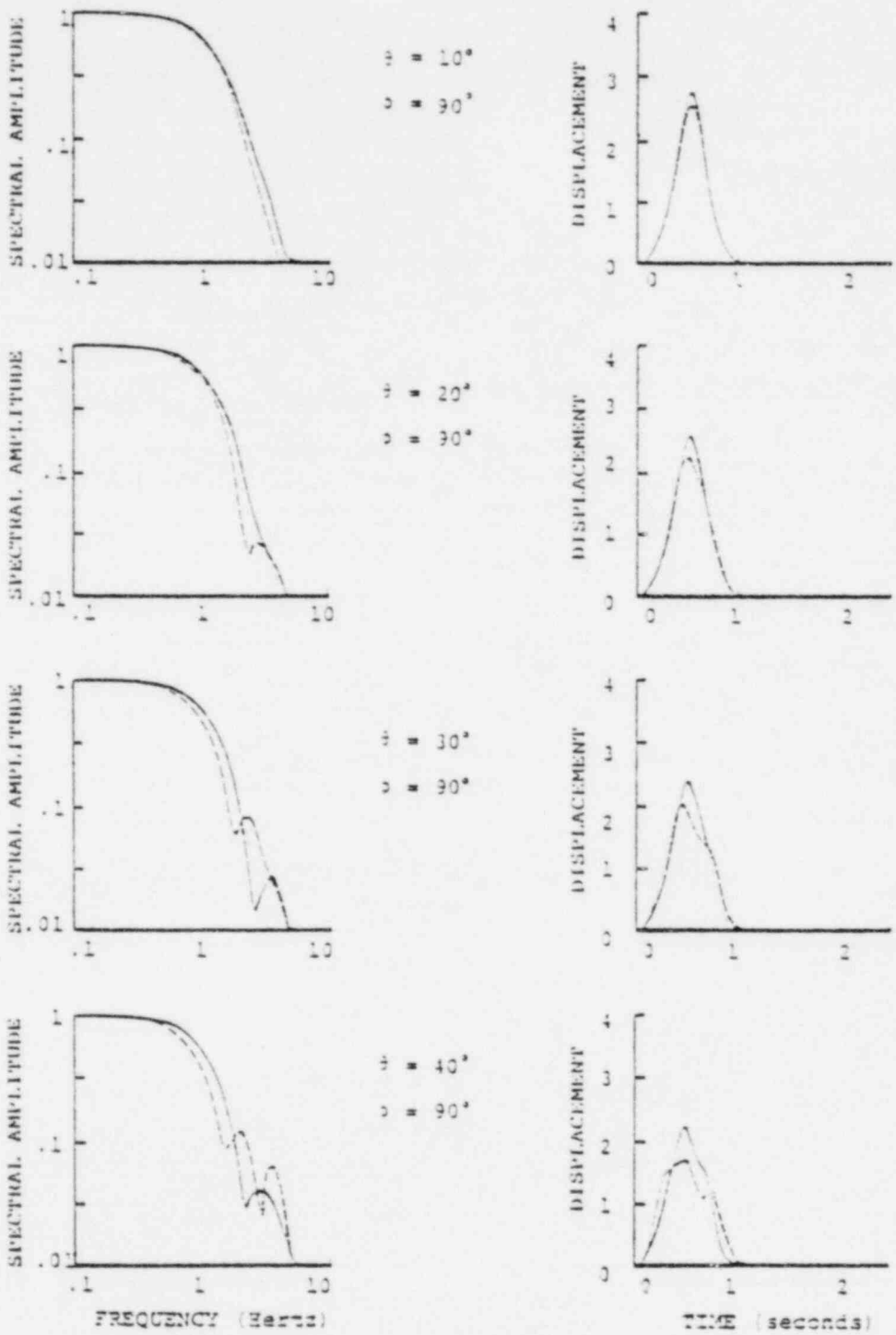

Figure 16. Normalized far field P wave (solid curves) and S wave (dashed curves) displacement spectra and time histories. Displacements are shown at 10° intervals in θ, for ϕ = 90°.

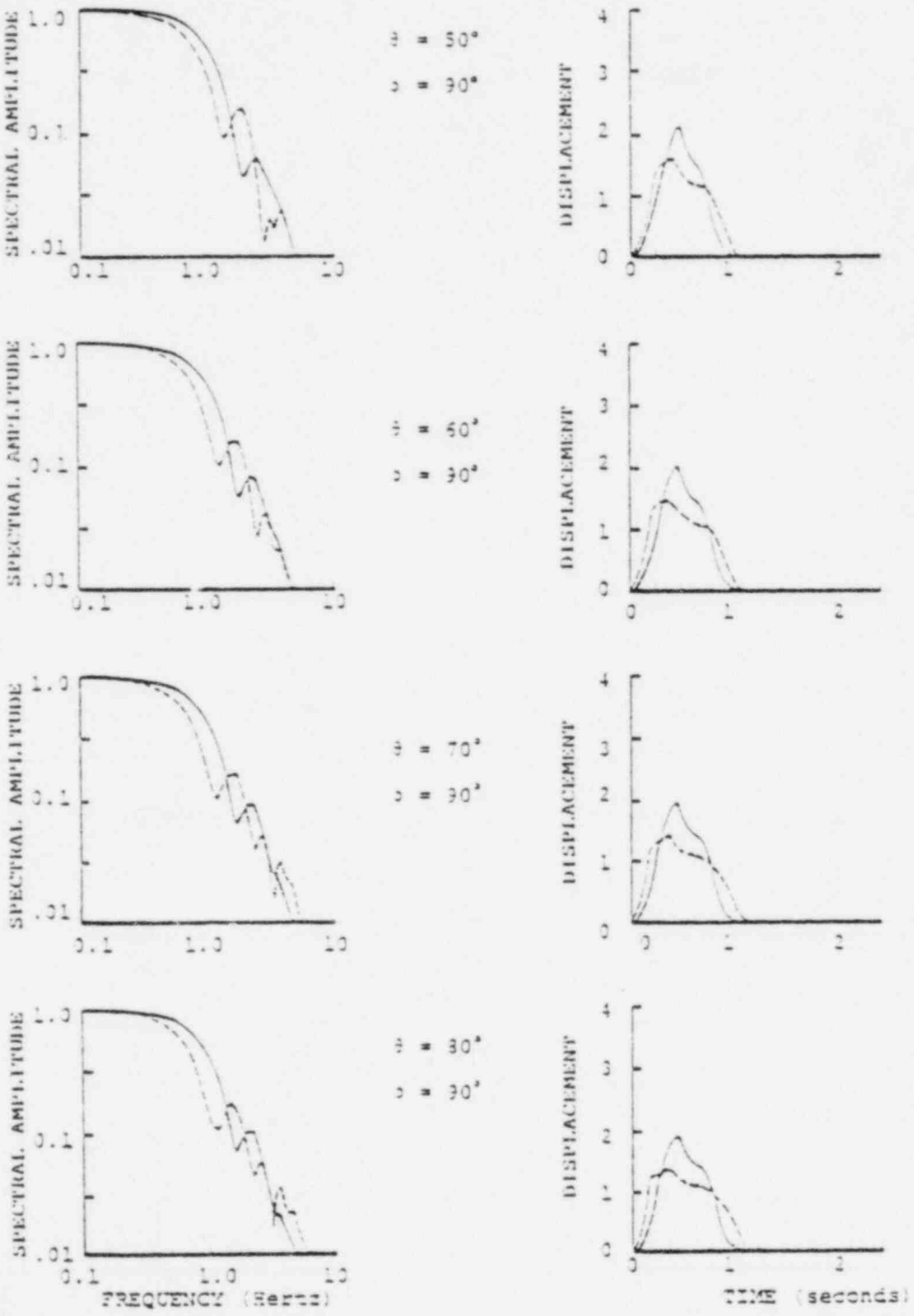

Figure 16 (Concluded)

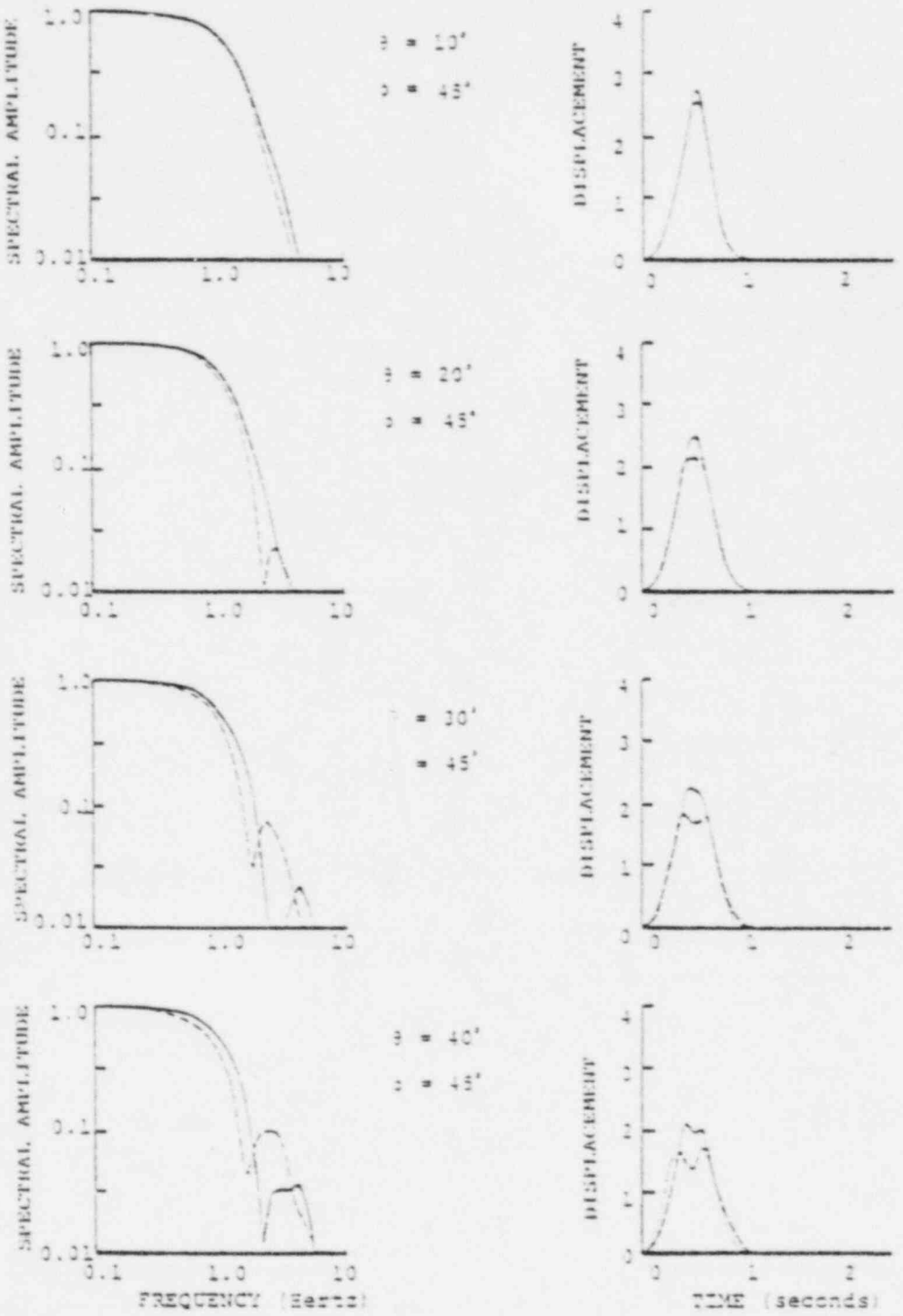

Figure 17. Normalized far field wave (solid curves) and S wave (dashed curves) displacement spectra and time histories. Displacements are shown at 10° intervals in ϑ, for ϕ = 45°.

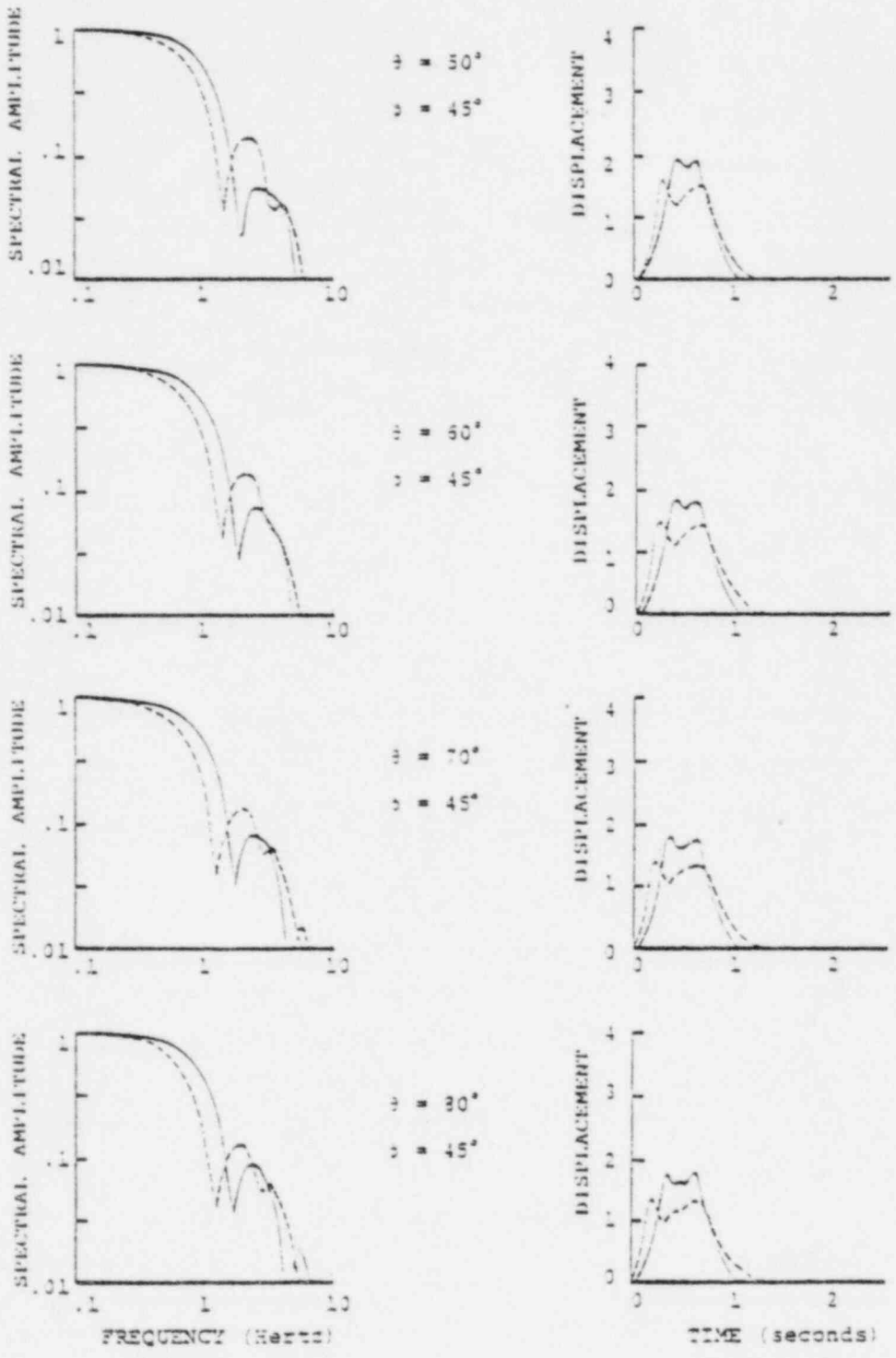

Figure 17 (Concluded)

there is only one apparent corner frequency. In most kinematic models of faulting, one assumes that there are corner frequencies associated with the characteristic dimension of faulting and the characteristic time of slip (rise time). For the dynamic model used here, there must be a strong interdpendence between the rupture propagation and the slip history since only one corner frequency is present.

The displacement time histories are larger and narrower for locations more nearly aligned with the fault plane. Even though seismic directivity effects are most severe for one dimensional rupture, as in a Haskell model, they are perceivable in two-dimensional models as well.

3.6.4 Constant Effective Stress Faulting on Rectangular Faults

Both the circular and the square faults have only one characteristic dimension and it is not surprising that they give similar results. It has been observed that many earthquakes are not so symmetric. For rectangular geometries one may expect quite different results. The Kostrov solution will apply only until the rupture reaches the narrower dimension. In the circular and square faults, all slippage terminates soon after the edge is reached, but for a long, thin fault the rupture continues. Dynamic calculations employing such geometry are few, but their results are enlightening. Madariaga (1977) performed dynamic calculations on elliptical and rectangular fault surfaces. In the Kostrov solution, the high frequencies in the slip function increase as the rupture front moves farther from the initiation point. Madariaga found that soon after the rupture front reaches the narrower dimension, the high frequencies in the slip function at the rupture front in the longer dimension appear to stop increasing. It was observed that the slip function remained essentially constant for the remainder of the faulting. Similar

findings have been made by Del Mar Technical Associates (1978) and Archuleta and Day (1979).

Archuleta and Day considered the slip history of a 30 km by 6 km strike slip fault for analysis of the Parkfield, California earthquake strong motion recordings. Their calculation was performed in an elastic halfspace with the top of the fault buried at 4 km and rupture was initiated on a narrow edge and at a depth of 8 km. The fault was sufficiently buried so that the free surface had little effect on the solution. Figure 18 shows the three components of displacement on the fault surface. The displacement in the direction of prestress (u_1) appears to reach a near constant form about one or two fault widths from the initiation point. The slip in the fault plane but normal to the prestress (u_2), is quite small. The displacement (u_3) is the motion normal to the fault plane. Motion of this type can be viewed as a slight warping of the fault surface as the rupture propagates.

Figure 19 shows the three components of velocity on the fault surface. Even though the displacements down the fault appear ramp- or step-like, the velocities show that the slip function is similar to that of the Kostrov solution except that the maximum velocity has stopped increasing as the rupture propagates away from the hypocenter.

All of the models mentioned above employ Coulomb-like friction models to govern the sliding process. It is assumed that there is a frictional stress which opposes slip while slip occurs, usually called a dynamic frictional stress, and higher values of stress appropriate to when slip is at rest, called a static frictional stress. A consequence of this model is that slip generally will not reverse itself. This is a very important feature of rectangular faults with large aspect ratios. Figure 20 from Archuleta and Day shows the sections of the fault plane which are slipping at various times after rupture initiation. The faulting process near th...

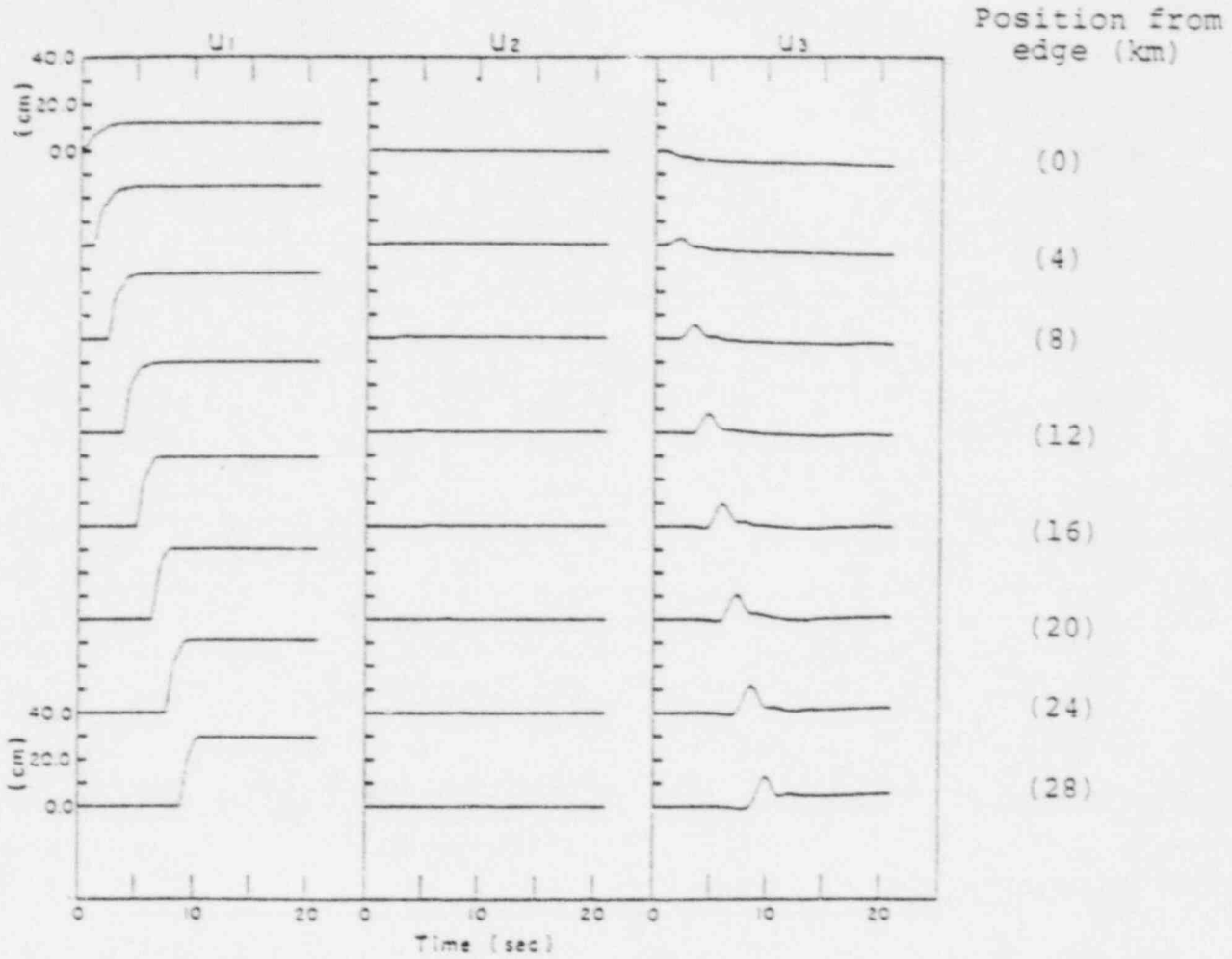

Figure 18. Three component displacements computed for a 30 x 6 km^2 rectangular fault. Observation points are at mid-width (from Archuleta and Day, 1979).

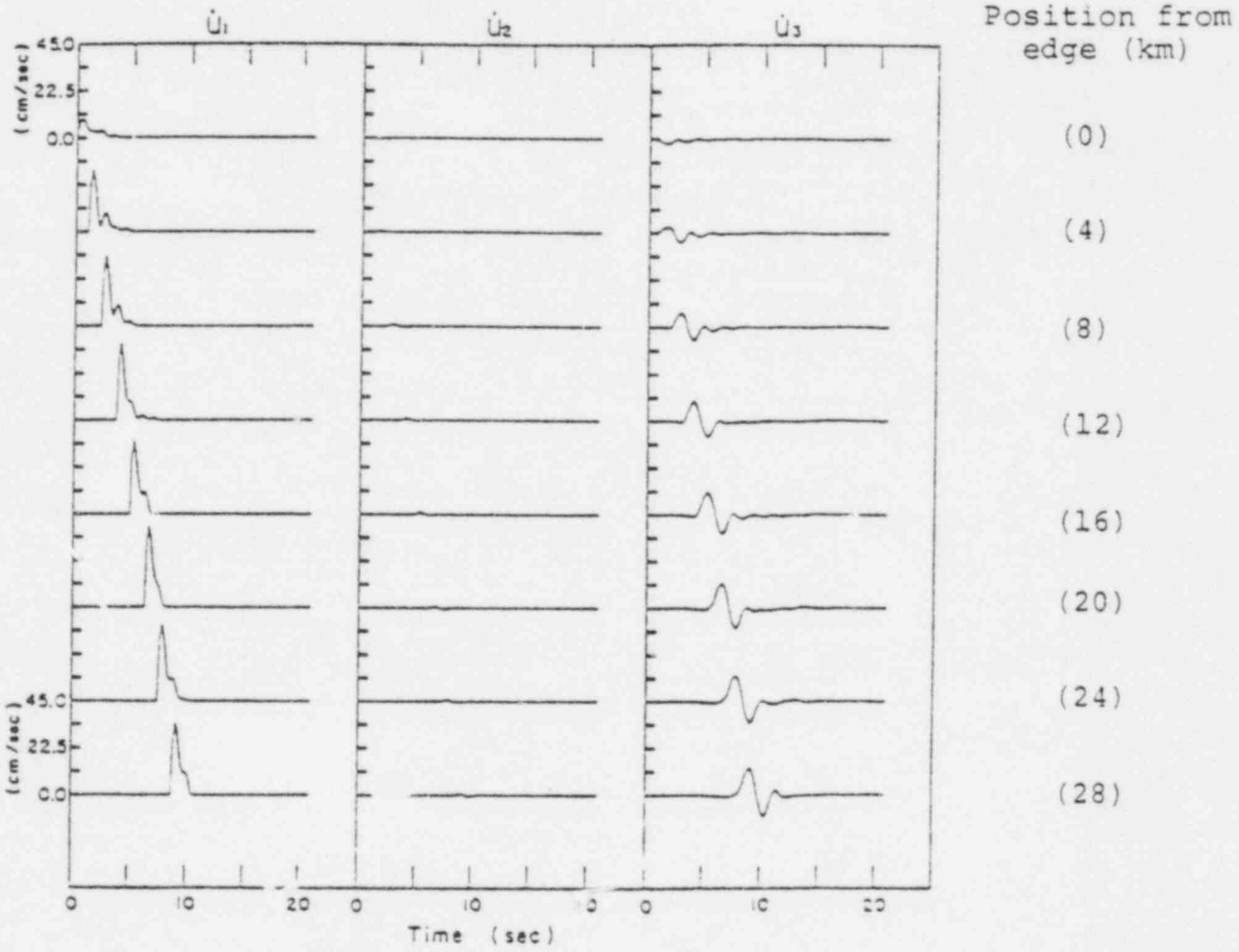

Figure 19. Three component velocities at various locations on a rectangular fault (from Archuleta and Day, 1979).

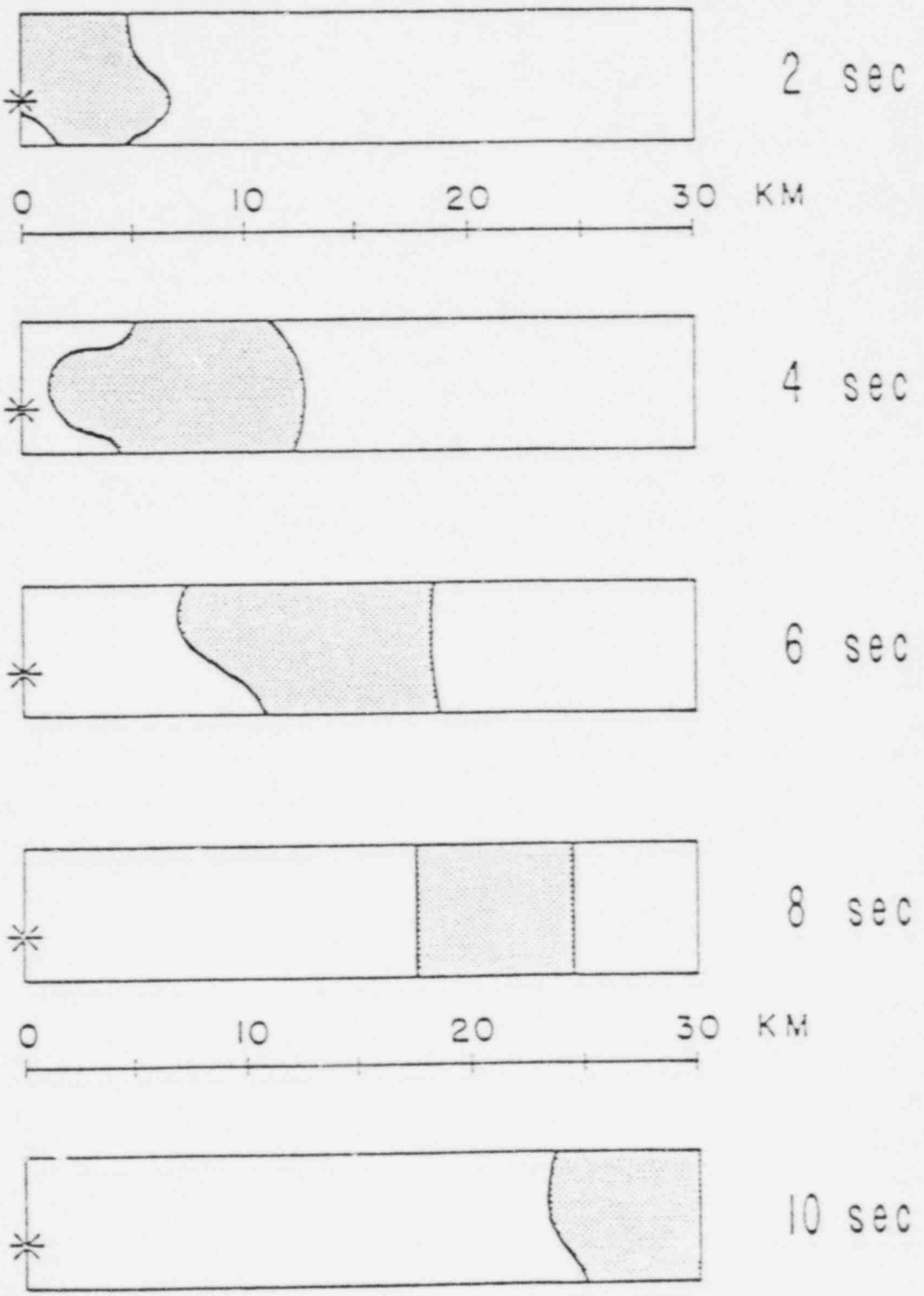

Figure 20. View of the rupture surface at various times. Shaded areas indicate slip is occurring. White areas to the left indicate a shutdown of the slip (from Archuleta and Day, 1979).

hypocenter terminates behind the moving rupture front until slip is confined to a region comparable to a fault width. Without the frictional stresses opposing slip reversals, slip could go on indefinitely exciting oscillatory modes of slip which could have a prominent effect on the energy radiated.

It is clear that asymmetries in the fault surface can cause the simple dynamic slip solutions to be altered. To be useful in seismogram synthesis these effects must be parameterized. Madariaga (1977) noted that the average slip velocity reached in long thin faults as the rupture front propagates away from the hypocenter appeared to be consistent with that suggested by Ida (1973). It was found that the velocity could be approximated by

$$\dot{u} = C \frac{\sigma_e}{\mu} V_r$$

where $\dot{u}$ is average slip velocity, σ_e the effective stress, V_r the rupture velocity, μ the rigidity and C a constant of order one. It is quite surprising that fault width does not enter into this relationship since the narrow width is the feature of the fault model which causes the solution to deviate from the Kostrov solution and approach a steady state.

The most detailed study of the effect of the geometry of rectangular faults with constant effective stress drop on the slip characteristics was performed by Day (1979). Day compared three faults with bilateral rupture over the same length (8 km) and differing widths (Table 3). Figures 21, 22 and 23 show the slip displacement histories at various points of the fault for fault widths of 8 km, 4 km and 1.5 km, respectively. The square fault results (Figure 21) are, of course, similar to that of Day, et al. (1978), and little difference is seen in the two to one aspect ratio case (Figure 22). The long, narrow fault shows quite different results

TABLE 3

PARAMETERS USED BY DAY (1979) FOR RECTANGULAR FAULT SIMULATIONS

P wave velocity	α = 6.0 km/sec
S wave velocity	β = 3.46 km/sec
Density	ρ = 2.7 gm/cm^3
Rupture velocity	V_R = 3.12 km/sec
Tectonic shear stress	σ_T = 1,000 bars
Frictional stress	σ_f = 900 bars
Fault length	ℓ = 8 km
Fault width	W = 1.5, 4, and 8 km

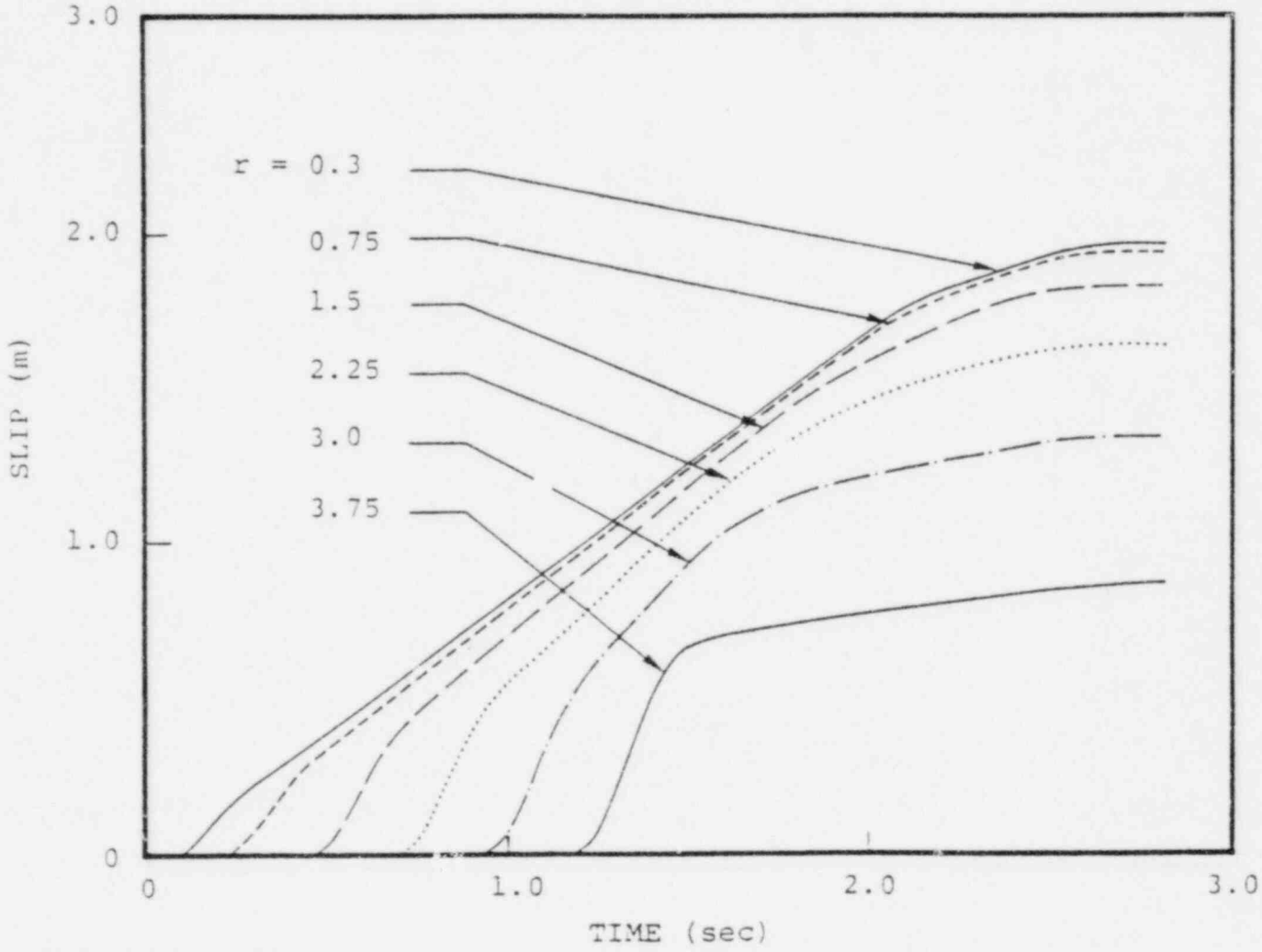

Figure 21. Slip histories along the center-line of the 8 km x 8 km fault plane, at several distances from the focus. The observation points are aligned with the direction of slip (Day, 1979).

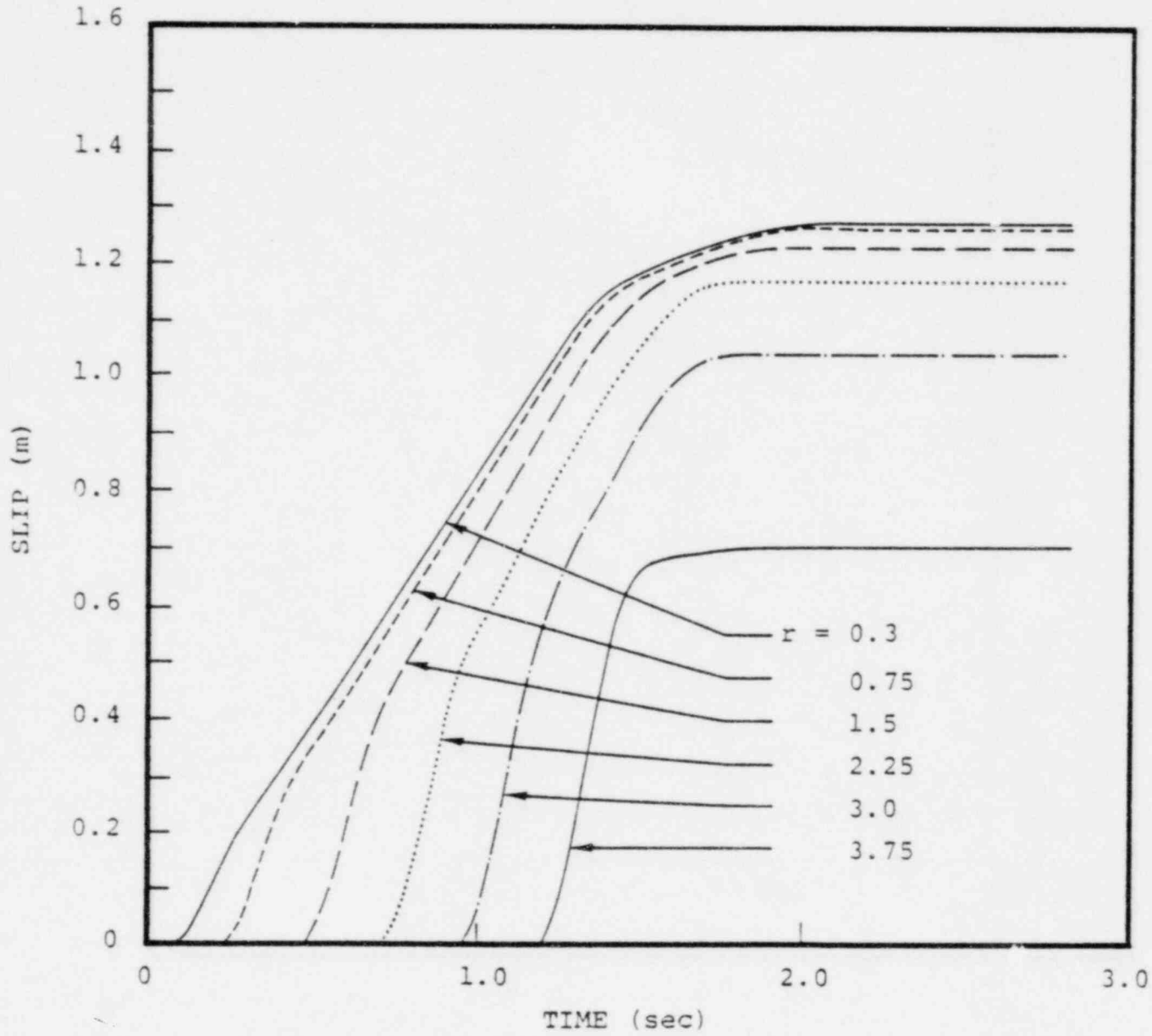

Figure 22. Slip histories along the center-line of the 4 km x 8 km fault plane. The observation points are aligned with the slip direction and the long dimension of the fault.

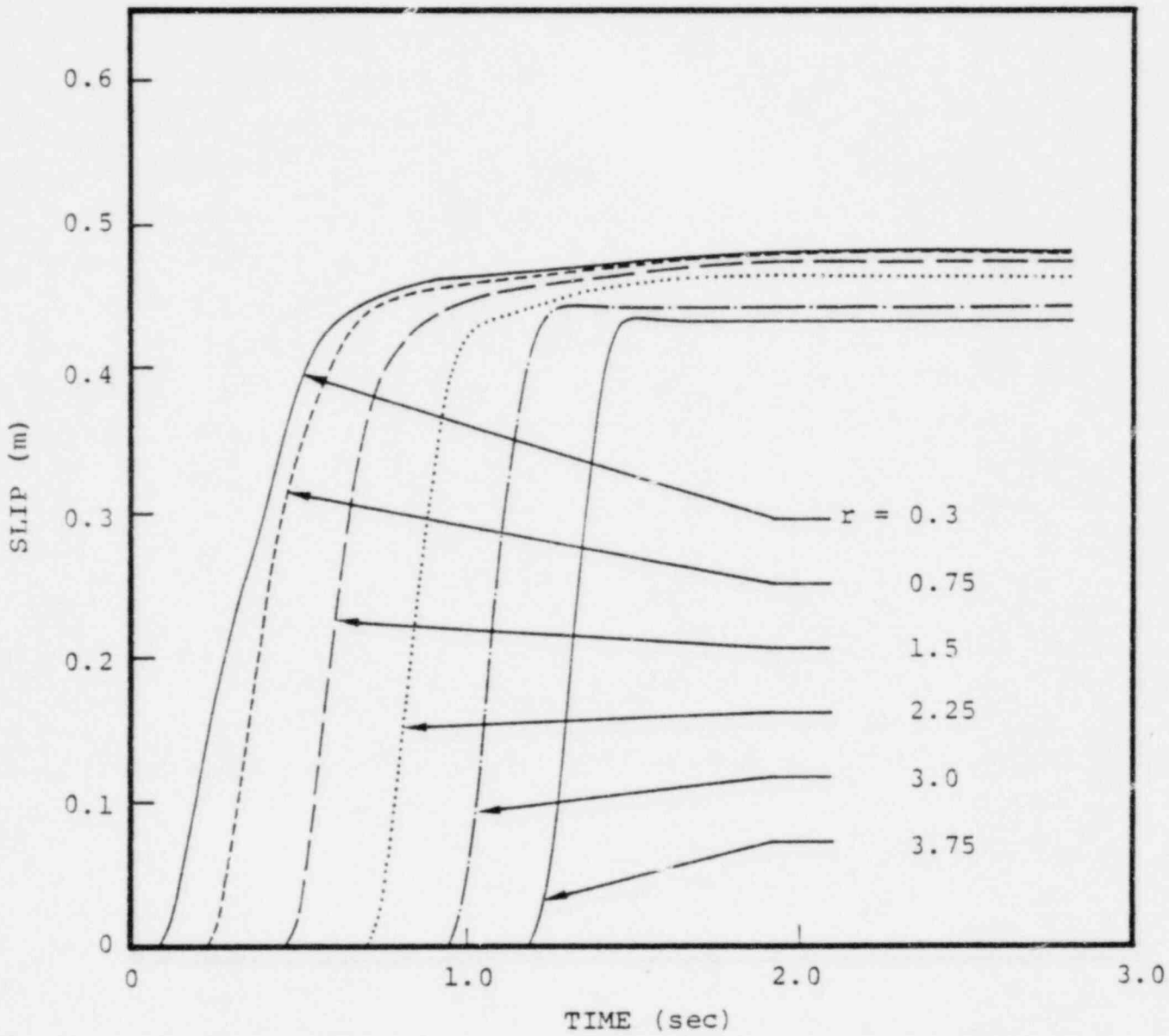

Figure 23. Slip histories along the center-line of the 1.5 km x 8 km fault plane. The observation points are aligned with the slip direction and the long dimension of the fault.

(Figure 23). Except for the point near the hypocenter, the slip histories are quite similar. It appears that the initial slopes of slip along the fault are roughly the same. The static displacements are the same within 10 percent. From the displacements it would appear that a ramp-like slip model would be appropriate in this case.

Figures 24, 25 and 26 show slip velocities for the three cases. The first two cases have characteristics like that of a low-pass Kostrov (1964) slip function which is to be expected. As we move away from the hypocenter, the high frequency content in the slip function increases. The slip velocities on the long narrow fault differ from the first cases in two respects. First, after the rupture has propagated approximately one fault width from the hypocenter, the slip velocity begins to increase with a much slower rate. The maximum velocity at distances at and beyond 1.5 km differ by no more than about 10 percent. Second, the duration of slip tends to stabilize as well beyond 1.5 km. Points farthest from the hypocenter appear to have a duration approaching a value of $W/2\beta$ where W is the fault width and β is the seismic shear velocity.

These calculations are, of course, severely limited in high frequency content, but there are physical constraints which can be used to infer the actual high frequency characteristics expected in a continuum analogy to the discrete grid problem solved by Day. It is clear that there must be stress concentrations at the rupture front which will result in a singular slip velocity. Day noted that the slip velocities observed are highly consistent with a low passed Kostrov-like slip function in which the strength in the velocity singularity stops increasing after the rupture has progressed beyond some point away from the hypocenter. The Kostrov slip velocity can be written

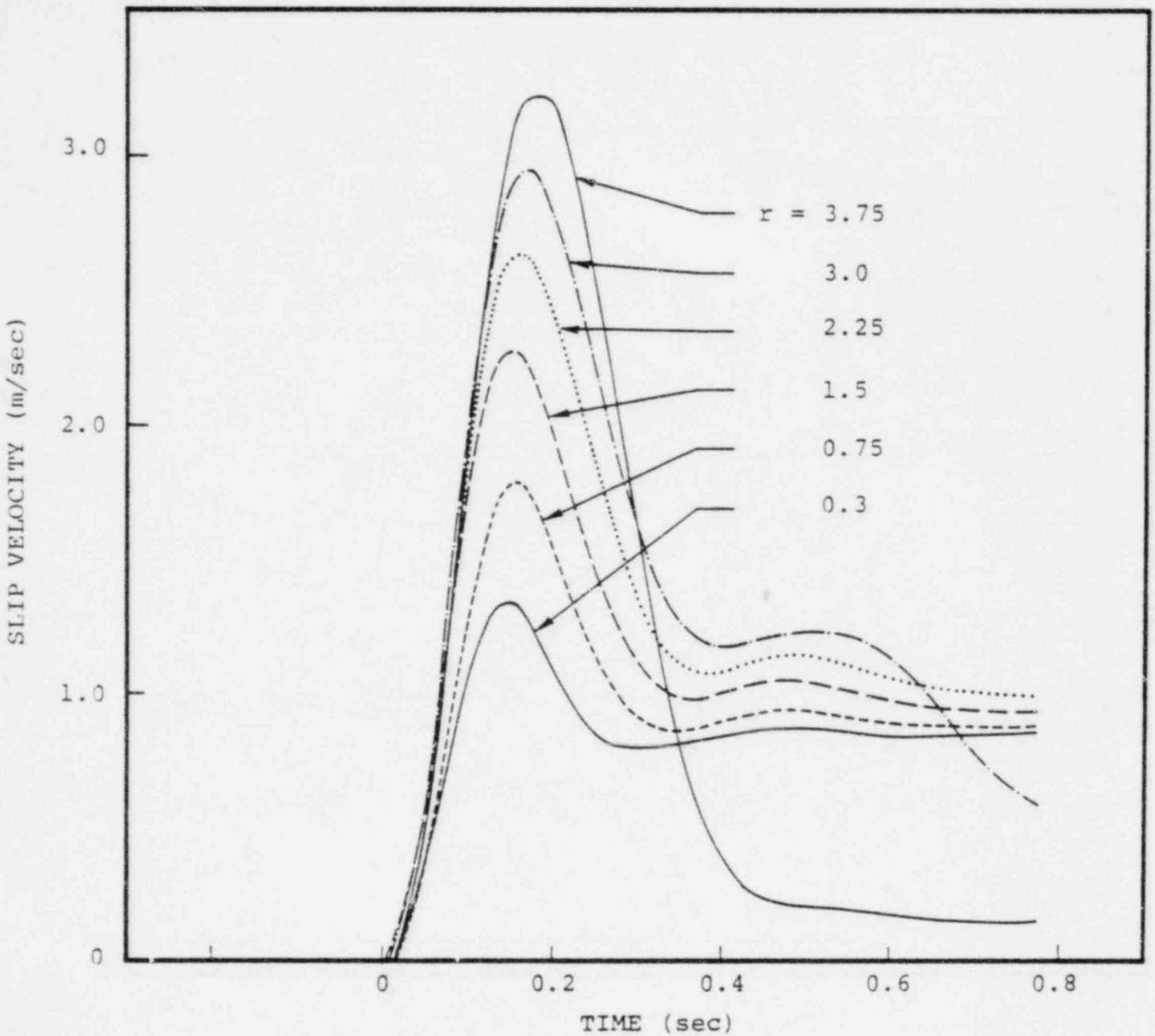

Figure 24. Slip velocity histories obtained along the center of the 8 km x 8 km fault, at several distances from the focus. The observation points are aligned with the slip direction. The time histories have been low-pass filtered with a 5 Hz cutoff, and the time delays corresponding to rupture arrival have been removed.

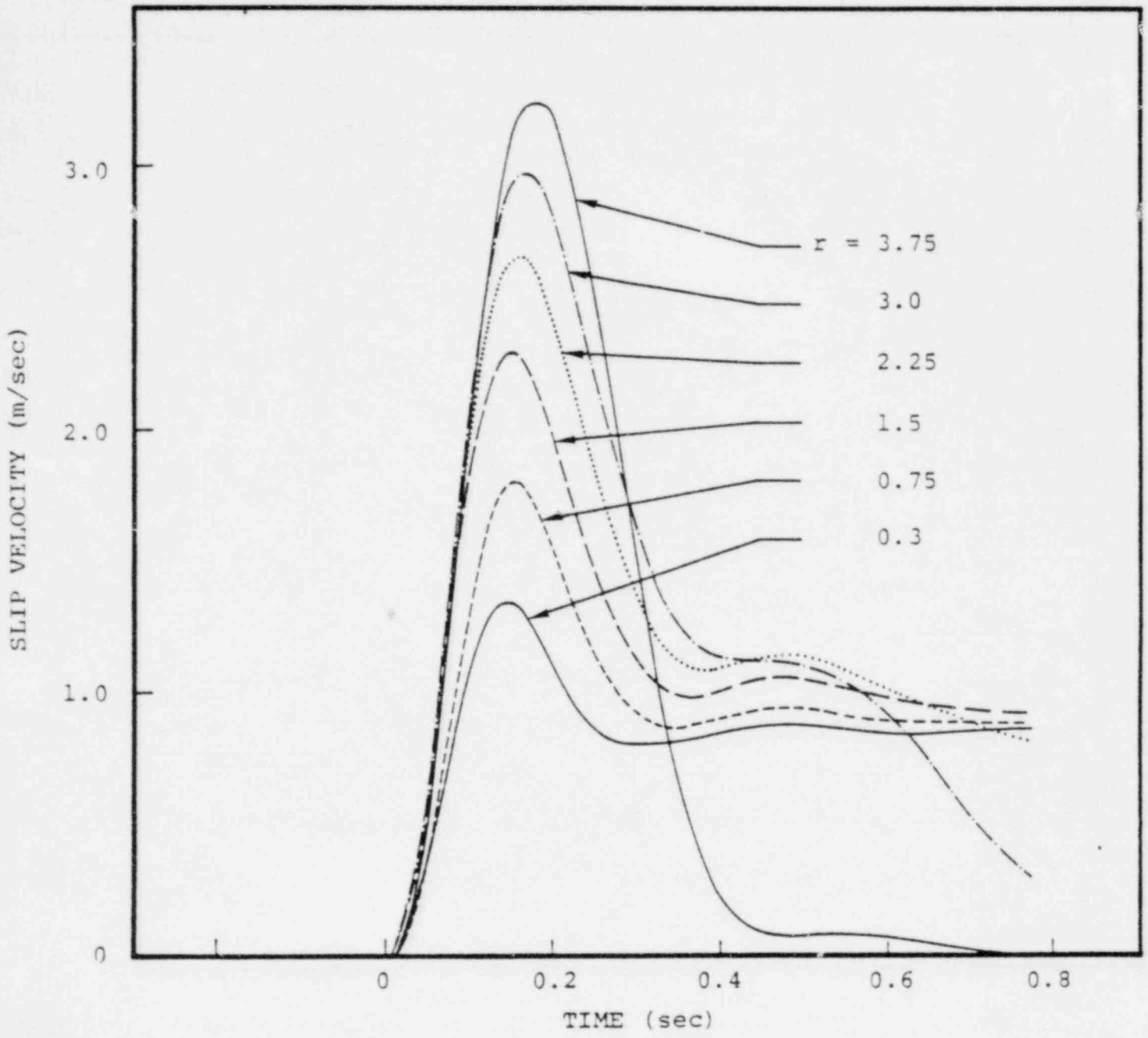

Figure 25. Slip velocity histories obtained along the center of the 4 km x 8 km fault, at several distances from the focus. Observation points are aligned with the slip direction and the long dimension of the fault. The time histories have been low-pass filtered with a 5 Hz cutoff and the time delays corresponding to rupture arrival have been removed.

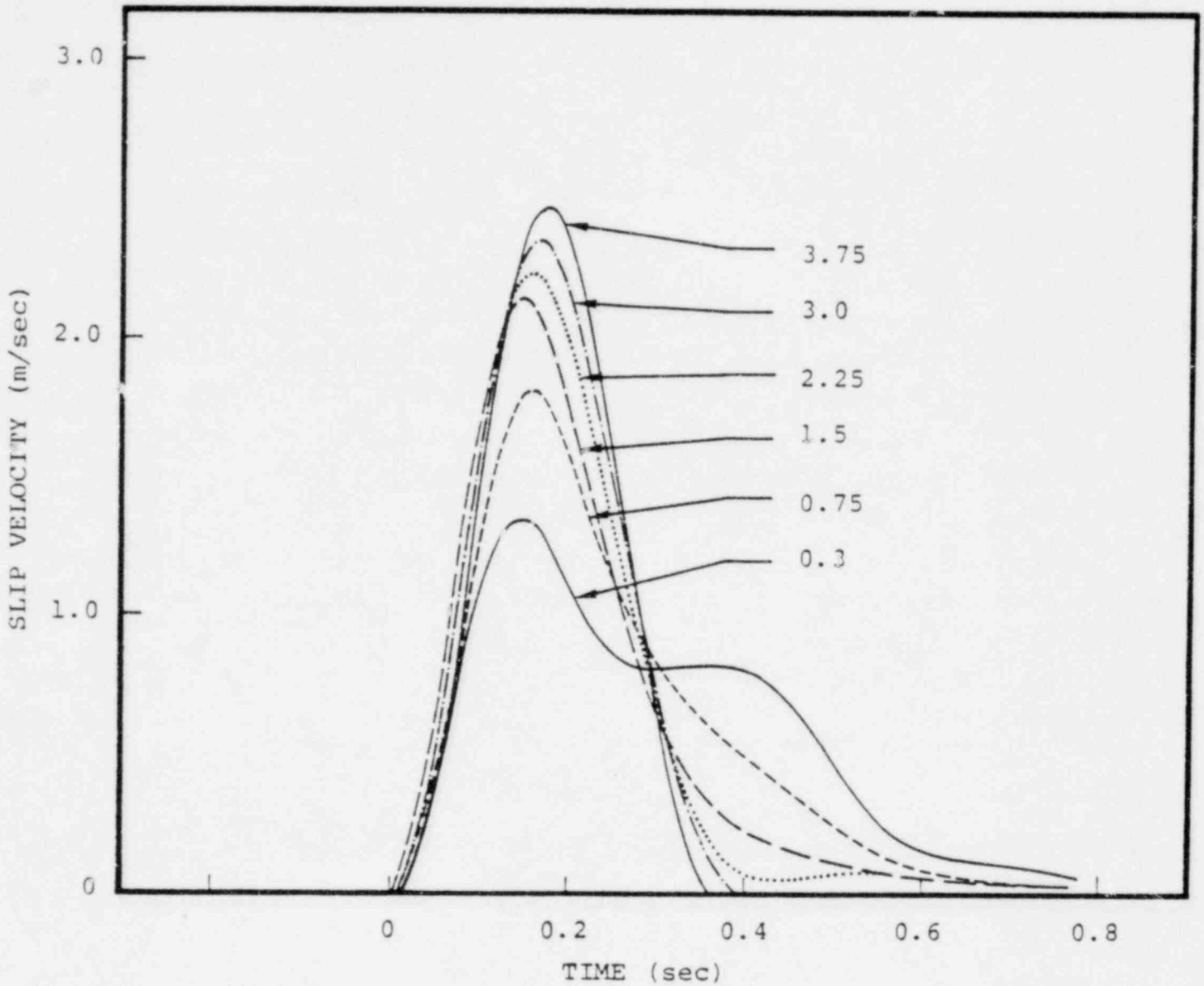

Figure 26. Slip velocity histories obtained along the center of the 1.5 km x 8 km fault, at several distances from the focus. Observation points are aligned with the slip direction and the long dimension of the fault. The time histories have been low-pass filtered with a 5 Hz cutoff, and the time delays corresponding to rupture arrival have been removed.

$$\dot{D}(\tau,r) = \frac{\dot{D}_0\left(\tau + \frac{r}{v}\right)}{\sqrt{\tau\left(\tau + \frac{2r}{v}\right)}} H(\tau)$$

where τ is a reduced time $t - r/v$, r is the distance from the hypocenter, v the rupture velocity and $\dot{D}_0$ the slip velocity at the center of the fault. The strength of the square root singularity is controlled by $\sqrt{r/v}$. The rectangular fault slip appears to follow this trend until the rupture progresses to approximately a fault width. For subsequent rupture the strength of the initial slip velocity changes very little. Even though the Kostrov solution suggests that the high frequency content in the slip function should continually increase, this appears to be the case only if the rupture is expanding uniformly in all directions. It appears that the internal dynamics of the source impede the growth of the high frequencies when rupture is terminated in some direction and in a surprisingly predictable manner.

3.6.5 Effect of the Free Surface

The calculations described above, except for those of Archuleta and Day (1979), involve stress release in a homogeneous elastic wholespace. The presence of a free surface or layer boundary, which require stress conditions to be satisfied, can influence the nature of stress release on the fault. For a constant applied stress static slips are known to be enhanced at very shallow depths, but the effect of the free surface is negligible unless the fault depth is significantly less than a fault width (Boore and Dunbar, 1977). Archuleta (1977) considered the effect of the free surface on th rupture dynamics for a strike slip fault of constant effective stress which breaks the surface. His calculations demonstrated that in cases where rupture begins at depth and is permitted to break the free surface, the high frequencies

in the slip function, as well as the static values, are enhanced by the free surface. This suggests that in cases of stress release at very shallow depths, there may be large high frequency motion associated with a "breakout" of the rupture.

Even though many shallow events are known to produce surface ground breakage, it is not known whether such slip is associated with effective stress drops comparable to those at depth. Bouchon and Aki (1977) noted that the largest accelerations observed in the Pacoima Dam recording of the San Fernando earthquake correspond quite well in time with the arrival of a Rayleigh wave from the surface breakage.

3.6.6 Discussion

There are several limitations to the numerical fault models just discussed. These models generally assume constant effective stress on a single fault surface. The assumption of constant prestress and constant frictional stress may not be appropriate for earthquakes. Several investigators have suggested this is probably not appropriate for the most widely studied earthquake, the 1971 San Fernando, California earthquake (Hanks, 1974; Bouchon, 1978; Bache and Barker, 1978). It has been suggested by Andrews (1979) and Hanks (1979) that the prestress must be inherently complicated to be consistent with observed distributions of earthquake b-values. McGarr, et al. (1979) gives strong evidence for large variations in local effective stresses from analyses of faulting in a South African mine.

Another weakness of this type of model is that the fault surface and rupture propagation is assumed to be known. The rupture velocity is usually chosen to be subsonic (less than shear velocity) at initiation. The fault growth accelerates instantaneously to the rupture velocity and decelerates to

zero instantaneously at the edges. Since the stopping of the rupture appears to be the most important source of high frequency radiation in these models, the specification of the rupture history is very important for engineering applications. Since a propagating rupture has no momentum, there is nothing physically wrong with terminating the rupture instantaneously. What is not clear is whether such a process occurs in earthquakes. When rupture propagation is determined by the slip and stress conditions by use of a fracture criterion, it has been found that such instantaneous stopping can occur only under certain conditions (Das and Aki, 1977).

Numerical studies suggest that two of the more important aspects of the rupture process which affect the high frequency radiation of seismic energy are, (1) increase of high frequencies in the slip history as rupture progresses, and (2) the stopping of the rupture. Both of these features are artifacts of the numerical models discussed. The infinite velocity of the Kostrov solution is permitted because stress at the rupture front is allowed to be infinite. Earth materials cannot support infinite shear stresses and fracture must occur at finite stresses (Cherry, et al., 1976). Rupture velocity cannot be considered an independent quantity. Since the tendency of a material to fracture is related to some distribution of stress in the vicinity of the rupture front, one must expect the rupture history to be linked in some way to the stress and constitutive properties of the medium. What is not clear is whether such considerations make any difference in the radiation of seismic energy in the frequency range of interest.

An important addition to numerical modeling in the past few years is the incorporation of more realistic physics governing the behavior of the rupture and fault slip in the vicinity of the rupture front. The physics of fracture is

not well understood, either theoretically or experimentally, but progress is being made. Most of the work in this area may not be too useful for immediate application, but some can be helpful in evaluating techniques commonly used in practice. A supplement to this review summarizing nonlinear source models will be submitted pending completion of a numerical study now being done at S^3 under NRC funding.

3.6.7 Summary

Numerical models of the earthquake source attempt to describe the rupture process resulting from given initial stress conditions. Most models of this type have assumed the effective stress to be constant in a prescribed fault geometry. In such cases the slip history during and just after initiation will resemble the self-similar crack solutions discussed in Section 3.5.2. When the rupture encounters a fault boundary, self-similarity is destroyed. Radiation from the fault boundary can cause rupture to terminate behind the rupture front and can slow the growth of high frequencies in the slip history at the rupture front. Generally, these models violate some physical constraint on the rupture process such as allowing infinite stresses to occur or specifying rupture history independent of the slip history and medium constitutive properties. It is not understood how such assumptions affect the high frequency radiation predicted by such models. Future work is needed to further study the details of the rupture process when all known physical constraints are included.

Cost might prohibit the direct use of numerical earthquake simulation for computing near-field, high frequency ground motion, but the results from such simulations can be important for suggesting kinematic models of earthquakes which could be used for such a purpose. Future work is also necessary to determine how numerical results can be used to obtain high frequency kinematic descriptions.

3.7 SUMMARY AND CONCLUSIONS

In the preceding sections we have described what we believe to be the most important earthquake source models that may be useful for simulating earthquake ground motions. These models have proved to be very useful for many seismological applications, but they have rarely been used for synthesis of ground motion of engineering interest.

The most commonly used source models are called kinematic models because the slip and rupture history is prescribed on the fault surface. Some kinematic models, like the original one proposed by Haskell, can quickly be dismissed as possible candidates for deterministic modeling of near-field ground motion. In fact, none of the proposed kinematic models have demonstrated an ability to model the characteristics of near-field data over wide frequency, magnitude and distance ranges. However, few serious attempts have been made, so one cannot conclude that it cannot be accomplished.

Even the simplest kinematic model has a large number of details which must be specified. The constraints on these parameters arise from interpretation of ground motion data and from consideration of the physics of rupture. Unfortunately, at this time, these only weakly constrain the form of the kinematic models. As far as details are concerned, much work is required before we will be able to fully understand the relative importance of various model characteristics for determining the high frequency radiation. In summary, what is needed to make the kinematic models more useful for strong motion prediction is both more study of the parametric dependence of the radiation predicted by these models and more detailed knowledge of the kinematic properties of actual earthquake faulting.

Dynamic models of the earthquake source attempt to simulate earthquakes as a stress relaxation process. Slip and rupture histories on the fault surface are determined

from initial stress conditions and the dynamic consequences of the stress relaxation. Such models have greatly helped the understanding of the physical processes of earthquakes and have been used to constrain the characteristics of kinematic models.

Simple dynamic models are probably too crude to be of direct use for synthesizing of near-field accelerations, but numerical dynamic modeling can be very important for simulating some of the physical properties of earthquakes which are important for near-field ground motion. Unfortunately, there are at present technological limitations to the frequencies which can be simulated in such calculations. Work is needed to develop methods for extending numerical results to frequencies of importance to acceleration.

Most of the numerical modeling performed to date have not satisfied all of the physical laws of rupture as we know them, and work is needed to determine the details of certain earthquake processes, like the stopping of rupture, when more reasonable physical constraints are applied. Work is also needed to constrain the initial stress conditions which are appropriate for earthquakes.

IV. PRELIMINARY PARAMETRIC INVESTIGATIONS OF SELECTED THEORETICAL EARTHQUAKE SOURCE MODELS

4.1 INTRODUCTION

Many different models of the earthquake source have been used to simulate the radiation of seismic waves. Most of these models are commonly used to infer characteristics of earthquake processes by the study of ground motion recordings in the far-field and geometrical far-field and usually at frequencies much lower than those of engineering interest. In only a few cases have such models been employed to simulate ground motion at close distances from moderate or large events at frequencies greater than one hertz. There are several reasons for the lack of calculations of this kind. Such calculations are generally costly. For most of the simple models the characteristics of the motion in the geometrical near-field cannot be expressed in simple analytic form like the motion in the far-field and geometrical far-field often can. Numerical integrations over the fault surface can be cumbersome. Expense limits severely the high frequency resolution of numerical source models for which the cost increases at least by a rate of frequency to the third power and usually much more. Another reason is the inability (until very recently) to properly account for the response of the earth. Wholespace calculations are often not adequate when describing the characteristics of strong ground motion. The transverse displacement at Parkfield Station #2, for example, has not been fit well using a reasonable source model without accounting for the effect of the near surface sediments. Another reason is that our near-field data source, strong motion accelerograms, appear too complicated to model in detail, like seismologists are now accustomed to doing with far-field data. "Wiggle for wiggle" fits may indeed by impossible, but few have even attempted to determine whether the gross characteristics of acceleration can be modeled deterministically.

The purpose of this study is to determine which source models are likely candidates for use in simulating near-field ground motion. An ideal source model would accurately describe the physical processes occurring on the rupture surface as well as predicting the ground motion. However, the most important characteristic for judging a model is its ability to approximate the important elements of near-field seismic radiation from earthquakes. Since there are so few cases of applications of any model to the simulation of high-frequency strong ground motion, it is not even clear what elements of these models are important. For example, Madariaga (1978) showed that a Haskell model with the correctly used ramp-like slip function can produce infinite near-field accelerations in certain geometries but it is not clear which characteristics of the model must be modified to produce more desirable results. To simplify model validation, it is desirable to first determine what specific elements of the models are important in determining the characteristics of the radiation of seismic energy from such models. It is reasonable to assume that such a model will probably be kinematic. Numerical models of the rupture process are much too costly to be used for the frequencies of interest, though the results of such models can be used in the construction of kinematic models which contain information in the frequency range of interest. The early phases of model validation will be concerned with the sensitivity of the near-field ground motion characteristics to the details of kinematic models.

4.2 RUPTURE SPECIFICATION IN KINEMATIC MODELS

4.2.1 Introduction

Kinematic models must contain some specification of the history of the advancement of the rupture front from the hypocenter of the source. Simple models assume coherency of rupture with constant rupture velocity. Rupture is usually allowed

to initiate instantaneously at a point or on a line, accelerating instantaneously to a terminal value and decelerating instantaneously to zero velocity at a prescribed boundary. The physics of rupture propagation is not understood very well. Though this is not of great concern in studies of low frequency radiation, it must be considered carefully when dealing with high frequency characteristics of ground motion. The purpose of this section is to examine some of the consequences of the simple assumptions about the rupture history commonly used in kinematic models. The results given here are preliminary since only a few calculations have been performed to date. The calculations will attempt to determine the sensitivies to various parameters used to specify the rupture history and isolate those parameters most important for determining the high frequency characteristics of motion.

The following sections will examine the sensitivity of near-field ground motion to the stopping and starting of rupture propagation in simple kinematic models. The specific questions which will be addressed are:

1. Can one-dimensional rupture propagation models give reasonable results when starting and stopping of rupture is smoothed?

2. What constraints on rupture and slip velocity are needed to produce reasonable accelerations from rupture initiation at a point?

3. What are the differences in the accelerations produced by one- and two-dimensional rupture models?

Attention will be focused on ground motion characteristics in the plane of the fault, but off the rupture surface, where directionalized rupture effects are mot severe. Future studies will be more detailed after the essential model characteristics are isolated.

4.2.2 One-Dimensional Rupture

One-dimensional rupture (simultaneous rupture over a fault width), as used in the original Haskell model, can lead to some undesirable characteristics in the predicted ground motion. Madariaga (1978) showed that infinite accelerations are produced in certain geometries in the geometrical near-field, even for a ramp-like slip time history. At all geometries the high frequency characteristics are related to phases due to the sudden starting and stopping of the rupture at the edges and/or corners of the fault surface. By high frequencies in this case we mean high in the asymptotic sense. There must be some frequency at which the starting and stopping phase will dominate the radiation produced. In the geometrical far-field accelerations consist only of starting and stopping phases.

It is not clear whether the sudden stopping of rupture is present in earthquakes. Das and Aki (1977) demonstrated that our present views of fracture mechanics do not prohibit sudden stopping of the rupture front when a fracture barrier is present. Bouchon (1979) has used such barriers to interpret the Pacoima Dam recordings of the 1971 San Fernando, California earthquake, but it has not been established from observations that ruptures in earthquakes, in general, stop suddenly.

As an example of how important the abrupt starting and stopping can be in near-field motion, velocities and accelerations were computed at near fault locations for a standard Haskell model and a Haskell-like model with varying rupture velocity on the fault. The geometry used is shown in Figure 27. Stations were chosen in the fault plane in the focused direction, since this is where the differences in the two cases should be most pronounced. A simple ramp slip history is used with a slip velocity of 1/msec and a duration of one

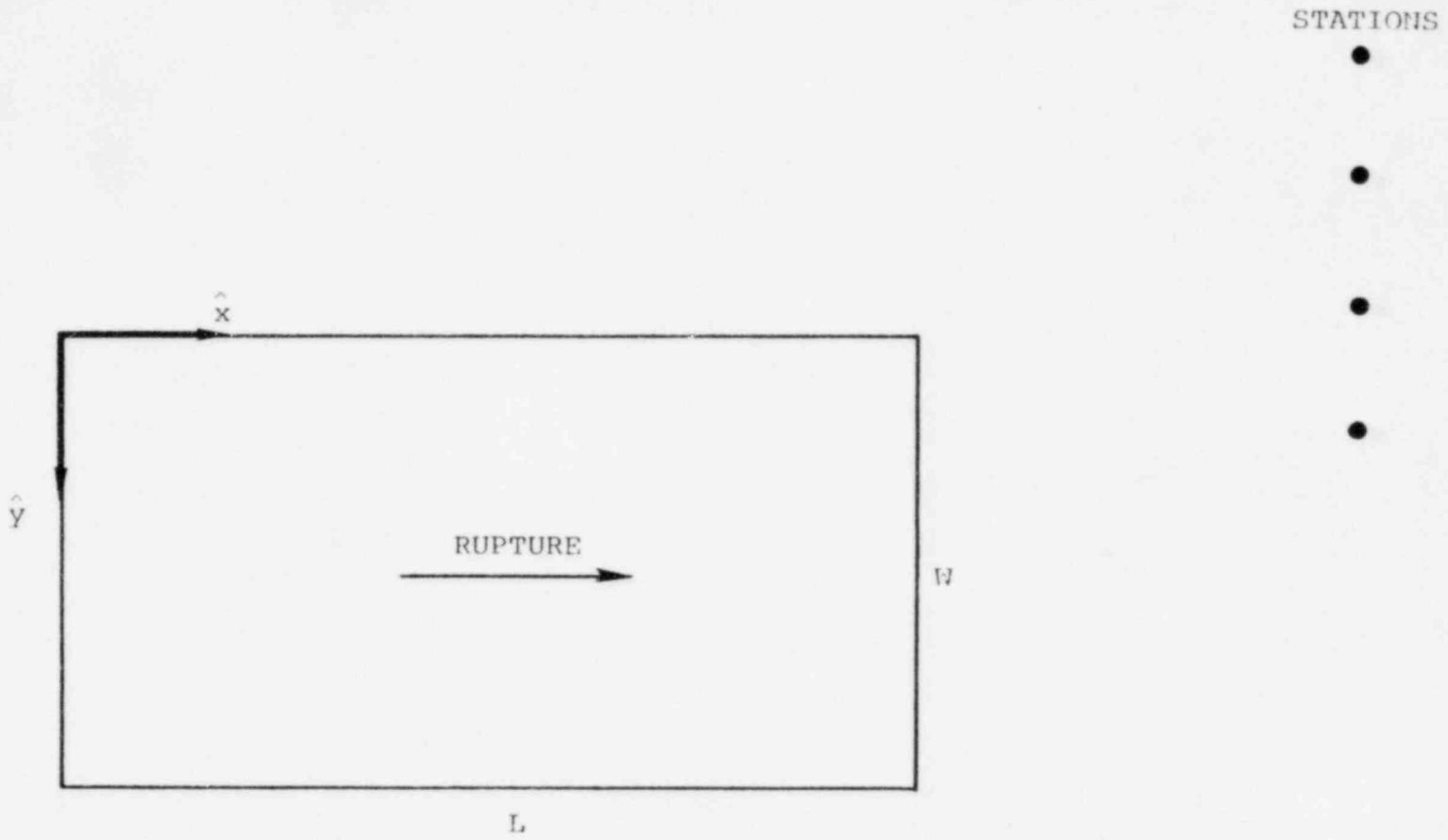

Figure 27. Geometry used in simulations. Fault length L = 10 km, W = 5 km and stations located at (x,y) = (15,-5), (15,-3), (15,-1), (15,1) in fault plane.

second. The source moment is 1.4×10^{25} dyne/cm and its approximate magnitude is about $M_L = 6.1$ (Hanks and Kanamori, 1979). Rupture velocity was chosen to be 0.9 of the shear velocity for constant rupture velocity cases and a maximum of that value for variable rupture cases.

Time series were obtained by numerical two-dimensional integration over the fault surface in the Fourier frequency domain, using transformed versions of Haskell's (1969) time domain solution and then transforming to the time domain by use of a fast Fourier Transform. The two-dimensional numerical integration was performed using a Gauss-Legendre (Davis and Rabinowitz, 1975) rule and was checked by comparison to a two-dimensional Romberg scheme which agreed to at least three decimal places in all checks made. A simple cosine tapering filter was applied from 5 Hz to the nyquist frequency of 6.25 Hz. Five hertz was chosen as the maximum frequency because it is high enough to correspond to wavelengths considerably shorter than any length scale in the problem and, therefore, would be representative of the high frequency behavior of the radiation. It is also low enough to keep cost manageable (expense is roughly proportional to maximum frequency cubed). For simplicity of interpretation, all calculations are done for an elastic wholespace. The final results were tested by comparisons to displacement solutions in Madariaga (1978).

Figures 28 and 29 show the velocities and accelerations computed at the four stations from the standard Haskell model. Since all four stations are in the plane of the fault, all of the ground motion is in the direction normal to the fault plane. This will be the case in all computations presented in this section. Accelerations in Figure 29 show many of the features noted by Madariaga (1978). At station (15, -5), for example, the motion is dominated by a series of steps

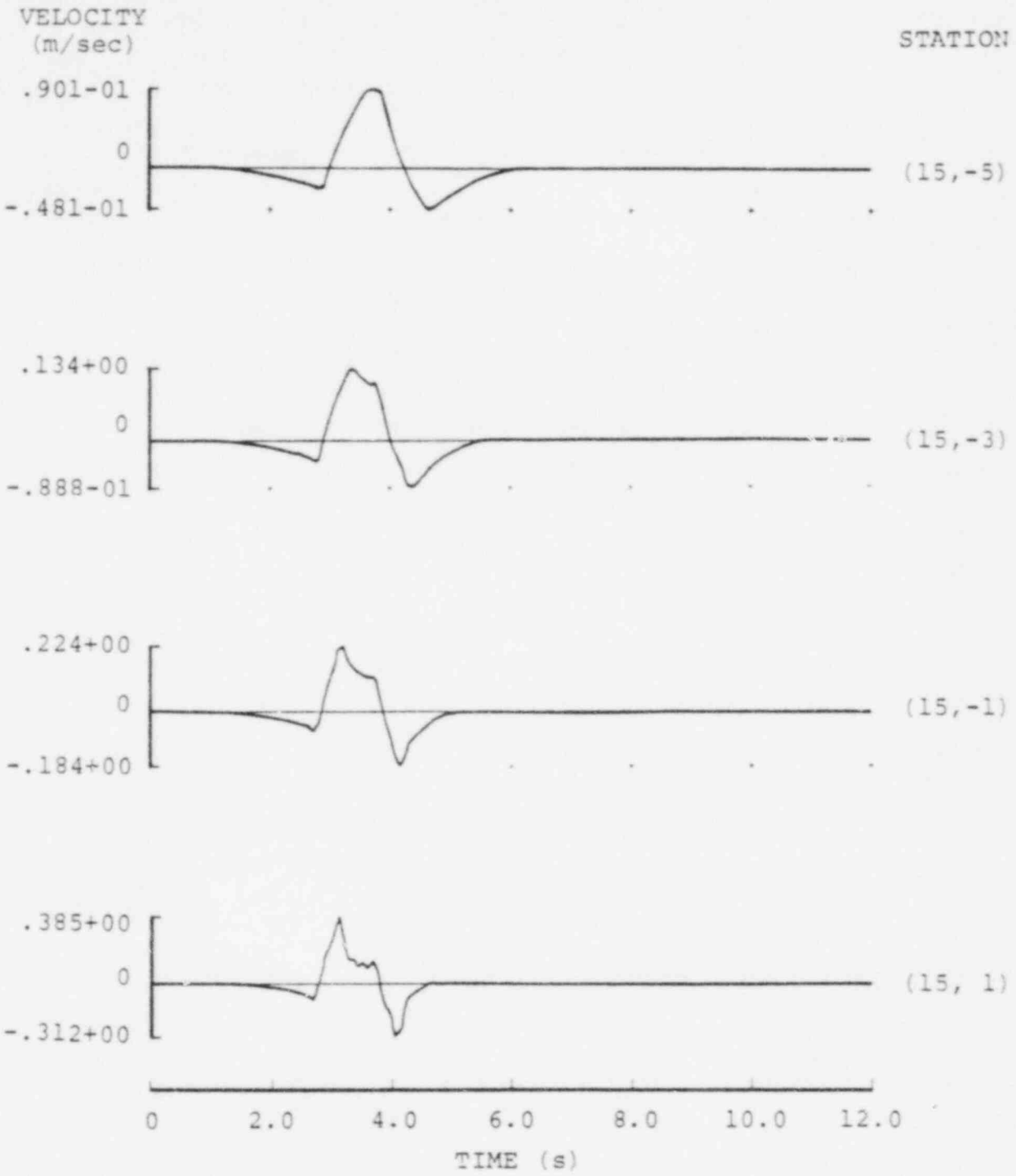

Figure 28. Ground velocities from the basic Haskell model.

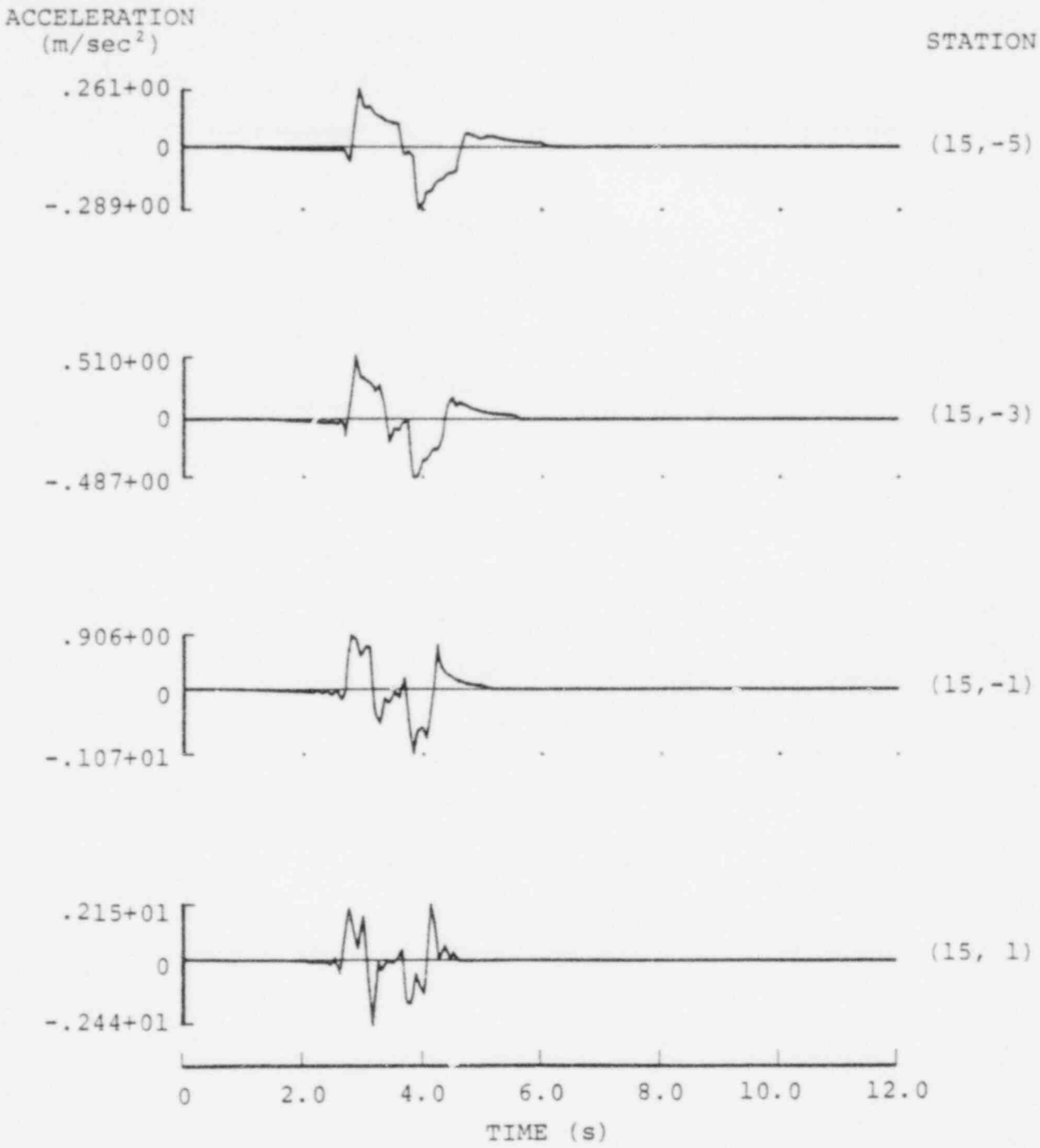

Figure 29. Accelerations from the basic Haskell model.

corresponding in time to arrivals from each of the far corners of the fault. There should be eight steps in this case because the slip history has both a starting and stopping contribution. Station (15, 1) is located in the cylindrical wave region noted by Madariaga where singular values of acceleration are to be expected. For the limited frequency band used in these calculations, the largest acceleration is not particularly high, 2.44 m/sec^2 or 0.24 g. The analytical solutions to this problem show that the singular accelerations are in the form of square-root singularities. The largest acceleration will roughly scale with the square-root of the frequency band passed. It is not desirable to have the maximum acceleration strongly dependent upon the frequency band used in processing, and there is little evidence to suggest that this is the case in strong ground motion recordings.

The distribution of amplitudes for the four stations is probably not very reasonable. Stations (15, 1) and (15,-5) differ in peak value by an order of magnitude and extending to high frequencies would probably increase the difference more. There are some slight differences in distance from the fault and radiation pattern between the two stations, but bulk of the difference is due to the location with respect to the rupture direction. Even though our density of strong motion recordings may not be sufficient to observe such differences if they are present in earthquake recordings, it is rather doubtful that differences of the magnitude shown here are physical.

It was suggested earlier that most of the effects seen here are primarily due to the abrupt starting and stopping of the rupture and not coherency over a large part of the fault. Calculations were made using the same fault model and stations, except the rupture velocity was tapered to zero at the edge of the fault. The rupture velocity was given the functional form

$$v(x) = 0.9\beta \sqrt{1 - \left(\frac{x - L/2}{L/2}\right)^2}$$

where v is rupture velocity, β the shear velocity and L the fault length. For most of the fault the rupture is very near or equal to the terminal value used in the previous calculation.

Figures 30 and 31 show the velocities and accelerations at the four stations for the varying rupture rate. The acceleration time histories are considerably simpler and appear to contain less high frequency energy, and the peak values of both velocity and acceleration are reduced to about 60 to 70 percent of those in the contant rupture velocity case. The reduction in amplitudes is quite similar to the ratio of average rupture velocities across the entire fault, 0.9β versus $2/\pi$ (0.9β) or 0.65. This is to be expected for the low frequencies which sense the fault processes as a whole, but it is somewhat surprising that acceleration gives similar results. In the geometrical far-field, the starting and stopping phase are the only motion seen in acceleration from dimensional models. One would expect removal of such phases to drastically change the peak values of acceleration. In the geometrical near-field it appears that internal points on the fault may also contribute significantly to acceleration.

The smoothing of starting and stopping of the rupture does lower the acceleration somewhat, but does very little to change the relative amplitudes at the four stations. The amplitude differences between Stations (15,-5) and (15,1) are unacceptable for the smoothed rupture as well as for abrupt starting and stopping case. One-dimensional rupture propagation is not acceptable approximation when acceleration is of interest.

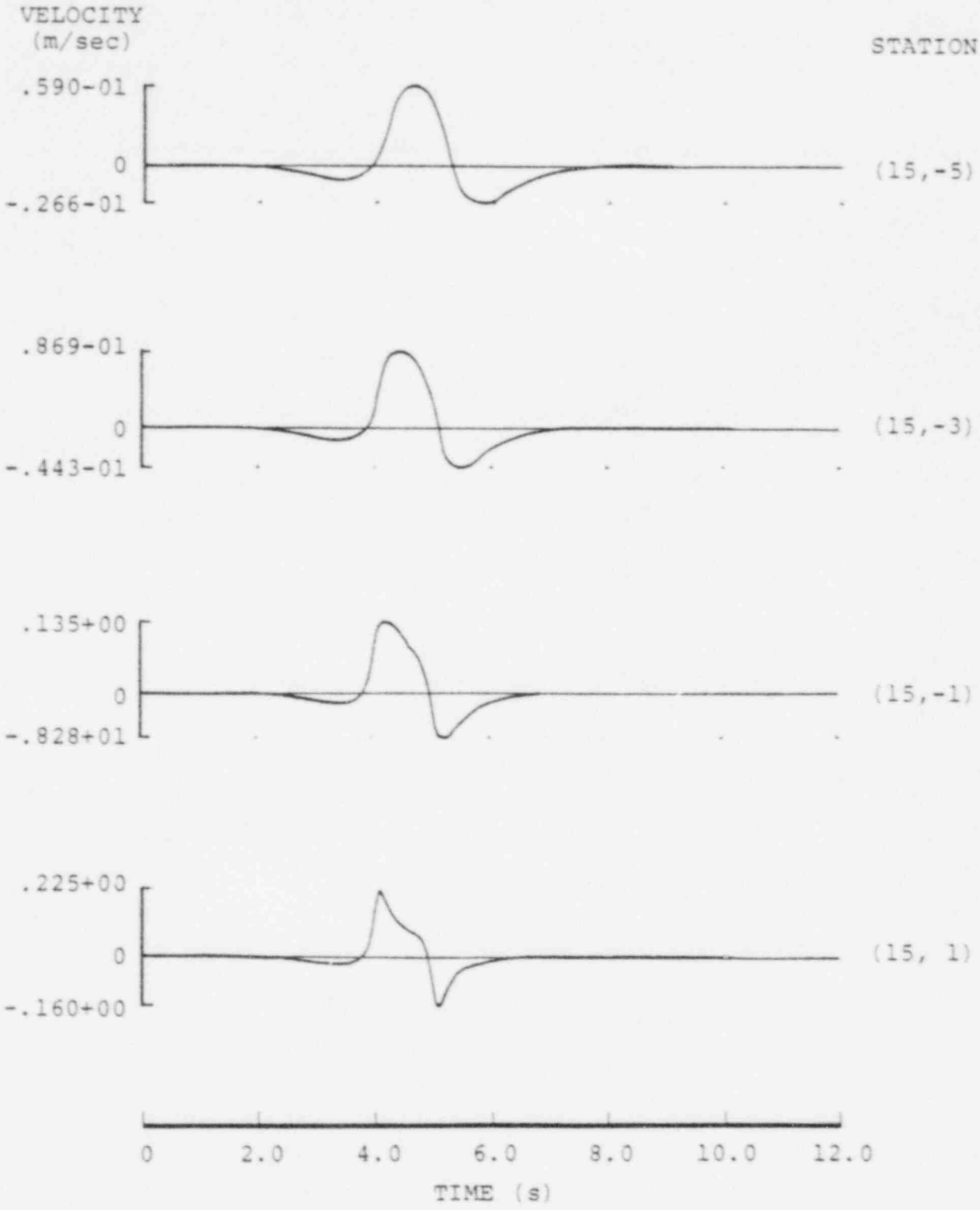

Figure 30. Velocities from variable rupture velocity model.

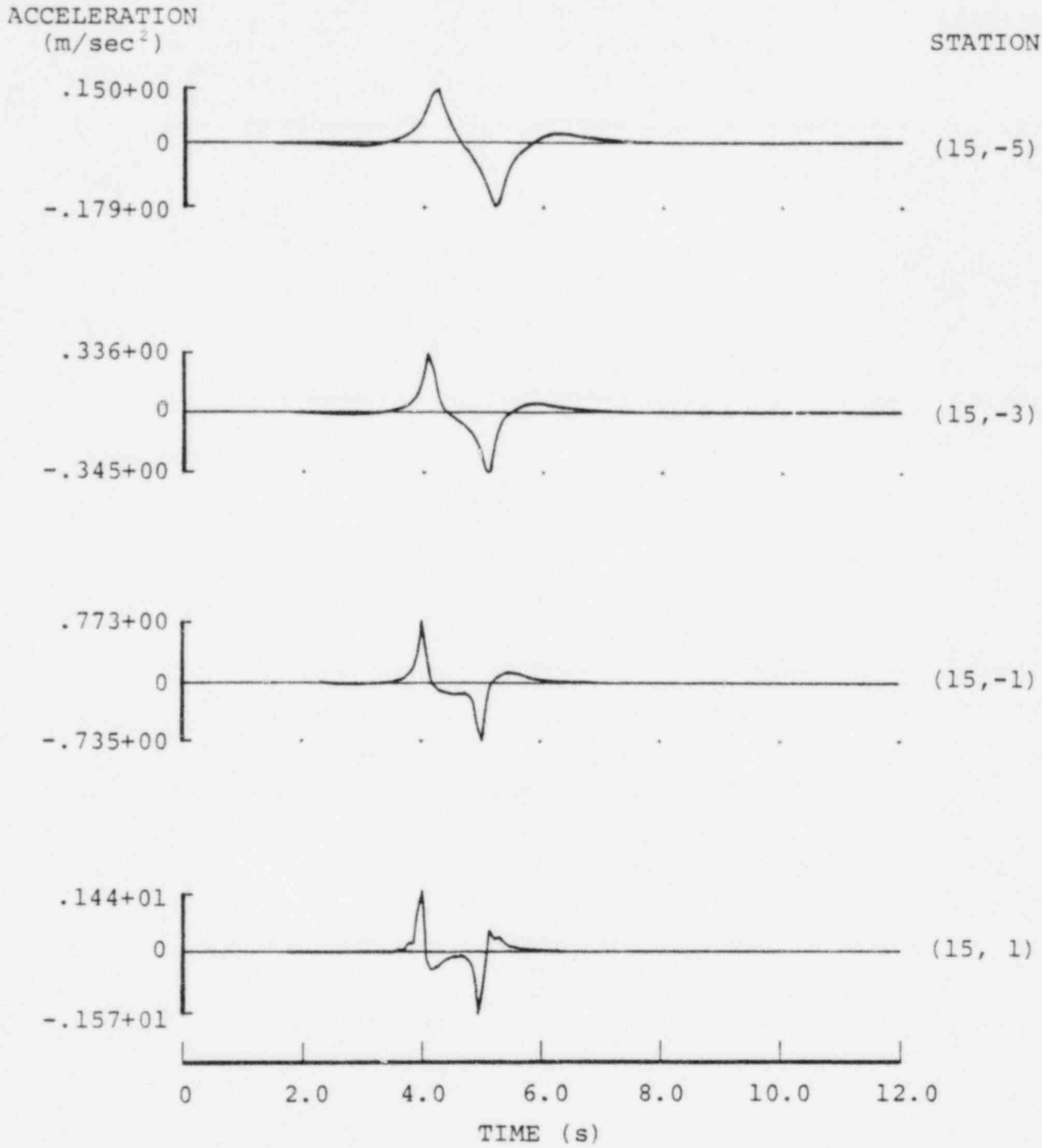

Figure 31. Accelerations from variable rupture velocity model.

4.2.3 Rupture Initiation from a Point

Most suggested models of the earthquake source included two-dimensional rupture initiating at a point. The high frequency radiation due to a sudden initiation in rupture is well known and analytical expressions are available for both expanding crack solutions and constant dislocation models. Contributions from stopping at the boundaries of the fault must be studied numerically. Approximations to the first motion due to the initiation of a shear crack have been formulated by Burridge and Willis (1969) and Richards (1973). For a circularly expanding rupture the shear wave accelerations due to initiation can be written

$$\ddot{u}(\bar{x},t) = \frac{v^2 \dot{D}_0 R(\bar{x})}{\beta \left(1 - \frac{v^2}{\beta^2} \sin^2\theta\right)^2} \frac{H(t-\tau_s)}{r}$$

where v is the rupture velocity, β the shear velocity, $\dot{D}_0$ the slip velocity at initiation, R the double couple radiation pattern, r the hypocentral distance, θ the angle from the fault normal, and τ_s the shear wave arrival time. The initial acceleration is proportional to slip velocity (which is proportional to effective stress) and is a rather sensitive function of rupture velocity. A similar expression for a constant dislocation model can be derived from Savage (1966) and it is identical except that

$$\left[1 - \frac{v^2}{\beta^2} \sin^2\theta\right]^2$$

must be replaced with

$$\left[1 - \frac{v^2}{\beta^2} \sin^2\theta\right]^{3/2} .$$

Because of the strong dependence of the acceleration on rupture velocity, there are only certain combinations of rupture velocities and slip velocity (or effective stress) which will result in reasonable values. Figure 32 shows the values of slip velocity as a function of rupture velocity necessary to produce a 0.5 g free field acceleration at the maximum of the radiation pattern in the fault plane and fault normal 10 km from the initiation. At the fault normal, the crack and constant dislocation solutions are the same. Note that large slip velocities and fast rupture velocities will produce enormous accelerations. For example, using a Mach number of 0.9, which is a quite popular value, one can produce a free-field acceleration of 0.5 g with as little as 67 cm/sec slip velocity with a crack model and 153 cm/sec using a constant dislocation model. These values are appropriate for the first motion only and possibly not even related to the largest acceleration predicted by a model. The above formulas are only appropriate for initiation of rupture in all directions. Rupture beginning on fault edges or corners will produce somewhat smaller values of initial acceleration.

Here we compare motion for a point initiation versus the one-dimension rupture propagation for the rectangular fault used in the Haskell model case. All source parameters are identical except that the rupture begins at the lower left hand corner, coordinate (0,5) and ruptures two-dimensional toward the stations at a velocity of 0.9, the shear wave velocity. Figures 33 and 34 show the velocities and accelerations at the four stations in the fault plane. For the Haskell model, the peak values are quite variable depending on the location of the station with respect to the rupture propagation direction. For rupture initiating at a point, the amplitudes of the four stations vary to a lesser degree and differences can probably be explained by slight differences in radiation pattern and distance from the fault. The peak

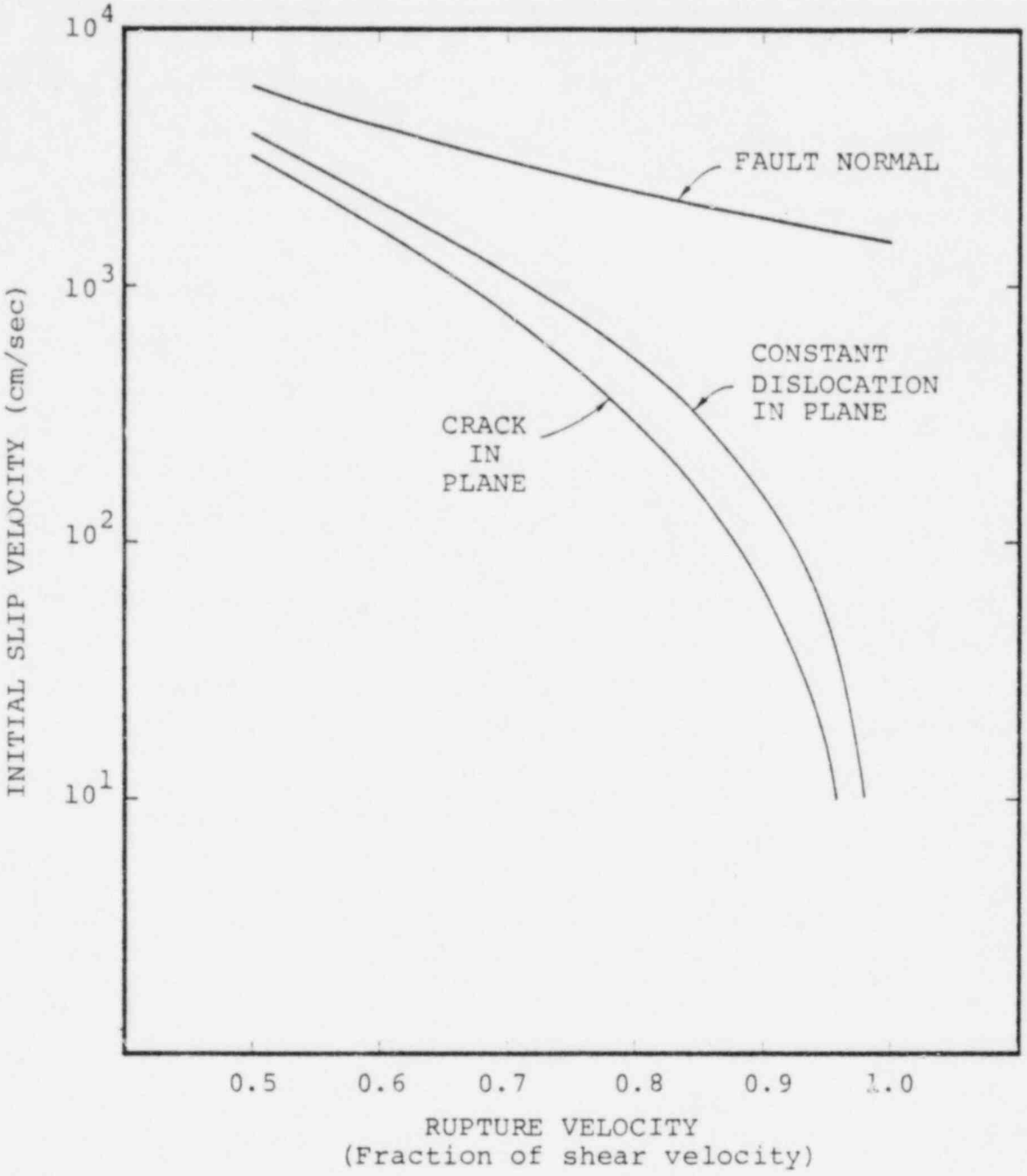

Figure 32. The initial slip velocity needed to produce 0.5 g free-field acceleration at 10 km distance from rupture initiation as a function of rupture velocity. Curves for an observer in the fault plane for both a crack and constant dislocation and at the fault normal (crack and dislocation solutions the same).

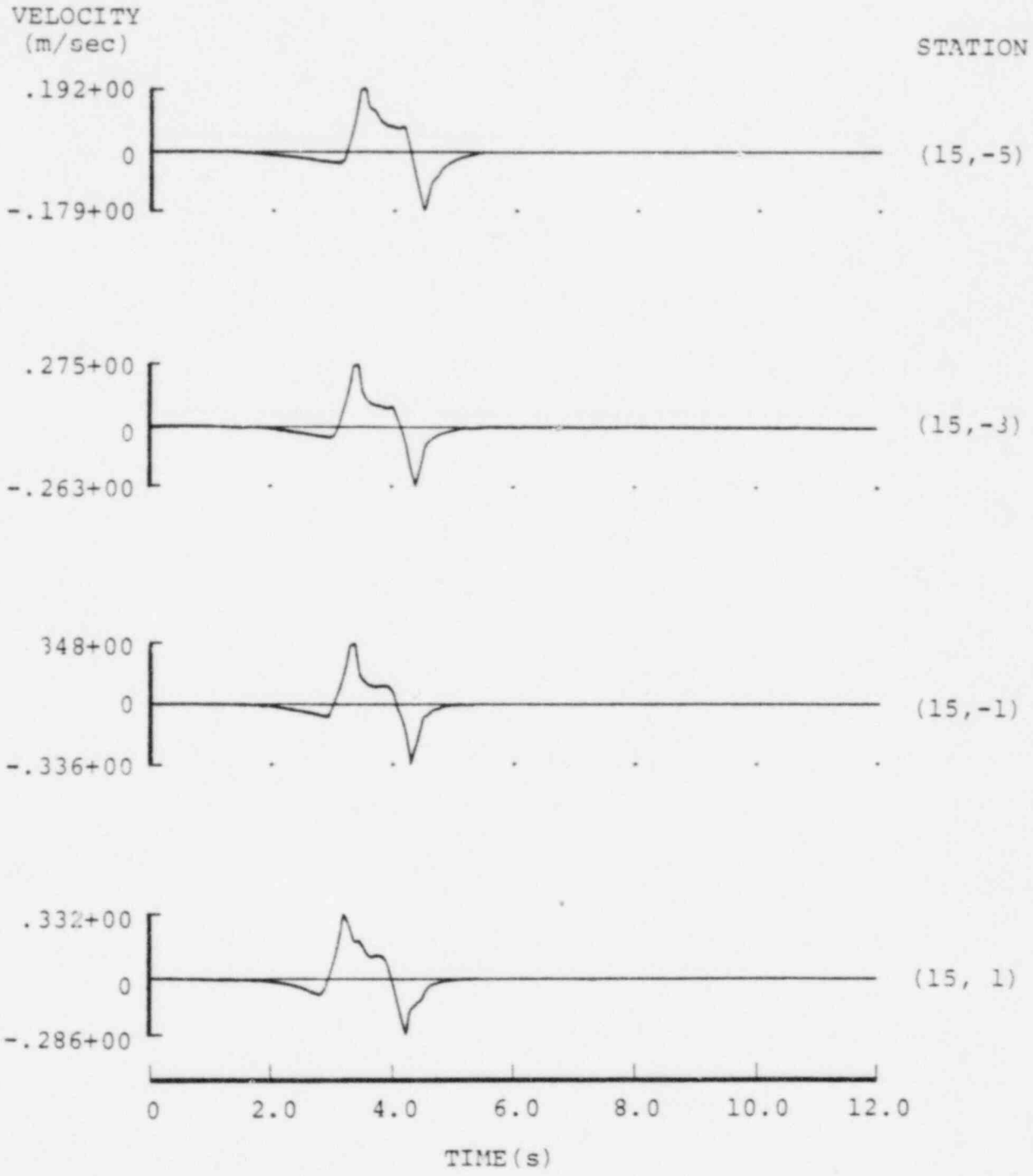

Figure 33. Velocities from point initiation of rupture at (O,W).

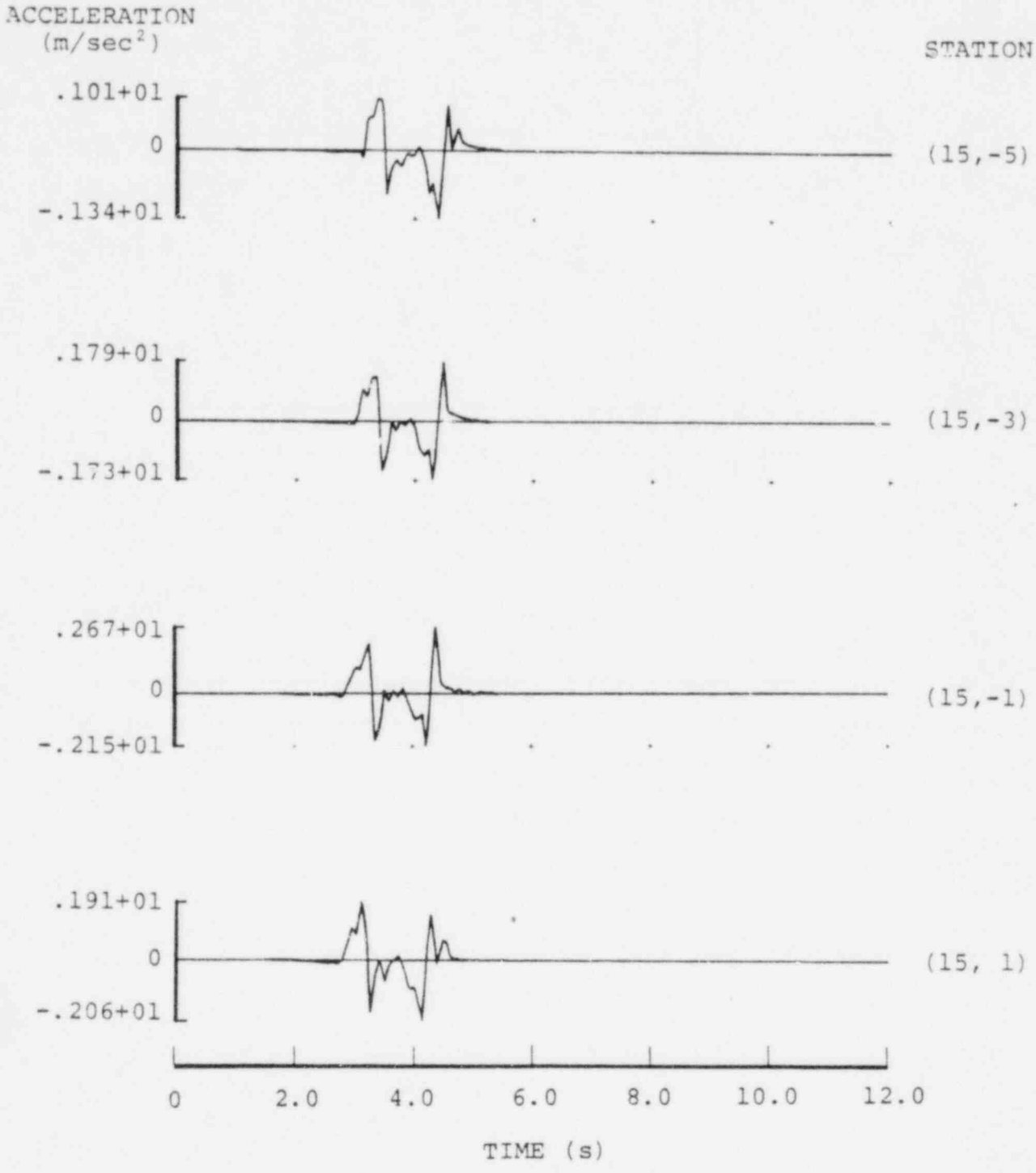

Figure 34. Accelerations from point initiation of ruptures.

amplitude at Station (15,1), which was in the line of rupture for the Haskell case, has been reduced in the two-dimensional rupture case. Station (15,-5), which now has rupture moving toward it, increased in amplitude significantly. One-dimensional rupture approximations will overestimate acceleration in some geometries and underestimate them in others.

The acceleration pulses are quite similar at the four stations. The initiation step in this case is very prominent, but only about one-half the size it would be if the rupture initiation was inside the fault boundary and not on a corner. The increase in acceleration after initiation may be due to contributions on the left and lower edges of the fault or possibly some internal slip. The first very sharp downward trend at all stations corresponds very well in time to a stopping phase radiated from the nearest corner of the fault. In this case, the slip duration is longer than the rupture time and the late characteristics in acceleration are due to the stopping of the slip and should mimic the early behavior except with a change in sign. This type of characteristic is unphysical since the slip duration should be coupled with the rupture history.

4.2.4 Summary

We have presented some preliminary results concerning the sensitivities of computed accelerations due to details in the specification of the rupture history in simple kinematic models. Calculations were limited to stations in the fault plane where directivity effects are thought to be most severe. More complete studies of the dependence of both time series and spectra quantities at various observation points will be necessary to clarify results.

One-dimensional rupture propagation is an unacceptable approximation when computing near-field acceleration. Directivity effects overestimate the ground motion in the rupture direction and underestimate the motion away from the rupture direction. Smoothing of the abrupt starting and stopping of the rupture reduces the accelerations produced from such models, but does not significantly alter the effects due to directionalized rupture.

Initiation of rupture propagation from a point appears to be a necessary element of a kinematic model used for computing near-field accelerations. If it is assumed that rupture accelerates instantaneously to a terminal value of rupture velocity, care must be taken to assure that the rupture velocity and slip velocity are compatible with one another. Otherwise, point initiation of rupture can produce very large accelerations in the plane of the fault. Radiation from the stopping of rupture is prominent in the near-field accelerations computed, particularly stopping at corners of the fault, but further work is necessary to clarify whether such stopping effects are actually present in observed accelerations.

V. SUMMARY, CONCLUSIONS AND FUTURE PLANS FOR THE STUDY PROGRAM

5.1 SUMMARY

This report has presented a status summary of a continuing investigation into the applicability of theoretical earthquake source modeling to the definition of design ground motion environments for nuclear power plants located in the near-field of potentially active faults. To date, most of the research effort has centered on a systematic evaluation and comparison of the various near-field ground motion prediction procedures which have been proposed by previous investigators. The results of this state-of-the-art review were presented in Sections II and III. This was followed in Section IV by a summary of some preliminary results of parametric studies conducted using specific source models with different assumptions concerning the initiation, propagation and stopping of the faulting process.

In Section II, a critical review of the various proposed empirical procedures for predicting near-field ground motion parameters (i.e. peak motions, spectra and time histories) was presented together with descriptions of some selected applications of these procedures. Six different, recently proposed peak motion prediction procedures were described and compared. In particular, each was used to predict the peak acceleration levels to be expected in the near-field ($R = 5$ km) of major earthquakes ($5.5 < M < 8.0$) and it was demonstrated that the range covered by these estimates exceeds an order of magnitude (cf. Figure 1). Three different ground motion spectra prediction techniques were also compared, including that specified in Regulatory Guide 1.60. Again, as with the peak estimates, it was demonstrated that there are significant differences between the near-field ground motion spectra predicted by these different methods, particularly in regard to overall spectral shape. Empirical time history prediction procedures were similarly reviewed and it was noted that all

the existing techniques rely heavily on empirical predictions of the peak amplitude and spectral characteristics of the expected motion and, consequently, are subject to all the uncertainties associated with the specification of these parameters at near-field distances.

Section III focused on an extensive and systematic review of the characteristics of the various proposed theoretical earthquake source models with particular emphasis on a critical evaluation of those assumptions which might affect the near-field ground motion characteristics predicted by the various models. For purposes of discussion, the models were subdivided into three classes: kinematic, simple dynamic and numerical. The kinematic class encompasses those models (e.g. Haskell, Savage) in which the displacement discontinuity (i.e. slip) across a predetermined rupture surface (i.e. fault plane) is specified independent of any explicit consideration of the forces driving the motion. It was noted that most of the strong ground motion calculations which have been performed to date, including those recently carried out by DELTA for the San Onofre Nuclear Generating Station site, have been kinematic in nature, despite the fact that simple dynamical considerations have been used to motivate the selection of the slip function in some cases. One feature common to all such models is the requirement to specify values for a variety of parameters in order to deterministically synthesize near-field ground motion. However, it was noted that in this approach the parameter values must be deduced empirically and, moreover, that the available empirical data do not provide very good constraints on the values for some of the parameters (e.g. stress drop, rupture velocity) which may have a strong influence on the computed ground motion.

The second class of models considered were the simple dynamic models typified by those of Kostrov (1964), Brune (1970) and Archambeau (1968). These theoretical models are simple approximations to the stress relaxation process. The limited

assumptions in these models make them unsatisfactory for synthesis of near-field motion, but they have proved useful in constraining certain physical parameters in earthquakes.

The final group of theoretical source models considered in Section III were those falling into the class of numerical models. For the most part, these can be viewed as extensions of the simple dynamic models to include consideration of a more realistic rupture which initiates at a point, propagates over a fault plane and stops when it reaches the boundaries of the predetermined rupture surface. It was noted that simulations performed using such models require extensive computations and consequently only a limited number are currently available. In spite of this limitation, these calculations have served to provide insight into the importance of the various simplifying assumptions commonly employed in the formulation of the kinematic models. It was noted, however, that even these relatively sophisticated models are oversimplified in that they assume that the fault surface and rupture propagation is known and that there is a constant effective stress acting on a single fault surface.

Some of these issues were addressed in more detail in Section IV where selected assumptions identified in the derivation of the theoretical models of Section III were evaluated through detailed parametric simulations. In particular, it was demonstrated that the computed near-field ground motion characteristics are sensitive to whether rupture is initiated at a point as opposed to simultaneously across the width of the fault and to whether the rupture gradually decelerates rather than stopping suddenly as is commonly assumed.

5.2 CONCLUSIONS

This report summarizes the research conducted during the first year of a two-year study program and, consequently,

definitive conclusions regarding the applicability of theoretical earthquake source models to the prediction of near-field ground motion characteristics are not yet available. However, some preliminary conclusions can be drawn on the basis of the research conducted to date. These are:

1. Existing empirical procedures for predicting peak motions are not adequately constrained by the available near-field data, as evidenced by the fact that the variability in near-field peak motions predicted using the different procedures can exceed an order of magnitude.

2. Detailed statistical analyses of strong ground motion spectra suggest that the spectral shape should be a function of magnitude and distance. The current Regulatory Guide 1.60 standard design spectra do not account for this variability and tend to be significantly broader than those predicted on the basis of the statistical analyses.

3. Evidence suggests that normalizing design response spectra to predicted peak acceleration levels at near-field distances is not only subject to the large uncertainties associated with the peak specification, but may lead to design spectra which are too conservative over much of the frequency band of interest, particularly if the acceleration peak is an isolated high frequency arrival.

4. Computation of broadband (up to 20 Hz) near-field ground motions using kinematic source models involves the specification of a number of poorly constrained parameters. The results

of such computations are subject to large uncertainties unless further constraints can be found either in the theory or in more detailed analyses of the observations.

5. Most dynamic models of earthquakes are deficient in that they contain no physical description of the process by which ruptures stop. Parametric calculations involving different, plausible approximations indicate that the selected mode of stopping can significantly affect the computed near-field, high frequency motions. It has not been determined which proposed descriptions of the stopping of rupture propagation are appropriate for the earthquake process.

6. Parametric studies indicate that the computed near-field ground motion characteristics are sensitive to whether rupture is initiated at a point or simultaneously across the width of the fault, as is sometimes assumed in kinematic modeling. Simultaneous rupture across the fault width, though often a reasonable assumption in far-field studies, is not acceptable for near-field ground motion simulations.

7. Parametric studies indicate that coherent rupture propagation over a fault plane with dimensions thought to be appropriate for earthquakes of interest does not necessarily lead to unreasonably high peak acceleration levels in the near-field. This is contrary to the assertions of some previous investigators.

5.3 FUTURE PLANS FOR THE STUDY EFFORT

As a result of the state-of-the-art review conducted during the past year, the various theoretical earthquake source models available for simulating near-field ground motion have been identified and characterized. In the coming year, the study will focus on more detailed evaluations of the applicability of these models to the problem of defining design ground motion characteristics for nuclear power plants located in the near-field of potentially active faults. In particular, parametric studies, such as those described in Section IV of this report, will be extended and used to assess the importance of various modeling assumptions on the near-field ground motion characteristics predicted by the models. Once this has been accomplished, those models which have been shown to be physically plausible will be tested against the available strong motion data sample. That is, selected source models will be used in conjunction with highly simplified models of the propagation path to make predictions corresponding to a number of near-field ground motion observations. Those models which are found to be consistent with the observed peak amplitudes, spectra and time histories will be identified and their relative strengths and weaknesses will be analyzed and documented.

Once these tasks have been completed, a comprehensive report will be prepared which will summarize the current level of understanding of near source ground motion characteristics and identify specific analytical earthquake source modeling procedures which appear to be applicable to the design process.

REFERENCES

Aki, K. (1967), "Scaling Law of Seismic Spectrum," JGR, 72, pp. 1217-1223.

Aki, K. (1968), "Seismic Displacements Near a Fault," JGR, 73, pp. 5359-5376.

Ambraseys, N. N. (1969), "Maximum Intensity of Ground Movements Caused by Faulting," Paper presented at the Fourth World Conference on Earthquake Engineering, Santiago, Chile.

Anderson, J. G. (1974), "A Dislocation Model for the Parkfield Earthquake," BSSA, 64, pp. 671-686.

Anderson, J. G. (1976), "Motions Near a Shallow Rupturing Fault: Evaluation of Effects Due to the Free Surface," Geophys. J., 46, pp. 575-593.

Anderson, J. G. and P. G. Richards (1975), "Comparison of Strong Ground Motion from Several Dislocation Models," Geophys. J., 42, pp. 347-374.

Andrews, D. J. (1979), "A Stochastic Fault Model," preprint.

Archambeau, C. B. (1968), "General Theory of Elastodynamic Source Fields," Rev. Geophys., 6, pp. 241-288.

Archuleta, R. J. (1976), "Experimental and Numerical Three-Dimensional Simulations of Strike-Slip Earthquakes," Ph.D. Dissertation, University of California at San Diego.

Archuleta, R. J. and J. N. Brune (1975), "Surface Strong Motion Associated with a Strike-Slip Event in a Foam Rubber Model of Earthquakes," BSSA, 65, pp. 1059-1072.

Archuleta, R. J. and S. M. Day (1979), "Dynamic Rupture in a Layered Medium: 1966 Parkfield Earthquake," in preparation.

Archuleta, R. J., W. B. Joyner and D. M. Boore (1978), "A Methodology for Predicting Ground Motion at Specific Sites," Proceedings of the Second International Conference on Microzonation for Safer Construction - Research and Application, San Francisco, California, November 26 - December 1, 1978, pp. 255-266.

Bache, T. C. and T. G. Barker (1978), "The San Fernando Earthquake - A Model Consistent with Near-Field and Far-Field Observations at Long and Short Periods," Systems, Science and Software Final Technical Report submitted to the U.S. Geological Survey, SSS-R-79-3552, January 1979.

Bache, T. C. and T. G. Barker (1979), "Earthquake Source Models Inferred from Long and Short Period Teleseismic Observations," Systems, Science and Software Final Technical Report sponsored by the U. S. Geological Survey, SSS-R-80-4206, October.

Bernreuter, D. L. (1977), "A Geophysical Assessment of Near-Field Ground Motion and the Implications for the Design of Nuclear Installations," Paper presented at the CSNI Specialist Meeting on the 1976 Friuli Earthquake and The Antiseismic Design of Nuclear Installations, Rome, Italy.

Boatwright, J. and D. M. Boore (1975), "A Simplification in the Calculation of Motions Near a Propagating Dislocation," BSSA, 65, pp. 133-138.

Boore, D. M. (1977), "Strong-Motion Recordings of the California Earthquake of April 18, 1906," BSSA, 60, pp. 651-678.

Boore, D. M. and W. B. Joyner (1978), "The Influence of Rupture Incoherence on Seismic Directivity," BSSA, 68, pp. 283-300.

Boore, D. M., A. A. Oliver, III, R. A. Page and W. B. Joyner (1978), "Estimation of Ground Motion Parameters," U. S. Geological Survey Open-File Report 78-509.

Boore, D. M. and D. J. Stierman (1976), "Source Parameters of the Point Mugu, California, Earthquake of February 21, 1973," BSSA, 66, pp. 385-404.

Boore, D. M. and M. D. Zoback (1974), "Near Field Motions from Kinematic Models of Propagating Faults," BSSA, 64, pp. 321-342.

Bouchon, M. (1978), "A Dynamic Source Model for the San Fernando Earthquake," BSSA, 68, pp. 1555-1576.

Bouchon, M. and K. Aki (1977), "Discrete Wave-Number Representation of Seismic-Source Wave Fields," BSSA, 67, pp. 259-278.

Brady, A. G. (1966), "Studies of Response to Earthquake Ground Motion," Ph.D. Thesis, California Institute of Technology.

Brady, A. G. and R. Husid (1966), "Distribution of Maximum Response to Random Excitation," RILEM Symposium.

Brune, J. N. (1970), "Tectonic Stress and the Spectra of Seismic Shear Waves from Earthquakes," JGR, 75, pp. 4997-5009.

Burridge, R. (1973), "Admissible Speeds for Plane-Strain Self-Similar Cracks with Friction but Lacking Cohersion," Geophys. J., 35, pp. 439-455.

Burridge, R. and L. Knopoff (1964), "Body Force Equivalents for Seismic Dislocations," BSSA, 54, pp. 1875-1888.

Burridge, R. and J. R. Willis (1969), "The Self-Similar Problem of the Expanding Elliptical Crack in an Anisotropic Solid," Proc. Cambridge Phil. Soc., 66, pp. 443-468.

Burridge, R. and C. Levy (1974), "Self-Similar Circular Shear Cracks Lacking Cohesion," BSSA, 64, pp. 1789-1808.

Bycroft, G. N. (1960), "White Noise Representation of Earthquakes," Proceedings ASCE, 86, EM2, pp. 1-16.

Cherry, J. T., E. J. Halda and K. G. Hamilton (1976), "A Deterministic Approach to the Prediction of Free Field Ground Motion and Response Spectra from Stick-Slip Earthquakes," Earthquake Engng. and Struct. Dyn., 4, pp. 315-332.

Crandall, S. H., K. L. Chandirmani and R. G. Cook (1966), "Some First-Passage Problems in Random Vibration," Transactions ASME, pp. 532-538.

Dahlen, F. A. (1974), "On the Ratio of P-Wave to S-Wave Corner Frequencies for Shallow Earthquake Sources," BSSA, 64, pp. 1159-1180.

Das, S. and K. Aki (1977), "Fault Plane with Barrieris: A Versatile Earthquake Model," JGR, 82, pp. 5658-5670.

Davis, P. J. and P. Rabinowitz (1975), "Methods of Numerical Integration," Academic Press, New York.

Day, S. M. (1979), "Three-Dimensional Simulation of Rectangular Fault Dynamics," Interim Report prepared for the Institute for Advanced Computation, Systems, Science and Software Report SSS-R-80-4161, September.

Day, S. M., T. C. Bache, T. G. Barker and J. T. Cherry (1978), "A Source Model for the 1975 Pocatello Valley Earthquake," Systems, Science and Software, Scientific Report to the Air Force Geophysics Laboratory, SSS-R-79-3893, December.

De Hoop, A. T. (1958), "Representation Theorems for the Displacement in an Elastic Solid and Their Applications to Elastodynamic Diffraction Theory," Thesis, Technische Hogeschool, Delft.

DELTA (Del Mar Technical Associates) (1978), "Simulation of Earthquake Ground Motions for San Onofre Nuclear Generating Station Unit 1," Final Report for Southern California Edison Company, submitted for review to the Nuclear Regulatory Commission.

Donovan, N. C. (1973), "A Statistical Evaluation of Strong Motion Data Including the February 9, 1971 San Fernando Earthquake," Paper presented at the Fifth World Conference on Earthquake Engineering, Rome, Italy.

Eaton, J. P. (1967), "The Parkfield-Cholame, California, Earthquakes of June-August, 1966; Instrumental Seismic Studies," U. S. Geological Survey Professional Paper 579.

Esteva, L. (1970), "Seismic Risk and Seismic Design Input for Nuclear Power Plants," in Seismic Design for Nuclear Power Plants, edited by R. J. Hansen, pp. 438-483.

Filson, J. and T. V. McEvilly (1967), "Love-Wave Spectra and the Mechanism of the 1966 Parkfield Sequence," BSSA, 57, pp. 1245-1257.

Geller, R. J. (1976), "Scaling Relations for Earthquake Source Parameters and Magnitude," BSSA, 66, pp. 1501-1524.

Gutenberg, B. and C. F. Richter (1956), "Earthquake Magnitude, Intensity, Energy and Acceleration," BSSA, 46, pp. 105-145.

Guzman, R. and P. C. Jennings (1976), "Design Spectrum for Nuclear Power Plants," J. Power Div., Am. Soc. Civil Engrs., 102, pp. 165-178.

Hanks, T. C. (1974), "The Faulting Mechanisms of the San Fernando Earthquake," JGR, 79, pp. 1215-1229.

Hanks, T. C. (1979), "b Values and $\omega^{-\gamma}$ Seismic Source Models: Implications for Tectonic Stress Variations Along Active Crustal Fault Zones and the Estimation of High Frequency Strong Ground Motion," JGR, 84, pp. 2235-2242.

Hanks, T. C. and H. Kanamori (1979), "A Moment Magnitude Scale," JGR, 84, pp. 2348-2350.

Hartzell, S. H., G. A. Frazier and J. M. Brune (1978), "Earthquake Modeling in a Homogeneous Half-Space," BSSA, 68, pp. 301-316.

Haskell, N. A. (1964), "Total Energy and Energy Spectral Density of Elastic Wave Radiation from Propagating Faults," BSSA, 54, pp. 1811-1841.

Haskell, N. A. (1966), "Total Energy and Energy Spectral Density of Elastic Wave Radiation from Propagating Fault, 2, a Statistical Source Model," BSSA, 56, pp. 125-140.

Haskell, N. A. (1969), "Elastic Displacements in the Near Field of a Propagating Fault," BSSA, 59, pp. 865-908.

Heaton, T. H. and D. V. Helmberger (1977), "A Study of the Strong Ground Motion of the Borrego Mountain, California Earthquake," BSSA, 67, pp. 315-330.

Herrmann, R. B. and O. W. Nuttli (1975), "Ground-Motion Modeling at Regional Distances for Earthquakes in a Continental Interior, II. Effect of Focal Depth, Azimuth and Attenuation," Earthquake Engng. and Struct. Dyn., 4, pp. 59-72.

Housner, G. W. (1947), "Characteristics of Strong-Motion Earthquakes," BSSA, 37, pp. 19-31.

Housner, G. W. (1955), "Properties of Strong Ground Motion Earthquakes," BSSA, 45, pp. 187-218.

Housner, G. W. (1965), "Intensity of Ground Shaking Near the Causative Fault," Paper presented at the Third World Conference on Earthquake Engineering, New Zealand.

Housner, G. W. and P. C. Jennings (1964), "Generation of Artificial Earthquakes," Proceedings ASCE, 90, EM1, pp. 113-150.

Husid, R. (1967), "Gravity Effects on the Earthquake Response of Yielding Structures, Report on Earthquake Engineering Research Laboratory, California Institute of Technology

Ida, Y. (1973), "The Maximum Acceleration of Seismic Ground Motion," BSSA, 63, pp. 959-968.

Israel, M. and R. Kovach (1977), "Near-Field Motions from a Propagating Strike-Slip Fault in an Elastic Half-Space," BSSA, 67, pp. 977-994.

Israel, M. and M. Vered (1977), "Near-Field Source Parameters by Finite Source Theoretical Seismograms," BSSA, 67, pp. 631-640.

Kanamori, H. and D. L. Anderson (1975), "Theoretical Basis of Some Empirical Relations in Seismology," BSSA, 65, pp. 1073-1098.

Kawasaki, I. (1975), "On the Dynamic Process of the Parkfield Earthquake of June 28, 1966," J. Phys. Earth, 23, pp. 127-144.

Keilis-Borok, V. (1959), "An Estimation of the Displacement in an Earthquake Source and of Source Dimensions," Ann. Geofis., 12, pp. 205-214.

Kostrov, B. V. (1964), "Self-Similar Problems of Propagating Shear Cracks," J. Appl. Math. Mech., 28, pp. 1077-1087.

Kostrov, B. V. (1968), "The Inverse Problem of the Theory of Earthquake Foci," Bull. (Izv.) Acad. Sci., USSR, Earth Physics, No. 9.

Levy, N. A. and A. K. Mal (1976), "Calculations of Ground Motion in a Three-Dimensional Model of the 1966 Parkfield Earthquake," BSSA, 66. pp. 405-424.

Madariaga, R. (1976), "Dynamics of an Expanding Circular Fault," BSSA, 66, pp. 639-666.

Madariaga, R. (1977), "Modeling of Three-Dimensional Earthquake Faults by Finite Differences," (Abstract) AGU Fall Meeting, San Francisco, December 5-9, 1977.

Madariaga, R. (1978), "The Dynamic Field of Haskell's Rectangular Dislocation Fault Model," BSSA, 68, pp. 869-888.

McGarr, A., S. M. Spottiswoode, N. C. Gay and W. D. Ortlepp (1979), "Observations Relevant to Seismic Driving Stress, Stress Drop and Efficiency," JGR, 84, pp. 2251-2261.

McGuire, R. K. (1978a), "Seismic Ground Motion Parameter Relations," J. Geotech. Engr. Div., Proceedings of the American Society of Civil Engineers, 104, pp. 481-490.

McGuire, R. K. (1978b), "A Simple Model for Estimating Fourier Amplitude Spectra of Horizontal Ground Acceleration," BSSA, 68, pp. 803-822.

Minster, J. B. (1973), "Elastodynamics of Failure in a Continuum," Ph.D. Thesis, California Institute of Technology, Pasadena, California.

Molnar, P., B. E. Tucker and J. N. Brune (1973), "Corner Frequencies of P and S Waves and Models at Earthquake Sources," BSSA, 63, pp. 2091-2104.

Murphy, J. R. and L. J. O'Brien (1977), "The Correlation of Peak Ground Acceleration Amplitude with Seismic Intensity and Other Physical Parameters," BSSA, 67, pp. 877-915.

Newmark, N. M., J. A. Blume and K. W. Kapur (1973), "Seismic Design Spectra for Nuclear Power Plants," J. of Power Div., Proceedings of the American Society of Civil Engineers, 99, pp. 287-303.

Niazy, A. (1975), "An Exact Solution for Finite, Two-Dimensional Moving Dislocation in an Elastic Half-Space with Application to the San Fernando Earthquake of 1971," BSSA, 65, pp. 1797-1826.

Ohnaka, M. (1973), "A Physical Understanding of the Earthquake Source Mechanism," J. Phys. Earth, 21, pp. 39-59.

Orphal, D. L. and J. A. Lahoud (1974), "Prediction of Peak Ground Motion from Earthquakes," BSSA, 64, pp. 1563-1574.

Page, R. A., D. M. Boore, W. B. Joyner and H. W. Coulter (1972), "Ground Motion Values for Use in the Seismic Design of the Trans-Alaska Pipeline System," U. S. Geological Survey Circular 672.

Rascon, O. A. and C. A. Cornell (1968), "Strong Motion Earthquake Simulation," Research Report R68-15, School of Engineering, Massachusetts Institute of Technology.

Reid, H. F. (1911), "Elastic Rebound Theory," Bull. Dept. Geol. Sci., 6, University of California Publication.

Richards, P. (1973), "The Dynamic Field at a Growing Plane Elliptical Shear Crack," Int. J. Solids and Structures, 9, pp. 843-861.

Richards, P. G. (1976), "Dynamic Motions Near an Earthquake Fault: A Three-Dimensional Solution," BSSA, 66, pp. 415-431.

Richter, C. F. (1958), Elementary Seismology.

Rosenblueth, E. and J. I. Bustamente (1962), "Distribution of Structural Response to Earthquakes," Proceedings ASCE, 88, EM3, pp. 75-106.

Sato, R. (1975), "Fast Computation of Theoretical Seismograms for an Infinite Medium, Part I. Rectangular Fault," J. Phys. Earth, 23, pp. 323-331.

Sato, T. and T. Hirasawa (1973), "Body Wave Spectra from Propagating Shear Cracks," J. Phys. Earth, 21, pp. 415-431.

Savage, J. C. (1966), "Radiation from a Realistic Model of Faulting," BSSA, 56, pp. 577-592.

Savage, J. C. (1972), "Relation of Corner Frequency to Fault Dimensions," JGR, 77, pp. 3788-3795.

Savage, J. C. (1974), "Relation Between P and S Corner Frequencies in the Seismic Spectrum," BSSA, 64, pp. 1621-1627.

Schnabel, P. B. and H. B. Seed (1973), "Accelerations in Rock for Earthquakes in the Western United States," BSSA, 63, pp. 501-516.

Somerville, P. G., R. A. Wiggins and R. M. Ellis (1976), "Time-Domain Determination of Earthquake Fault Parameters from Short-Period P Waves," BSSA, 66, pp. 1459-1484.

Swanger, H. J. and D. M. Boore (1978a), "Simulation of Strong-Motion Displacements Using Surface-Wave Modal Superposition," BSSA, 68, pp. 907-922.

Swanger, H. J. and D. M. Boore (1978b), "Importance of Surface Waves in Strong Ground Motion in the Period Range of 1 to 10 Seconds," Proceedings of the Second International Conference on Microzonation for Safer Construction - Research and Application, San Francisco, California, November 26 - December 1, 1978, pp. 1447-1457.

Swanger, H. J., J. R. Murphy and R. Guzman (1979), "State-of-the-Art Study Concerning Near-Field Earthquake Ground Motion," Systems, Science and Software Quarterly Technical Report to the Nuclear Regulatory Commission, SSS-R-79-4021, April.

Thatcher, W. and T. C. Hanks (1973), "Source Parameters of Southern California Earthquakes," JGR, 78, pp. 8547-8576.

Trifunac, M. D. (1976a), "Preliminary Analysis of the Peaks of Strong Earthquake Ground Motion: Dependence of Peaks on Earthquake Magnitude, Epicentral Distance, and Recording Site Conditions," BSSA, 66, pp. 189-219.

Trifunac, M. D. (1976b), "Preliminary Empirical Model for Scaling Fourier Amplitude Spectra of Strong Ground Acceleration in Terms of Earthquake Magnitude, Source-to-Site Distance, and Recording Site Conditions," BSSA, 66, pp. 1343-1373.

Trifunac, M. D. and A. G. Brady (1975), "On the Correlation of Seismic Intensity Scales with the Peaks of Recorded Strong Ground Motion," BSSA, 65, pp. 139-162.

Trifunac, M. D. and F. E. Udwadia (1974), "Parkfield, California Earthquake of June 27, 1966: A Three-Dimensional Moving Dislocation," BSSA, 64, pp. 511-534.

Wiggins, J. H., Jr. (1964), "Effect of Site Conditions on Earthquake Intensity," J. of Struc. Div., Am. Soc. of Civil Engrs., 90, pp. 279-313.

Wiggins, R. A., G. A. Frazier, J. Sweet and R. Apsel (1978), "Modeling Strong Motions from Major Earthquakes," Proceedings of the Second International Conference on Microzonation for Safer Construction - Research and Application, San Francisco, California, November 26 - December 1, 1978, pp. 693-700.

NRC FORM 335 (7-77)

U.S. NUCLEAR REGULATORY COMMISSION

BIBLIOGRAPHIC DATA SHEET

1. REPORT NUMBER (Assigned by DDC)
NUREG/CR-1340
SSS-R-80-4217

4. TITLE AND SUBTITLE (Add Volume No., if appropriate)
State-of-the-Art Study Concerning Near-Field Earthquake Ground Motion

2. (Leave blank)

3. RECIPIENT'S ACCESSION NO.

7. AUTHOR(S)
H. J. Swanger, J. R. Murphy, et al.

5. DATE REPORT COMPLETED
MONTH: January YEAR: 1980

9. PERFORMING ORGANIZATION NAME AND MAILING ADDRESS (Include Zip Code)
Systems, Science and Software
P.O. Box 1620
La Jolla, California 92038

DATE REPORT ISSUED
MONTH: August YEAR: 1980

6. (Leave blank)

8. (Leave blank)

12. SPONSORING ORGANIZATION NAME AND MAILING ADDRESS (Include Zip Code)
Site Safety Research Branch
Division of Reactor Safety Research
U.S. Nuclear Regulatory Commission
Washington, D.C. 20555

10. PROJECT/TASK/WORK UNIT NO.

11. CONTRACT NO.
FIN No. B6491

13. TYPE OF REPORT
Annual Technical Report

PERIOD COVERED (Inclusive dates)
September 18, 1978-September 18, 1979

15. SUPPLEMENTARY NOTES

14. (Leave blank)

16. ABSTRACT (200 words or less)

This report presents a status summary of a continuing investigation into the applicability of theoretical earthquake source modeling to the definition of design ground motion environments for nuclear power plants located in the near-field of potentially active faults. A wide variety of proposed near-field ground motion prediction procedures are described and evaluated. It is concluded that existing empirical procedures for predicting near-field ground motion characteristics are not adequately constrained by the available strong motion data, leading to order of magnitude uncertainty in the prediction of some parameters. On the other hand, the review of the proposed theoretical source descriptions has identified a number of model parameters and assumptions which are also not well constrained either by data or theiry and which may affect the near-field ground motion estimates predicted by those models. Preliminary parametric study results are presented, for example, which demonstrate that different, commonly employed assumptions concerning the initiation and stopping of earthquake faulting can have a significant effect on the computed near-field ground motion characteristics.

17. KEY WORDS AND DOCUMENT ANALYSIS

17a. DESCRIPTORS

17b. IDENTIFIERS/OPEN-ENDED TERMS

18. AVAILABILITY STATEMENT
Unlimited

19. SECURITY CLASS (This report)
Unclassified

21. NO. OF PAGES

20. SECURITY CLASS (This page)

22. PRICE
$

NRC FORM 335 (7-77)